

REASONS FOR SOIL EROSION AND SURFACE RUNOFF IN THE SOUTH EASTERN PART OF THE SWISS ALPS

MASTERARBEIT GEO 511
SUBMITTED ON APRIL 30, 2014

Submitted by:

Pascale Polich
09-733-676
Hochstrasse 108
8044 Zürich
papolich@hotmail.com

Supervisor:

Prof. Dr. Markus Egli
markus.egli@geo.uzh.ch
Winterthurerstrasse 190
8057 Zürich

Co-Supervisor:

Barbara Zollinger PhD Student
barbara.zollinger@geo.uzh.ch
Winterthurerstr. 190, 8057 Zürich
Institute of Geography
University of Zürich

PD Dr. Christof Kneisel
kneisel@uni-wuerzburg.de
Am Hubland, 97074 Würzburg
University of Würzburg

DEPARTMENT PHYSICAL GEOGRAPHY
DEPARTMENT OF GEOGRAPHY
UNIVERSITY OF ZURICH

Abstract

Soil erosion and surface runoff are natural geological phenomena and important components of the global geochemical cycle. However, the constantly increasing demand for food and fresh water has required a change in land useage, resulting in increasingly severe soil erosion. This has now become a global problem, affecting large parts of the world population.

Various scientific studies have been done, implementing different types of rainfall simulators, in order to ascertain the natural factors influencing soil erosion as well as the impact of changes in land usage on the rates of that erosion. The question regarding the possible effects of climate change has also been investigated. Most of this erosion research has been done on land used for agricultural purposes. Very little research has been done in alpine and subalpine areas, although soil erosion is a process that plays a major role in both areas.

The objective of the present study was to investigate the effect of several natural variables such as slope inclination, vegetation cover and gravel content, as well as the influence of permafrost soil on soil erosion and surface runoff. Sixty rainfall simulations were performed on permafrost-influenced soil and soil with no permafrost conditions at two different study sites.

During each of the rainfall simulations surface runoff and sediment yield were collected on the downhill side of a soil plot. Besides the actual simulations, a dataset of various soil properties (e.g. vegetation cover, slope, and soil moisture) was also created and soil investigations made in order to generate digitalized maps of the two study sites showing the prevailing soil orders.

The two investigated areas differed on several points. One study site was located in a subalpine region (Spinas, 1750m asl), one in an alpine region (Bever, 2800m asl). At Spinas the rainfall simulations were performed on a northerly exposed scree slope covered with conifers and a dense layer of moss. There were local occurrences of permafrost because of the interaction of climatic conditions and topography, as well as surface and subsurface factors (chimney effect). At the upper study site, Bever, the measurements were conducted on a glacier forefield with marginal vegetation cover (alpine tundra). Here the permafrost occurrence was a residue of the melted glacier.

The results indicated a variation in the amount of surface runoff and sediment yield collected during the rainfall simulations, induced by the absence or presence of permafrost, although this effect was not always statistically significant. The soil properties that seemed to have the strongest influence at the subalpine site were the gravel content of the soil and the slope inclination. In the alpine region, by contrast, the ratio between fine and coarse-grained soil components had the strongest influence. There was a difference not only in the results of the statistical tests, but also in soil characteristics (e.g. C/N ratio) and vegetation cover (forest versus marginal vegetation) of the two study areas.

The findings of this study support the view that the melting of the alpine permafrost has an effect on soil erosion. However, it was also found that there are other factors that have an equal influence on this phenomenon.

Acknowledgements

First I would like to thank Prof. Dr. Markus Egli and Barbara Zollinger for their kind support and leading ideas, as well as for giving me the opportunity to work within the framework of an ongoing dissertation with a lot of freedom to pursue my own goals within my own project.

Special thanks go to Dr. Christian Rixen and the SLF in Davos for the allocation of the rainfall simulator and the collection boxes, which accompanied me during my summer of fieldwork in the Swiss Alps.

I thank Sandra Röthlisberger for the instruction and support during my time at the laboratory at the University of Zürich, as well as Rahel Wanner from the ZAHW in Wädenswil for the CHN measurements of the large number of soil samples.

And last but not least I thank Henning Deblitz, Alexandr Ossipov and Dominique Polich for their assistance and mental support in the field.



Figure 1 Lej Verd (Source: P. Polich).

Contents

Abstract	I
Acknowledgements	III
Contents.....	V
Figures	IX
Tables	XIII
Abbreviations	XV
1 Introduction	1
1.1 Problem Definition	1
1.2 Theoretical background.....	3
1.2.1 Wind erosion	3
1.2.2 Pluvial erosion.....	5
1.2.3 Calculation of soil erosion.....	9
1.2.4 Measurement of soil erosion	10
1.2.5 Permafrost degradation.....	13
1.3 Aim of the study and hypotheses.....	16
2 Material and methods	17
2.1 Study Sites.....	17
2.2 Experimental design	22
2.3 Eijkelkamp rainfall simulator	24
2.4 Rainfall simulation procedure	25
2.5 Plot survey	27
2.6 Laboratory work and data preparation	29
2.6.1 Sediment yield and runoff measurement	29
2.6.2 Soil Samples	29
2.7 Statistical analyses.....	31
2.8 Soil cartography	33

3	Results	35
3.1	General results	35
3.1.1	Sediment yield	35
3.1.2	Surface runoff	37
3.1.3	Correlation: surface runoff and sediment yield	38
3.1.4	C/N-Ratio	40
3.1.5	pH value	44
3.2	Hypothesis 1	47
3.2.1	Spinas	47
3.2.2	Bever	49
3.3	Hypothesis 2	51
3.3.1	Spinas	51
3.3.2	Bever	54
3.4	Soil cartography	57
3.4.1	Spinas	57
3.4.2	Bever	58
4	Discussion	59
4.1	Surface runoff and sediment yield.....	59
4.2	PH Value and Vegetation	60
4.3	C/N ratio	61
4.4	Rainfall simulator	62
5	Conclusion.....	63
6	Bibliography	65
7	Source of Figures.....	73
8	Appendix	75
8.1	Appendix A: Illustrations of the plot survey	75
	Slope.....	76
	Vegetation cover.....	77
	Gravel content	78
	Soil moisture.....	79

8.2	Appendix B: Descriptive statistics	81
	Sediment yield.....	81
	Surface runoff.....	82
	C/N ratio.....	83
	pH value (laboratory)	84
8.3	Appendix C: C/N ratios of alpine soils.....	85
8.4	Appendix D: pH values Zollinger et al., 2013.....	86
8.5	Appendix E: Data sets	87
8.5.1	Spinas	87
8.5.2	Bever	91

Figures

Figure 1 Lej Verd (Source: P. Polich).....	III
Figure 2 Gully erosion in Kenya (Source: WWF).....	1
Figure 3 Soil erosion in the Swiss Alps (Source: P. Polich).	2
Figure 4 Wind erosion transport modes: creep, saltation and suspension (Source: WER).	3
Figure 5 Example of a spray-type rainfall simulator (Source: Landloch).	10
Figure 6 Example of a drip-type rainfall simulator (Source: Clark et al., 2002).....	11
Figure 7 Schematic plot of permafrost (important terms) (Source: Permos).	13
Figure 8 Permafrost degradation and thaw settlement in Alaska (Source: NGEE).....	14
Figure 9 Overview of Switzerland and the Val Bever with the two study sites (Source: geo.admin). .	17
Figure 10 Map of the lower study site Spinas (Source: geo.admin).....	18
Figure 11 Soil profile at Spinas with permafrost (Source: B. Zollinger).	19
Figure 12 Soil profile at Spinas without permafrost (Source: B. Zollinger).	19
Figure 13 Picture of the scree slope at Spinas (Source: P. Polich).....	19
Figure 14 Map of the upper study site, Bever (Source: geo.admin).....	20
Figure 15 Soil profile at Bever with permafrost (Source: B. Zollinger).	21
Figure 16 Soil profile at Bever without permafrost (Source: B. Zollinger).	21
Figure 17 Slope at Bever with sparse vegetation cover (Source: P. Polich).	21
Figure 18 Visual presentation of areas at Spinas where rainfall simulations were conducted, indicated by GPS way points (Source: Google earth).....	22
Figure 19 GPS way points indicating rainfall simulation sites at Bever (Source: Google earth).....	23
Figure 20 Eijkelkamp rainfall simulator (Source: Eijkelkamp).	24
Figure 22 Rainfall simulator installed at the study site Spinas (Source: P. Polich).	25
Figure 21 Rainfall simulator (Source: Eijkelkamp).	25
Figure 23 Plot survey (GPS measurement) of plot 22 at Bever (Source: P. Polich).	27
Figure 24 Step 1	33
Figure 25 Step 2	33
Figure 26 Step 3	33
Figure 27 Box plot of the sediment yield at Spinas (SPSS).	35
Figure 28 Box plot of the sediment yield at Bever (SPSS).	35
Figure 29 Box plot of the surface runoff at Spinas (SPSS).....	37
Figure 30 Box plot of the surface runoff at Bever (SPSS).	37
Figure 31 Amount of surface runoff (ml) and sediment yield (g) at Spinas (SPSS).	38
Figure 32 Scatter plot of surface runoff (ml) and sediment yield (g) at Spinas (SPSS).....	38
Figure 33 Amount of surface runoff (ml) and sediment yield (g) at Bever (SPSS).	39

Figure 34 Scatter plot of surface runoff (ml) and sediment yield (g) at Bever (SPSS).....	39
Figure 35 C/N ratio of the investigated soil plots at Spinas (with mean) (SPSS).	40
Figure 36 C/N ratio of the investigated soil plots at Bever (with mean) (SPSS).	40
Figure 37 Histogram of the pH value (Laboratory) at the investigated soil plots at Spinas (SPSS).	44
Figure 38 Histogram of the pH value (Laboratory) at the investigated soil plots at Bever (SPSS).	44
Figure 39 Box plot of the pH value (Laboratory) at the investigated soil plots at Spinas (SPSS).	44
Figure 40 Box plot of the pH value (Laboratory) at the investigated soil plots at Bever (SPSS).	44
Figure 41 Box plots of the surface runoff on PF and on soil without PF at Spinas (SPSS).	47
Figure 42 Box plots of the surface runoff on PF and on soil without PF at Spinas, logarithmic scale (SPSS).	47
Figure 43 Box plots of the sediment yield on soil with PF and on soil without PF at Spinas (SPSS).	48
Figure 44 Box plots of the surface runoff on PF and on soil without PF at Bever (SPSS).	49
Figure 45 Box plots of the surface runoff on PF and on soil without PF at Bever, logarithmic scale (SPSS)	49
Figure 46 Box plot of the sediment yield on PF and on soil without PF at Bever (SPSS).....	50
Figure 47 Box plot of the sediment yield on PF and on soil without PF at Bever, logarithmic scale (SPSS).	50
Figure 48 Gravel content (%) and sediment yield (g) at Spinas (SPSS).	52
Figure 49 Gravel content (%) and surface runoff (ml) at Spinas (SPSS).	52
Figure 50 Slope (°) and surface runoff (ml) at Spinas (without outliers) (SPSS).	53
Figure 51 Gravel content (%) and sediment yield (g) at Spinas (without outliers) (SPSS).	53
Figure 53 Scatter plot of the average amount of carbon in the soil and surface runoff (ml) at Bever (without outliers) (SPSS).....	56
Figure 52 Scatter plot of the ratio fine/coarse grained and surface runoff (ml) at Bever (without outliers) (SPSS).	56
Figure 54 Scatter plot of the C/N ratio and surface runoff (ml) at Bever (without outliers) (SPSS). ...	56
Figure 55 Representation of the different soil types at Spinas (ArcGIS).	57
Figure 56 Representation of the different soil types at Bever (ArcGIS).	58
Figure 57 Photo of soil patch nr. 5 at Spinas (Source: P. Polich).	59
Figure 59 Caricetum curvulae at soil patch nr. 30 at Bever (Source: P. Polich).	60
Figure 58 Alpine rose at Spinas (Source: P. Polich).	60
Figure 60 Histogram of the slope inclination at the investigated soil plots at Spinas (SPSS).....	76
Figure 61 Histogram of the slope inclination at the investigated soil plots at Bever (SPSS).....	76
Figure 62 Box plot of the slope inclination at the investigated soil plots at Spinas (SPSS).....	76
Figure 63 Box plot of the slope inclination at the investigated soil plots at Bever (SPSS).....	76
Figure 65 Histogram of the vegetation cover at the investigated soil plots at Bever (SPSS).....	77
Figure 64 Histogram of the vegetation cover at the investigated soil plots at Spinas (SPSS).....	77

Figure 67 Box plot of the vegetation cover at the investigated soil plots at Bever (SPSS).....	77
Figure 66 Box plot of the vegetation cover at the investigated soil plots at Bever (SPSS).....	77
Figure 68 Histogram of the gravel content at the investigated soil plots at Spinas (SPSS).	78
Figure 69 Histogram of the gravel content at the investigated soil plots at Bever (SPSS).	78
Figure 71 Box plot of the gravel content at the investigated soil plots at Bever (SPSS).	78
Figure 70 Box plot of the gravel content at the investigated soil plots at Spinas (SPSS).	78
Figure 72 Soil moisture before and after the rain simulations and the soil moisture difference at Spinas (SPSS).	79
Figure 73 Soil moisture before and after the rain simulations and the soil moisture difference at Bever (SPSS).	80

Tables

Table 1 Explanations of the levels of significance.....	31
Table 2 Outliers removed from the dataset of Spinas.	32
Table 3 Outliers removed from the dataset of Bever.....	32
Table 4 Amount of sediment yield (raw data and without outliers) at Spinas and Bever.	36
Table 5 Amount of surface runoff (raw data and without outliers) at Spinas and Bever.	37
Table 6 Correlation analysis between surface runoff (ml) and sediment yield (g) at Spinas (SPSS)....	38
Table 7 Correlation analysis between surface runoff (ml) and sediment yield (g) at Bever (SPSS)....	39
Table 8 C/N ratio and the amount of carbon and nitrogen in the 40 soil samples of Spinas.....	41
Table 9 C/N ratio and the amount of carbon and nitrogen in the 60 soil samples of Bever (Part 1)....	42
Table 10 C/N ratio and the amount of carbon and nitrogen in the 60 soil samples of Bever (Part 2)...	43
Table 11 List of the pH-values measured in the laboratory (Spinas).	45
Table 12 List of the pH-values measured in the laboratory (Bever).	46
Table 13 Independent T-Test for surface runoff at Spinas (SPSS)	47
Table 14 Independent T-Test for the sediment yield at Spinas (SPSS).....	48
Table 15 Independent T-Test for surface runoff at Bever (SPSS).....	49
Table 16 Signed-Rank Test for sediment yield at Bever (SPSS)	50
Table 17 Correlation analysis of soil parameters and soil erosion at Spinas (SPSS).....	51
Table 18 Correlation analysis of soil parameters and soil erosion at Spinas (without outliers) (SPSS)	52
Table 19 Correlation analysis of soil parameters and soil erosion in Bever (SPSS).....	54
Table 20 Correlation analysis of soil parameters and soil erosion at Bever (without outliers).....	55
Table 21 Sources of the used figures (Part 1).....	73
Table 22 Sources of the used figures (Part 2).....	74
Table 23 Spinas: descriptive statistics of the sediment yield (raw data).	81
Table 24 Spinas: descriptive statistics of the sediment yield (without outliers).....	81
Table 25 Bever descriptive statistics of the sediment yield (raw data).	81
Table 26 Bever descriptive statistics of the sediment yield (without outliers).....	82
Table 27 Spinas: descriptive statistics of the surface runoff (raw data).	82
Table 28 Spinas: descriptive statistics of the surface runoff (without outliers).	82
Table 29 Bever descriptive statistics of the surface runoff (raw data).	82
Table 30 Bever descriptive statistics of the surface runoff (without outliers).....	82
Table 31 Descriptive statistics of the C/N ration at Spinas (SPSS).....	83
Table 32 Descriptive statistics of the C/N ration at Bever (SPSS).....	83
Table 33 Descriptice statistics of the carbon and nitrogen at Spinas.	83
Table 34 Descriptice statistics of the carbon and nitrogen at Bever.....	83

Table 35 Descriptive statistics of the measured pH value (laboratory) at Spinas.	84
Table 36 Descriptive statistics of the measured pH value (laboratory) at Bever.....	84
Table 37 C/N ratio and the amount of carbon and nitrogen in alpine soils.	85
Table 38 C/N ratio and the amount of carbon and nitrogen in the topsoil of “Albula”, “Bever”, and “Spinas”.....	85
Table 39 Measured pH values at Spinas in Zollinger et al., 2013.	86
Table 40 Measured pH values at Bever in Zollinger et al., 2013.	86
Table 41 Dataset of Spinas (Part 1).....	88
Table 42 Dataset of Spinas (Part 2).....	89
Table 43 Dataset of Spinas (Part 3).....	90
Table 44 Dataset of Bever (Part 1.1).....	91
Table 45 Dataset of Bever (Part 1.2).....	92
Table 46 Dataset of Bever (Part 2.1).....	93
Table 47 Dataset of Bever (Part 2.2).....	94
Table 48 Dataset of Bever (Part 3.1).....	95
Table 49 Dataset of Bever (Part 3.2).....	96

Abbreviations

C	Carbon
e.g.	for example
FAL	Eidgenössische Forschungsanstalt für Agronomie und Landbau
GPS	Global positioning system
i.e.	id est
K-S Test	Kolgomorov Smirnov Test
M	molar
m	meter
MAAT	Mean annual air temperature
M. asl	Meters above sea level
N	Nitrogen
Pf	Permafrost
RUSLE	Revised Universal Soil Loss Equation
r/s	rotations per second
SLR	Soil loss ratio
SPSS	Statistical Package for the Social Science
TDR	Time-domain reflectometer
USLE	Universal Soil Loss Equation

1 Introduction

1.1 Problem Definition

Soil erosion is a worldwide problem affecting large parts of the world's population. About 75 billion tons of soil are eroded each year from the world's terrestrial ecosystems (Pimentel & Kounang, 1998). Because soil is formed very slowly, the soil is lost 13-40 times faster than it is renewed and sustained (Pimentel & Kounang, 1998). Soil erosion from land areas is widespread and adversely affects all natural and managed ecosystems, including those of agriculture and forestry. Soil erosion is also increasingly recognized as being more hazardous in mountain areas (Figure 3) (Millward & Mersey, 1999; Angima et al., 2003; Jasrotia & Singh, 2006). For these reasons and because soil is a vital and largely non-renewable resource (Gobin et al, 2004), soil erosion ranks as one of the most serious environmental problems in the world (Pimentel & Kounang, 1998).



Figure 2 Gully erosion in Kenya (Source: WWF).

On-site issues

These facts lead to several linked problems. Soil erosion reduces the overall productivity of terrestrial ecosystems in several ways. Firstly, erosion leads to an increase in water runoff, thereby preventing water infiltration and decreasing the water storage capacity of the soil. Secondly, organic matter and essential plant nutrients are lost during the erosion process and soil depth is reduced (Pimentel & Kounang, 1998) (Figure 2), so that roots and biota are less supported (Pimentel et al., 1995; Wardle et al., 2004). Because all these processes interact with one another, it is almost impossible to isolate and identify their specific impact on the processes of soil erosion (Pimentel & Kounang, 1998).



Figure 3 Soil erosion in the Swiss Alps (Source: P. Polich).

Off-site issues

The concept of off-site impact is associated with events in which soil is dislocated (i.e. mud-slides). Negative impacts include economic damage associated with the “muddy flooding” of homes, villages and infrastructure (Boardman, 2010; Mullan, 2013). Additionally, environmental damage is caused by the sedimentation of sand- and gravel-bedded rivers (Boardman et al., 2009) and the adsorption of chemicals onto soil particles and their resultant eutrophication in water bodies (Morgan, 2005).

Rainfall simulations are a common method in scientific studies to measure soil erosion. The majority of erosion research has been implemented on agriculturally used land, but not much research has been done in subalpine areas with extensively farmed meadows and forests, even though these regions could also behave similarly in terms of soil erosion. In the present study rainfall simulations were performed in two alpine regions in order to investigate their effect on soil erosion.

In the future and in the changing environment of the 21st century these adverse impacts may become a more serious problem, since future climate change is expected to have an impact on the extent, frequency and magnitude of soil erosion in a number of ways (Pruski & Nearing, 2002).

1.2 Theoretical background

Rain and wind energy are the two primary causes of erosion on tilled or bare land (Pimentel & Kounang, 1998). The focus of this study is on soil erosion caused by rain. In this chapter the causes and influencing factors of soil erosion and surface runoff are explained.

1.2.1 Wind erosion

Wind erosion (deflation) is a major conservation problem in arid and semi-arid regions around the world because of low precipitation and high evaporation rates (Skidmore, 2000). Wind energy dislodges soil particles and carries them off the land (Pimentel & Kounang, 1998). The most common consequences of wind erosion are: the removal of the most fertile part of the soil and a decrease in productivity, deposition of sediment in ditches and waterways, pollution of the air and reduction of visibility, as well as the deterioration of machinery (Hagen et al., 2010).

1.2.1.1 Processes of wind erosion

The three types of wind erosion are shown in Figure 4 below:

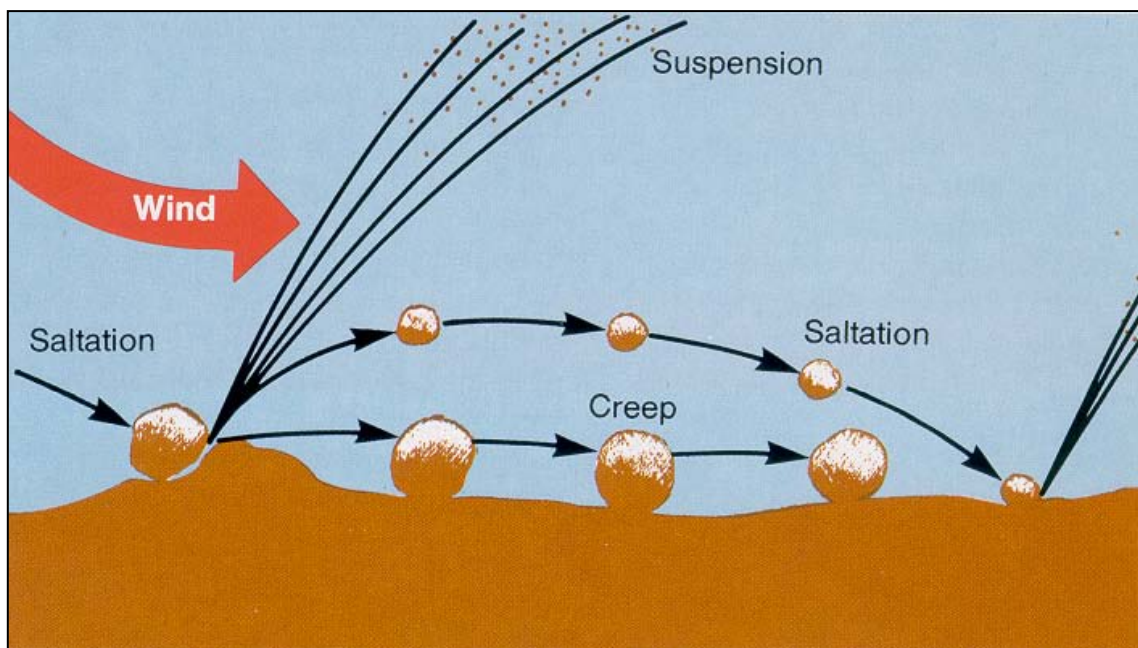


Figure 4 Wind erosion transport modes: creep, saltation and suspension (Source: WER).

Suspension

Fine soil aggregates / particles less than 0.1 mm in size are transported parallel to the surface (horizontally) and vertically upward into the atmosphere by strong winds. In the erosive processes these particles can be carried high into the atmosphere, returning to earth only when the wind subsides or they are carried downward with precipitation. Suspended particles can travel hundreds of miles. Suspension impacts productivity indirectly through the removal of organic matter and plant nutrients or, conversely, by leaving behind the less-fertile soil constituents (Lyles et al., 1985).

Saltation

During saltation individual soil aggregates / particles are lifted from the surface at 50 ° to 90 ° angles, rotate at 115–1000 r/s, and follow distinctive trajectories under the influence of air resistance and gravity (Chepil, 1945; White & Schulz, 1977). The size range for saltation excludes coarse and very coarse sand particles, which remain in the local area; the bouncing particles therefore range in size from 0.1 to 0.5 mm in diameter. During erosion saltating aggregates may shift to suspension mode because of abrasion and this may cause other aggregates on the surface to shift modes. Saltation is the major cause of aggregate breakdown during erosion. Its role is to initiate and sustain suspension and to drive the creep transport (Lyles et al., 1985).

Soil creep

In the course of soil creep, large soil particles roll and slide along the surface of the soil. Soil creep can move coarse, sand-sized particles ranging from 0.5 to 1 mm in diameter – particles too large to leave the surface in ordinary erosive winds. These particles can be set in motion by the impact of saltating soil aggregates / particles. It is estimated that surface creep constitutes 7% to 25% of total transport (Bagnold, 1941; Chepil, 1945; Horikowa & Shen, 1960; Lyles et al., 1985).

1.2.2 Pluvial erosion

1.2.2.1 Processes of pluvial erosion

In Europe soil erosion is caused mainly by water and, to a smaller extent, by wind (Gobin et al., 2004). Soil erosion caused by water consists of two sub-processes, namely the detachment of the soil particles and their transport. The degree of soil erosion depends on the amount of detached soil material and the ability of the erosive agent to transport the soil particles (Morgan, 1999).

Detachment

Rain splash is the most important detaching agent (Morgan, 1999). During events of highly intense precipitation air gets trapped and compressed in the soil aggregates, and this can result in high pressures, at a magnitude of 100 Pa. The unequal maceration of the aggregates lead to an increased shear stress which causes fissures (Auerswald, 1998) and facilitates erosion.

Erosion occurs when soil is exposed to water energy (Pimentel & Kounang, 1998). Since the falling raindrops cannot infiltrate the soil at their fall velocity, they are repulsed radially. Due to the high shear stress arising during this process, small particles become dissolved out of the aggregate compound and the already weakened aggregates are further disrupted. This process is called splash erosion (Auerswald, 1998). The primary force causing erosion in this process is gravity, acting through precipitation and water flow down a terrain slope (Vahabi & Nikkami, 2008; Canali, 1992; Assouline & Ben-Hur, 2006).

Soil surface affected by rainfall becomes subject to processes of wetting and drop impact which can lead to the formation of a seal during rainfall. A consequence of this sealing process can be reduced infiltration and increased erosion, as runoff is simultaneously increased (Ramos et al., 2003; Assouline & Ben-Hur, 2006).

Transport

In the instance of water saturated soil or a formed seal that prevents precipitation from infiltrating the soil, the excessive water first gets collected in depressions on the soil surface. Surface runoff does not start until the depression capacity is exhausted (Morgan, 1999). The water, flowing faster in rills and gullies, causes turbulences. In this way small pieces of gravel, of up to two centimeters in diameter, can be dissolved and transported. Transport capacity depends substantially on the amount of water and the downhill gradient. If there is a decrease in the amount of water or in the gradient, transport capacity decreases. The heaviest particles are deposited first and then the smaller and lighter ones (Auenwald, 1998).

1.2.2.2 Types of pluvial erosion

Soil erosion by water can be divided into different manifestations.

Rill and interrill erosion

The small scale (point and plot scale) types of soil erosion are interrill erosion and rill erosion. The mechanisms of these two processes are completely different (Wirtz et al., 2012). The soil detachment in interrill erosion is induced and enhanced by splash (raindrop impact) and shallow overland flow (Beuselinck et al., 2002; Meyer et al., 1975). In contrast, rill erosion is caused by a concentrated overland flow (Bryan, 2000; Govers et al., 2007; Knapen et al., 2007). Govers and Poesen (1988) measured the amount of interrill, rill and gully erosion in an upland field and found that most of the erosion in the field occurred in the rill and gully systems. Only 22% of total sediment removed came from interrill areas (Govers & Poesen, 1988). But these results should be treated with caution, since other authors (e.g. Wirtz et al., 2012) find it extremely difficult (or practically impossible) to determine the percentage of interrill, rill, and gully erosion on the total soil loss in a catchment area.

Rills are shallow drainage lines at a depth of less than 30 cm. During rill erosion surface water concentrates in depressions and cuts into the soil surface. This process leads to linear shapes of erosion. In sandy soils the shear strength of the soil is relatively small and easy to overcome (Scheffer & Schachtschabel, 2002). These newly formed rills can become persistent and evolve into gullies, potentially constraining further land use as the duration or the intensity of rain contributes to increase and runoff volumes continue to accelerate (Woodward, 1999; Hancock et al., 2008; Auerswald, 1998).

Gully erosion

Gully erosion is defined as the erosion process whereby runoff water accumulates and often recurs in narrow channels and - over short periods of time - removes the soil from this narrow area to considerable depths (Poesen et al., 2003). The gullies that emerge in this way are linear channels formed by a concentrated flow of water (Kirkby & Bracken, 2009). They can grow up to several meters in width and depth and typically present as a rectangular or V-shaped cross section (Bull & Kirkby, 1997). In the case of gully erosion, the raindrop as an erosion agent is only minimally important (Auerswald, 1998).

Gullies need high-intensity rainfall events to take place. For this reason several authors (e.g. Faust & Schmidt, 2009) consider the geomorphological importance of gullies to be quite low, corresponding to the rare activity of the gullies. Faust and Schmidt (2009) state an activity frequency of one single event in 20 years, compared to an assumed activity of the rills of about four times per year.

Sheet erosion

Sheet erosion is characterized by the detachment and uniform removal of fine topsoil particles, caused by rainfall impact and shallow overland surface flow. A mixture of water and solid soil elements flow down the slope as a sheet and erodes the soil in successive layers (Descroix et al., 2008). In this process fine particles of the soil are mostly transported (clay and silts) (Biot, 1981). This form of erosion has long been thought to be of very slow progression but is now recognized as a major threat to the sustainability of natural ecosystems. The reason for this is that the part that is removed, the upper horizon, is often the most fertile part of the soil. These fine particles contain most of the available nutrients and organic matter in the soil (UNEP, 1994). There are countless direct and indirect consequences of sheet erosion on ecosystems which could potentially have a negative impact on the overall economic development of a society. These include, for example: (1) a threat to soil functions (e.g. food production, water flow regulation), (2) an increase in the occurrence of floods, (3) a decrease of groundwater

recharge, (4) an increase in eutrophication of surface waters, (5) water pollution by heavy metals and pesticides, and (6) sedimentation in valleys and reservoirs (Dlamini, 2011).

1.2.2.3 Influencing factors

Several other factors can influence soil erosion, such as soil texture, permeability and antecedent moisture, rainfall intensity, land use and the type and density of the vegetation cover as well as land slope (Vahabi & Nikkami, 2008). Several of these factors and their influence on soil erosion will be discussed below.

Vegetation

The mechanisms by which vegetation stabilizes the soil are manifold. Land areas covered by both living and dead plant biomass are protected and experience reduced soil erosion because raindrop and wind energy is dissipated by the biomass layer (Pimentel & Kounang, 1998). The biomass layer causes raindrops to be intercepted and enhances infiltration, and also allows the transpiring of soil water and the trapping of the eroded sediment (Shit et al., 2012; Styczen & Morgan, 1995; Bochet et al., 2000; Rey et al., 2007). Moreover, the above-ground components of the vegetation increase the surface roughness and act as a windbreak (Gray & Sotir 1996). Gross et al. (1991) observed the runoff and sediment yield for areas with different canopy covers and concluded that even low density vegetation coverage remarkably decreases the sediment yield.

Erosion occurs when the soil lacks this protective vegetative cover, something which is especially widespread in developing countries due to higher population densities and inadequate agricultural practices (Pimentel & Kounang, 1998).

The benefits of the below-ground components of vegetation are considerable. Root systems form anchors that stabilize loose soil and control both the hydrological and mechanical properties of a slope (Gyssels & Poesen, 2003; Mattia et al., 2005; Nilaweera & Nutalaya, 1999; De Baets et al., 2006; Reubens et al., 2007). Roots affect important soil properties such as aggregate stability, soil bulk density, soil texture, infiltration capacity, organic and chemical content as well as shear strength (Miller & Jastrow, 1990; Reubens et al., 2007). Additionally, vegetation roots increase the infiltration capacity of the soil by creating macro-pores and thereby reducing the volume and the flow velocity of the surface runoff (Gyssels et al., 2005).

Pohl et al. (2009) and Martin et al. (2010) also proved that not only the amount of vegetation cover and root system but also plant diversity has an influence on the erosion susceptibility of the soil. This statement is founded on the relation between plant diversity and root type diversity. Several rainfall simulations were conducted on plots on ski slopes in the Swiss Alps which had different plant covers and had been graded by machine.

Forest

Forests, a special form of vegetation, also provide excellent protection against soil erosion. As a general rule, wooded areas are rumored to have a cushioning effect on surface runoff. Due to the higher interception and good transpiration of forest soil, soil moisture in a forested area - in summer and autumn - is lower than in the surrounding area. This leads to a higher water uptake capacity of the soil in forested areas during this time (Kohl et al., 2008). Another important factor is the stabilization of the soil caused by the tree roots (Dhakal & Sidle, 2003).

Singh & Kaur (1989) stated that a minimum of 60% forest cover of the landscape is necessary to prevent soil erosion in forested areas. The ongoing deforestation in many equatorial countries could therefore worsen the problem of soil erosion in those areas.

Slope inclination and slope length

An increasing slope inclination and slope length lead to a higher amount of surface runoff. And so that the detachment and transport capacity of surface runoff are also increased (Kinnel & McLachlan, 1989). Many articles have been written about the linear or less than linear relationship between soil erosion and slope aspect (McCool et al., 1987; Huang & Brandford, 1993; Lattanzi et al., 1974; Watson & Laflen, 1986). Erosion rates on sloping land are exceedingly high, especially on marginal, steep land (Lal & Steward, 1990; Warrington et al., 1989).

Other authors (Fox & Bryan, 1999; Moss, 1988; Kinnell, 1990) described slope gradient only as an indirect factor in the formation of soil erosion, as it influences the flow velocity of water running downhill. Flow velocity was observed to be directly proportional to interrill erosion rate, since runoff velocity increases the transport capacity of runoff in rain-impacted flow erosion conditions. A direct consequence of this is that on longer slopes interrill runoff will attain a greater runoff velocity and therefore an increased interrill erosion rate (Fox & Bryan, 1999).

Erodibility of soil

The erodibility of soil corresponds to the susceptibility of the soil to detachment as well as to the transport of soil particles (Morgan, 1999). The structure of the soil itself and its grain size distribution influence the facility with which it can be eroded and soil particles can be transported. Soils with medium to fine texture, low organic matter content and weak structural development are most easily eroded. Typically, these soils have low infiltration rates and are therefore subject to high rates of water runoff, the eroded soil being carried away in the water flow (Forster et al., 1985; Pimentel & Kounang, 1998). Stony soils, in contrast, are particularly well protected against erosion. Stones cannot be detached and transported easily (Auerswald, 1998).

In addition, aggregate stability is considered to be one of the main soil properties regulating soil erodibility (De Ploey & Poesen, 1985; Cerdà, 1998; Cantón et al., 2008). Soil aggregates are defined as soil particles that consist of several mineral single grains which are self-adhesive or bonded with humus or mineral substance (Scheffer & Schachtschabel, 2002). Aggregate breakdown produces small soil particles that may then be displaced and reoriented into a more continuous structure, forming a surface seal (Ramos et al., 2003).

Infiltration and soil moisture

Important for the process of infiltration into the soil is the water conductivity of the superficial soil matrix. In situations where this conductivity is reduced due to capping, destruction of the soil aggregates or the forming of a seal, the rate of infiltration decreases significantly. This increases surface runoff and the danger of erosion (Scheffer & Schachtschabel, 2002). Another important factor seems to be the antecedent soil moisture (Ward & Bolton, 1991).

Anthropogenic influences

On cultivated land soil tillage is the most important influencing factor in soil erosion except for slope inclination (Auerswald et al., 1991). Areas which are increasingly being cleared of trees, bushes and grass for the sake of agricultural usage are prone to erosion. Tillage in the direction of the slope, ground compaction with heavy machines and the unsuitable use of mineral and organic fertilizers will also increase the possibility of erosion (Morgan, 1999).

1.2.3 Calculation of soil erosion

1.2.3.1 USLE (Universal Soil Loss Equation)

The USLE (Universal Soil Loss Equation) was developed in the late 1950s by W. H. Wischmeier and D. D. Smith et al., together with the U. S. Department of Agriculture (USDA), Agriculture Research Service (ARS), Soil Conservation Service (SCS) and Purdue University (Renard et al., 1991). Its field use began in the 1960s in the Midwest of the USA and it became a tool used all over the world by soil conservationists to estimate rill and sheet erosion. It was revised 1978 so that soil loss from both crop and rangeland areas could be estimated more accurately (Renard et al, 1991; McCool et al., 1995).

1.2.3.2 RUSLE (Revised Universal Soil Loss Equation)

The Revised Universal Soil Loss Equation (RUSLE) replaced the Universal Soil Loss Equation (USLE) and is used for predicting the average annual soil loss from interrill and rill erosion caused by rainfall and associated overland flow. RUSLE retains the equation structure of USLE, but each of its factor relationships have either been updated with recent data, or new relationships have been derived based on modern erosion theory and data (Renard et al., 1997; USDA & NRCS, 2000).

This equation is a function of five input factors in raster data format:

$$A = R * K * L * S * C * P$$

where

A	Computed mean (annual) soil loss
R	Rainfall-runoff erosivity factor
K	Soil erodibility factor
L	Slope length factor
S	Slope steepness factor
C	Cover management factor
P	Supporting practices factor

(McCool et al., 1995; Prasannakumar et al., 2012).

This empirically based equation was derived from a large mass of field data. It computes combined interrill and rill erosion, using values representing the four major factors affecting erosion. These factors are:

(1) climatic erosivity represented by R, (2) soil erodibility represented by K, (3) topography represented by L and S, and (4) land use and management represented by C and P. While the former USLE structure has been retained in RUSLE, the algorithms used to calculate the individual factors have been changed significantly. Perhaps most important has been the computerization of the technology to assist with the determination of individual factors. This allows computation of the soil loss ratio (SLR) by 15-day intervals rather than by longer crop stage periods, and improves estimates of the factors affecting the SLR, such as surface roughness, crop growth and residue decomposition (McCool et al, 1995).

1.2.4 Measurement of soil erosion

Rainfall simulation or natural rainstorm

A natural rainstorm is characterized by its intensity distribution, duration, drop size distribution and rainfall energy (Agassi & Bradford, 1999). To develop the relationships between rainstorm and soil erosion processes, control over intensity, energy and duration is required (Meyer, 1965). This is obtained with a rainfall simulator that imitates the physical characteristics of natural rainfall as far as possible. Such a simulator is an ideal tool for infiltration, soil erosion, and other related research areas as it can replicate the process and characteristics of natural rainfall (Aksoy et al., 2012). It produces rain with the correct (1) rainfall intensity, (2) raindrop-size distribution, (3) raindrop-impact energy, (4) spatial variability over the plot and (5) temporal variability over the plot on demand and wherever necessary (Stroosdnijder, 2005; Bowyer-Bower & Burt, 1989; Clarke & Walsh, 2007). Small-scale portable rainfall simulators are therefore an essential research tool for investigating the process dynamics of soil erosion and surface hydrology (Iserloh et al., 2013).

Types of rainfall simulators

There is no standardization in rainfall simulation and rainfall simulators differ in design, rainfall intensities, rain spectra and research questions (Iserloh et al., 2013). Therefore there are many different definitions of the various rainfall simulators. Meyer (1988) listed a compilation of many different rainfall simulator systems.

In the present instance the following diversification into four main kinds of rainfall simulators is sufficient. Bowyer-Bower & Burt (1989) and Aksoy et al. (2012) separated the rainfall simulators into two main groups according to the way in which the raindrops are produced:



Figure 5 Example of a spray-type rainfall simulator (Source: Landloch).

The (1) spray-type simulators (pressurized nozzle simulators) use water sprayed from standard irrigation sprinkler nozzles under high pressure (see Figure 5). In this way, high rainfall intensities - which are more typical of natural rainstorms - can be generated. These systems also allow the simulation of rainfall fields on a larger scale, but still with uniform spatial distribution and reasonable drop size distribution (Corona et al., 2013).

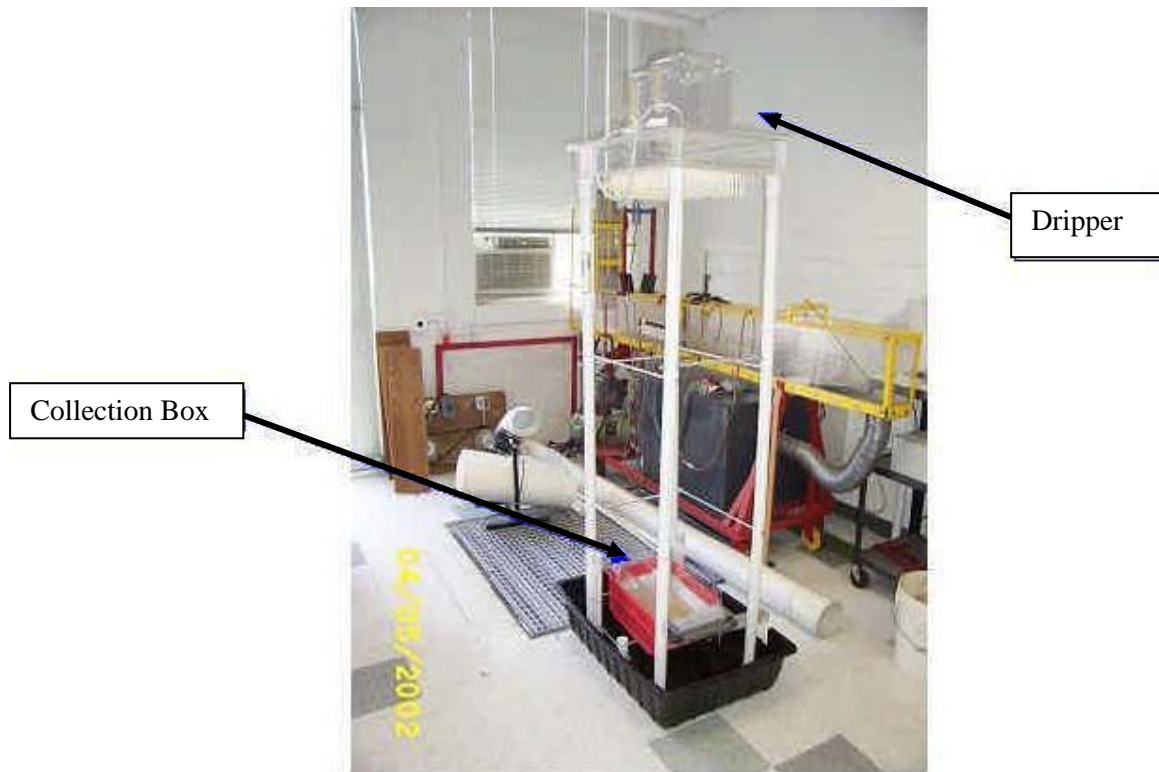


Figure 6 Example of a drip-type rainfall simulator (Source: Clark et al., 2002).

In contrast to that, (2) drip-type simulators (see Figure 6) are non-pressurized nozzle simulators (drop forming), from which water drips from a suitable apparatus under the effect of gravity (Bowyer-Bower & Burt, 1989; Aksoy, 2012). These systems are characterized by a uniform intensity spatial distribution. They are easily portable and use water very efficiently. However, drip type rainfall simulators generally have a limited drop size distribution, the velocity of the drops is limited by the height of the tank and they are limited to small plots (Corona et al., 2013).

On the other hand, Agassi & Bradford (1999) distinguished between rainfall simulators with (3) uniformly sized drops and those with (4) multi-sized drops. Rainfall simulators with uniformly sized drops usually consist of an open or closed chamber with protruding hypodermic needles, producing only one drop size. The drops fall vertically to the soil surface below. Changes in rainfall intensity are achieved by controlling the head of water above the drop forming tubes in the open chamber type or by altering the pressure in the closed chamber type. Changes in water pressure or in the water head also change the size and velocity of the drops which in turn change the kinetic energy of the simulated rainstorm (Agassi & Bradford, 1999; Munn & Huntington, 1976). Rainfall simulators with multi-sized drops are designed to produce drop characteristics close to those of natural rainstorms. They vary in type and number of nozzles and their spraying is either continuous or intermittent (Agassi & Bradford, 1999).

The need to distinguish the different partial processes of runoff formation and erosion led to the development of rainfall simulations on small plots. The outstanding advantages of small portable rainfall simulators are, among others, their low cost, easy transportation to remote areas and low water consumption. Small portable rainfall simulators also allow data collection under controlled conditions and over relatively short time periods (Iserloh et al., 2013).

Field or Laboratory

One can conduct rainfall simulations in the laboratory or in the field. Advantages of erosion measurements in the laboratory are that they allow better control of the range of dependent variables as well as the use of advanced equipment and the possibility to conduct replicated measurements. Rainfall simulators in the laboratory are less affected by wind, temperature and humidity (Clarke & Walsh, 2007). The advantages for field work are the possibility to conduct measurements on a proper scale, with realistic soil and plant characteristics and temporal changes in environmental variables (Agassi & Bradford, 1999). On the other hand, rainfall simulators used in the field may also have disadvantages, precisely because they are usually cheap, simple, and small simulators which rain onto a small test plot. Although large rainfall simulators also exist for field studies, they are generally impractical, non-portable and therefore difficult to use in field research in difficult to reach areas (Aksoy et al., 2012).

Measurements and scales

There are many different erosion processes which operate on different scales, spatially and temporally. Stroosnijder (2005) defines five relevant spatial scales for erosion measurement: (1) the point scale (1 m^2) for interrill erosion, (2) the plot ($<100 \text{ m}^2$) for rill erosion, (3) the hill slope ($<500 \text{ m}^2$) for sediment deposition, (4) the field ($<1 \text{ ha}$) for channels and (5) the small watershed ($<50 \text{ ha}$) for spatial interaction effects (Stroosnijder, 2005). For measurement on the different spatial scales different sizes of rainfall simulators can be used, from a very small portable infiltrometer with a 15 cm diameter rainfall area (Bhardwaj and Singh, 1992) to the complex Kentucky rainfall simulator that covers $4.5\text{m}\times 22\text{m}$ (Moore et al., 1983).

Furthermore, two temporal scales are described: (1) the single rainstorm and (2) the annual average (Stroosnijder, 2005). Time of the year, tillage history and wetting and drying history also affect results (Agassi & Bradford, 1999). The suggested plot shape should be square or rectangular with a length to width ratio close to 1. In addition, the plot must be representative of the field (Agassi & Bradford, 1999).

Because of all these facts it should be clear that a universal rainfall simulator applicable to all situations does not exist. Each specific condition requires specific designs for rainfall simulators. In the following study a small and portable drip-type rainfall simulator with one-sized drops was used. The rainfall simulations were conducted in the field on point scale (1 m^2) soil plots.

1.2.5 Permafrost degradation

In this master thesis the effect of permafrost degradation on soil erosion was explored by comparing erosion data of rainfall simulations on soil patches with permafrost and soil patches without permafrost. In this section the sequence of permafrost formation as well as the causes and process of permafrost degradation are described.

Permafrost formation

Permanently frozen soil (permafrost) is especially well-known in Siberia and Alaska. In the Alps this temperature-dependent phenomenon has been investigated more intensively since the 1970s (Vonder Mühll et al., 2001). Across the world, permafrost is widespread in high latitudes and in high-elevation regions (Zhang et al., 2007). The permafrost regions cover about a quarter of the terrestrial Northern Hemisphere (Zhang et al., 1999; Wu et al., 2009) and permafrost is one of the key components of terrestrial ecosystems in cold regions (Yang et al., 2010). Permafrost is primarily defined as soil that remains at or below 0 °C continuously for two or more years (Muller, 1974) (Figure 7). The phenomenon is defined by soil temperature and has nothing to do with the ice or water content of the soil. The ice within the permafrost, formed out of subcooled water, is only the consequence. Accordingly, dry permafrost is also found (Vonder Mühll et al., 2001).

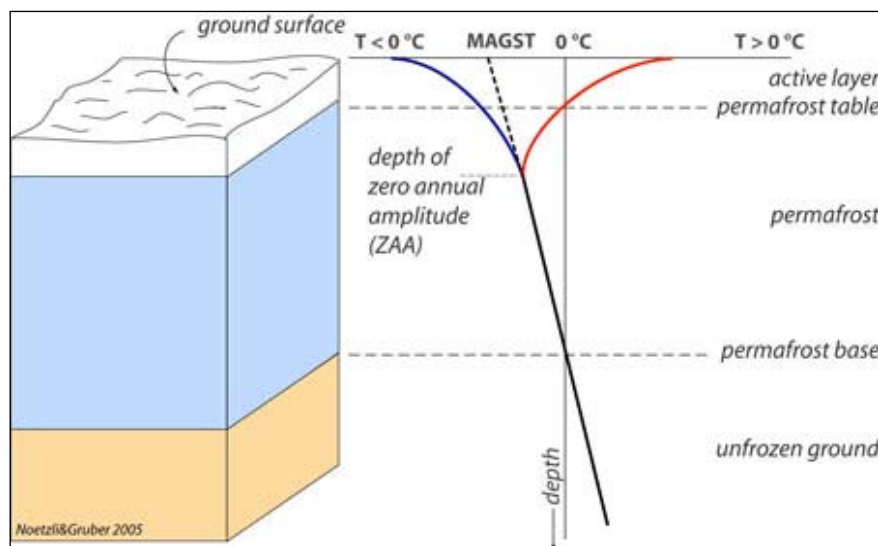


Figure 7 Schematic plot of permafrost (important terms) (Source: Permos).

Permafrost at any point in time is a product of both the present climate and of warmer and colder climates that dominated during changes over the past hundreds of thousands of years (Péwé, 1975). Contemporary permafrost formation differs in the continuous and the discontinuous permafrost zones. Permafrost occurs on all exposed soil surfaces in the continuous permafrost zone independent of the ecosystem structure, but it only forms during late-successional stages of ecosystem development in the discontinuous zone (Shur & Jorgenson, 2007). Simplified, the process of the formation of permafrost can be explained in the following way: If the cold that were stored in the soil during winter is not fully compensated in summer, the temperatures below a certain depth (permafrost table) remain colder than 0°C. Only the upper part, the active layer, record temperatures above freezing point. The actual permafrost can be found beneath this layer (Vonder Mühll et al., 2001).

In the Alps discontinuous permafrost distribution is a function of the altitude and exposure. It can be assumed that permafrost has the potential to occur in northerly exposed areas above an altitude of

2400m asl, and on south-facing sites above 3000m asl (Nötzli and Gruber, 2005). Due to local microclimates, sporadic permafrost can exist below the timberline at deeply shaded sites (Kneisel et al., 2000). In the south-eastern part of Switzerland permafrost has been present in areas above 1950m asl on northerly exposed slopes and above 2450m asl on south-facing slopes in the Younger Dryas (late Pleistocene). This means that permafrost was prevalent 500m to 600m below the present-day limits of discontinuous permafrost (Zollinger et al., 2013).

Source of permafrost degradation

Climatic change can affect permafrost directly or indirectly through changes in air temperature and soil heat conduction (Jorgenson et al., 2001). In most situations, however, climate change only has an indirect impact on permafrost, since permafrost is a component of a complex geo-ecological system with both positive and negative feedbacks associated with vegetation succession and changing soil properties. Furthermore, climate-ecosystem interactions differ between continuous, discontinuous and sporadic permafrost zones (Shur & Jorgenson, 2007). Shur and Jorgenson (2007) described five different patterns of permafrost formation: (1) climate-driven; (2) climate-driven, ecosystem-modified; (3) climate-driven, ecosystem-protected; (4) ecosystem-driven; and (5) ecosystem-protected permafrost. These distinctions are important because the various types react differently to climate change and surface disturbances (Shur & Jorgenson, 2007).



Figure 8 Permafrost degradation and thaw settlement in Alaska (Source: NGEE).

The process of permafrost degradation

Permafrost degradation refers to a decrease in the thickness and/or areal extent of permafrost. These changes can be caused naturally or artificially. Evidence has been found of a shifting in the southern edge of the discontinuous permafrost zone in the past decades (Halsey et al., 1995). When the top of the permafrost warms up, this heat eventually penetrates to the base of the permafrost. If the new surface temperature remains stable, thawing at the base of the ice-bearing permafrost occurs (i.e. basal thawing). This applies especially to thin discontinuous permafrost (Lemke et al., 2007). In regions influenced by ice-rich permafrost thawing, the ground surface caves in. This downward shifting pro-

cess is called thaw settlement. Since thaw settlement does not occur in a uniform manner, the result is a chaotic surface with small hills and wet depressions known as thermokarst terrain (Figure 8). Thermokarst processes pose a serious threat to arctic biota through either oversaturation or drying (Hinzman et al., 2005; Walsh et al., 2005). On slopes the thawing of ice-rich, near-surface permafrost layers can create mechanical discontinuities in the substrate, leading to active-layer detachment slides (Lewkowicz, 1992), which have the capacity to damage structures in the same way that other types of rapid mass movements do.

Consequences of permafrost degradation

The thawing of ice-rich permafrost can lead to a subsiding of the soil surface as a consequence of the masses of ground-ice melting. This process can lead to the formation of an uneven topography known as thermokarst, generating dramatic changes in ecosystems, landscape, land use and infrastructure performance that rely on permafrost for its foundation (Nelson et al., 2001; Walsh et al., 2005; Osterkamp, 1983; Osterkamp et al., 1998).

Consequences of melting permafrost are often closely linked to glacier melting. A serious threat is, for instance, the appearance of large quantities of unconsolidated, unvegetated sediments as a consequence of general glacier retreat and permafrost degradation (Kääb et al., 2007). Deeply frozen rock walls destabilize and impact waves caused by high-magnitude rock falls and landslides into new lakes forming in de-glaciating high-mountain ranges increase the danger of flooding (Haeberli, 2013).

Understanding glacier and permafrost changes is equally important because of their impact on human life and the environment. These changes have a crucial influence on the water cycle in cold mountains and their surrounding lowlands, on landscape evolution and tourism, and – in this instance of particular concern – can cause glacier- and permafrost-related hazards (Kääb et al., 2007).

1.3 Aim of the study and hypotheses

The aim of the study was to explore the effect of different soil and environment parameters on the susceptibility of the soil to erosion and surface runoff. The focused question was whether the degradation of permafrost significantly influences the soil's susceptibility to erosion. Rainfall simulations were therefore conducted on soil plots with permafrost influence and also on plots without permafrost influence, while various factors which could also affect the amount of soil erosion and surface runoff were also recorded. Surface runoff and sediment yield were collected on the downhill side of the plot and evaluated in the laboratory. The plots were selected according to whether they were influenced by permafrost (50%) or not (50%) and according to their varied slopes and vegetation cover.

In the context of the present master thesis the following hypotheses were tested:

Hypothesis 1

There is a significant difference in susceptibility to soil erosion (sediment yield and surface runoff) between soil with permafrost and soil without permafrost.

Hypothesis 2

Independent of the influence of permafrost, a decrease in soil erosion (sediment yield and surface runoff) is expected with increasing vegetation cover and decreasing slope.

An additional aim was to generate soil maps of the two study sites. Soil investigations were therefore made in the field and afterwards applied digitally on a map.

2 Material and methods

2.1 Study Sites

The rainfall simulations for the present master thesis were conducted at two different study sites. Both sites were located in the Canton of Grisons in the south-eastern part of Switzerland. In the present master thesis they are named Spinas and Bever (Figure 9).

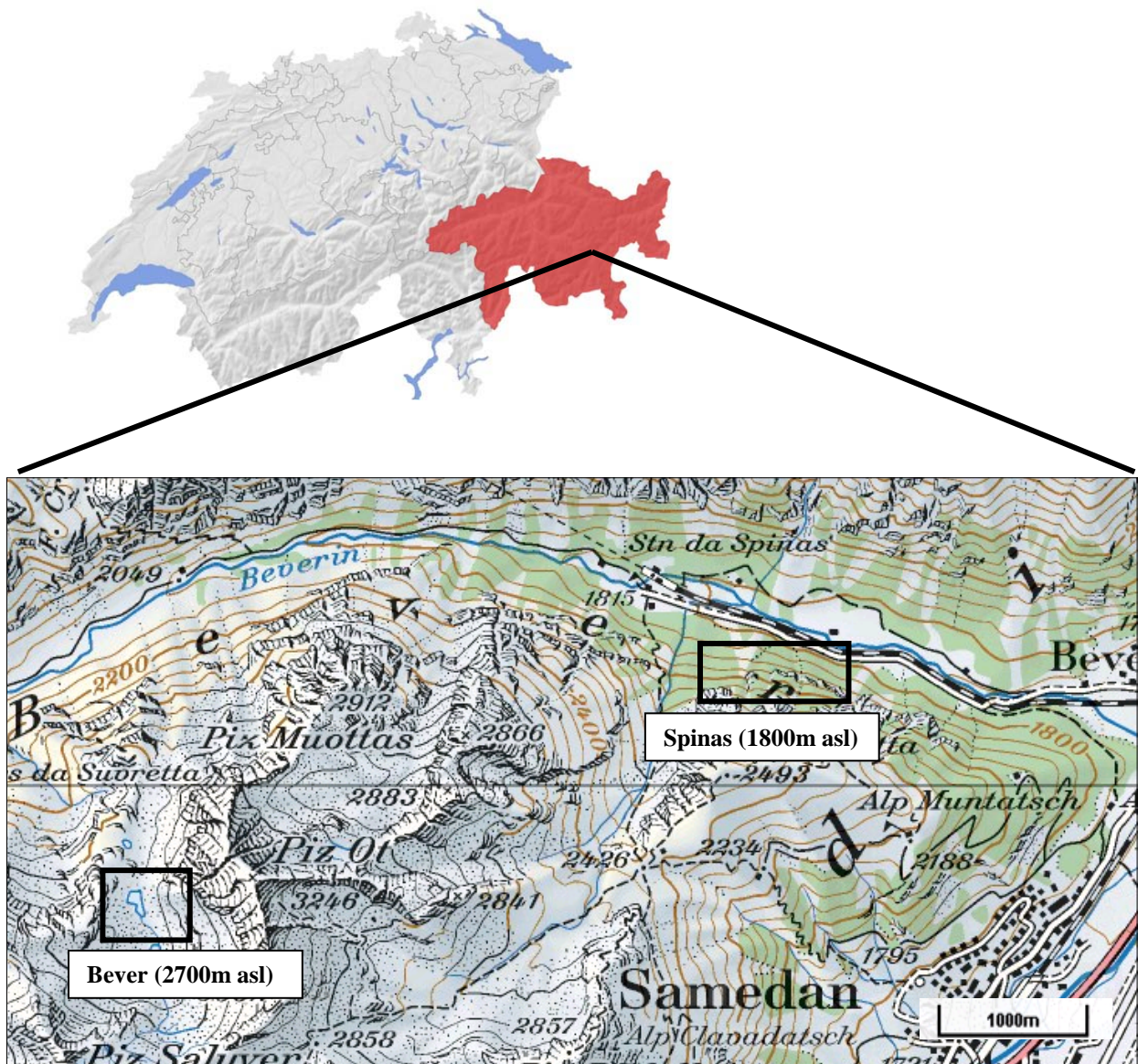


Figure 9 Overview of Switzerland and the Val Bever with the two study sites (Source: geo.admin).

The choice of these specific study areas was determined by the PhD project of Barbara Zollinger at the University of Zürich. This ongoing study on “The chemical weathering and soil erosion in the south eastern part of Swiss Alps” is supported by the DACH countries (Deutschland, Österreich, Schweiz), and a collaboration between the three countries Germany, Austria and Switzerland. In this study the chemical weathering, the organic carbon and the soil erosion of permafrost-influenced soil and non-permafrost soil are investigated with different scientific methods.

Spinas

The lower subalpine study site is situated in the Val Bever, a tributary valley of the Upper Engadine, and is about 4 km from the village Bever in the eastern Swiss Alps (Figure 10). The Bever Valley is a trough-shaped valley with an elevation of 1730 m asl to 1800 m asl at its lower end. The regional climate is quite continental with rather low precipitation and a comparatively high temperature range. Mean annual precipitation is 1050 mm and the mean annual air temperature (MAAT) is 1°C (Schwarb et al., 2000).



Figure 10 Map of the lower study site Spinas (Source: geo.admin).

The rainfall simulations were performed on 20 different soil plots on a northerly exposed scree slope (1780 m asl, 46°33'N, 9°51'E) (World Geodetic System (WGS84)) covered by conifers (*Larix deciduas*, *Pinus cembra*) (Figure 13). Most of the study site is well covered with vegetation. The soil is poorly developed and covered by an organic layer that is up to 30 cm thick. Below the organic layer there are only a few centimeters of mineral soil (Kneisel et al., 2000) with granite-rich slope deposits (Zollinger et al., 2013). The steep and rocky valley walls are incised by distinct rock couloirs and torrents which form part of the starting zones of several minor debris flows. Recent morphodynamics also include rock falls and snow avalanches (Kneisel et al., 2000). This specific slope has been the subject of previous studies investigating the permafrost occurrence in this area.

Below the timberline permafrost is assumed to exist only in deeply shaded sites, according to Haeberli's "rule of thumb" for predicting mountain permafrost (1975). A permafrost occurrence in terms of isolated permafrost lenses has been confirmed and characterized (see Kneisel & Hauck, 2003) in this study site at the low altitude of 1780m asl. It was assumed that this permafrost occurrence is a result of the interaction of climatic conditions and topography as well as surface and subsurface factors. The organic layers were considered to play an important role in insulating the subsurface and controlling the ground thermal regime (Kneisel et al., 2000). Indications are that the ground thermal regime of this site is not particularly dependent on weather conditions, but mainly driven by seasonal air circulation between the blocks, the so-called chimney effect (Punz et al., 2005; Harris & Pedersen, 1998). According to the patterns of permafrost formation described in chapter 1.2.5, this would be an ecosystem-driven permafrost formation (see Shur & Jorgenson, 2007).

The following figures show a permafrost-influenced soil profile (Figure 11) and one without permafrost (Figure 12) at the study site Spinas. One can see the coarse blocks of rock in the soil profile.



Figure 11 Soil profile at Spinas with permafrost (Source: B. Zollinger).



Figure 12 Soil profile at Spinas without permafrost (Source: B. Zollinger).



Figure 13 Picture of the scree slope at Spinas (Source: P. Polich).

Bever

The upper study site, Bever, is situated at 2800 m above sea level, next to the Piz Ot, on the glacier forefield of the melted Vadret Palüd Marscha glacier (2700 m asl, 46°54'N, 9°80'E), and beyond the timberline (Figure 14). The prevailing climate can be described as alpine as well as somewhat continental, with cold winters and cool summers. The climate is characterized by a mean annual temperature of $-2.6\text{ }^{\circ}\text{C}$ and a mean annual precipitation of $>1000\text{ mm}$. According to the Köppen-Geiger classification the climate is defined as an ET-climate (Kottek et al., 2006).

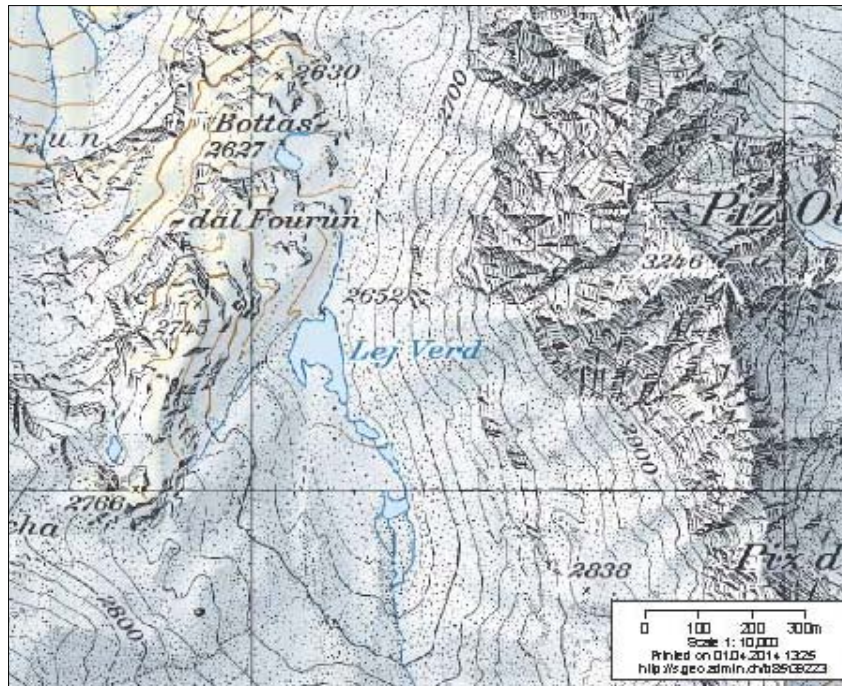


Figure 14 Map of the upper study site, Bever (Source: geo.admin).

The melting glacier left behind a glacier lake (Lej Verd), which is situated between steep slopes and former moraines. The soils are quite acidic, with a measured pH value of 3.7-4.8. The moraine of 1850 and several other sections of the slopes are still influenced by permafrost. In these cases the vegetation cover is often underdeveloped, and the soil is coarse and poorly mineralized (see Figure 17). The glacial till deposited in this area consists of granite/gneiss (Julier Granite) (Zollinger et al., 2013). In permafrost-free areas the vegetation cover is denser than on permafrost and the soil is brown colored. The vegetation can be described as alpine tundra, dominated by grasses and herbaceous plants (*Caricetum curvulae*, *Geomontani-Nardetum* (curved sedge)) (Zollinger et al., 2013).

The pictures below show a typical soil profile with permafrost (Figure 15) and one without permafrost (Figure 16) at the study site Bever.



Figure 15 Soil profile at Bever with permafrost (Source: B. Zollinger).



Figure 16 Soil profile at Bever without permafrost (Source: B. Zollinger).



Figure 17 Slope at Bever with sparse vegetation cover (Source: P. Polich).

2.2 Experimental design

For the collection of the erosion data, 60 rainfall simulations on different soil patches were performed over a three month period between June 2013 and August 2013. Twenty simulations were done at the lower study site Spinass and forty at Bever.

In order to investigate the validity of the first hypothesis, the soil patches had to be equally distributed in areas with permafrost-affected soil (50%) and areas not affected by permafrost (50%). In addition to that, features such as vegetation cover (%) and slope inclination (°) had to be variable. Several soil parameters were also measured (see chapter 2.5) to explore their possible influence on the surface runoff and sediment yield. It was also attempted to conduct all rainfall simulations during more or less constant weather conditions, so that the prerequisites would be as similar as possible during every simulation.

In total the data sets of the two study sites include 60 point scale measurements of surface runoff and sediment yield. Some characteristics of every investigated soil plot were also recorded.

Spinass

At Spinass the slope varied between 10° and 25°, while the vegetation cover varied between 0% and 100%. The rainfall simulations were performed on three different sub-areas on the slope with different types of vegetation covers: one with conifers, moss and dwarf shrub on massive rock, a second with light forest and moss on the topsoil, and the last subarea sparsely covered by trees or grass.

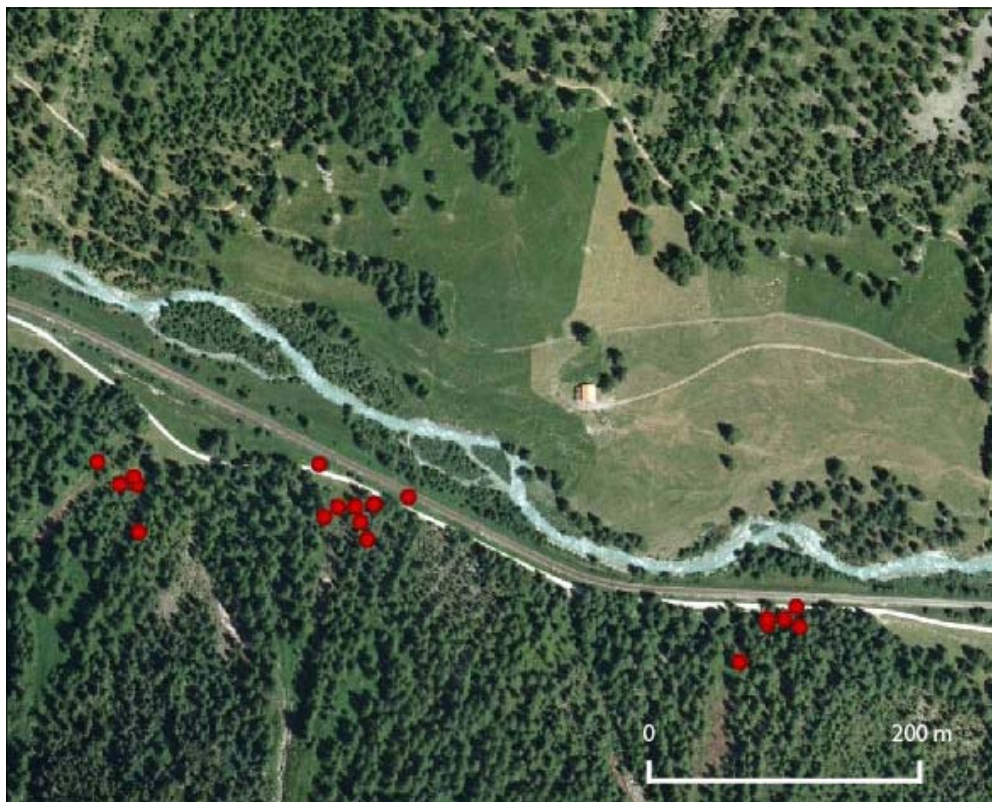


Figure 18 Visual presentation of areas at Spinass where rainfall simulations were conducted, indicated by GPS way points (Source: Google earth).

Figure 18 shows the GPS way points of every investigated soil plot. Even though the GPS measurements in the forest were not very accurate (± 8 m), one can recognize the general distribution and the three sub-areas at the study site Spinass.

Bever

At Bever the 40 rainfall simulations were performed on slopes on the western shore of the glacial lake Lej Verd. These slopes were covered with either vegetation and brown topsoil or coarse gravel without any vegetation cover. The slope inclination varied between 5° and 30° , and the vegetation cover between 0% and 100%.

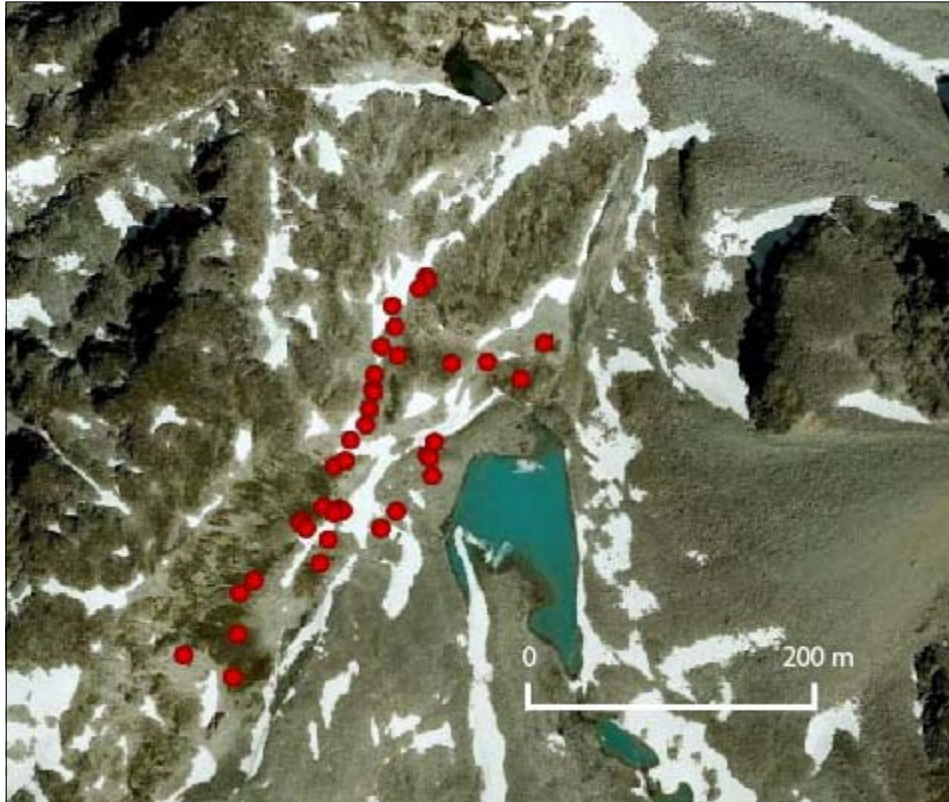


Figure 19 GPS way points indicating rainfall simulation sites at Bever (Source: Google earth).

In Figure 19 the distribution of the investigated soil plots at the study site Bever can be seen.

2.3 Eijkelkamp rainfall simulator

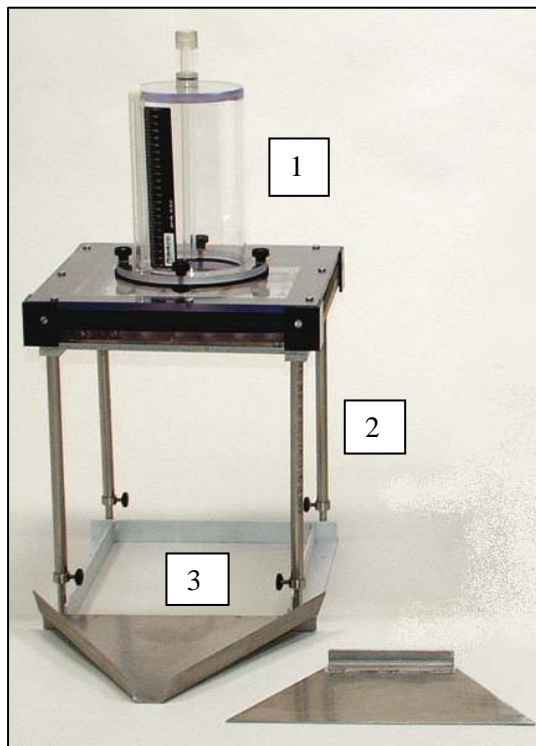


Figure 20 Eijkelkamp rainfall simulator (Source: Eijkelkamp).

A rainfall simulator allows the creation of an artificial precipitation event and the simultaneous control of many relevant factors such as intensity, energy and duration.

The 09.06 rainfall simulator of Eijkelkamp Agrisearch was used for the erosion measurements in this study (Figure 20). This gadget generates a standardized rain shower over a standard surface area of 25cm×25cm and allows the measurement of sediment yield and surface runoff by collecting the erosion products with a gutter. Essentially, the rainfall simulator consists of three parts: (1) the sprinkler head, (2) an adjustable support for the sprinkler and (3) an aluminum ground frame (see chapter 2.4). The water for the rainfall simulation is stored in a portable water tank. Water supply for the study was guaranteed because of the proximity of Lej Verd (at Bever) and the stream Beverin (at Spinus) to the study sites.

On every investigated soil patch, a rainfall simulation with the intensity of 375mlmin^{-1} (360mmh^{-1}) and duration of 3 minutes was applied, resulting in a 1125ml rain shower. The discharge rate of 375mlmin^{-1} was suggested by Eijkelkamp (2005) to generate representative measurements.

Technical specifications of the Eijkelkamp rainfall simulator (Eijkelkamp, 2005)

Surface area of test plot:	0.0625 m^2
Average fall height of test plot:	400 mm
Diameter of drops:	5.9 mm
Mass of drops:	0.106 g
Number of papillary tubes for drops:	49
Intensity of rainfall simulations:	360 mm h^{-1}

2.4 Rainfall simulation procedure

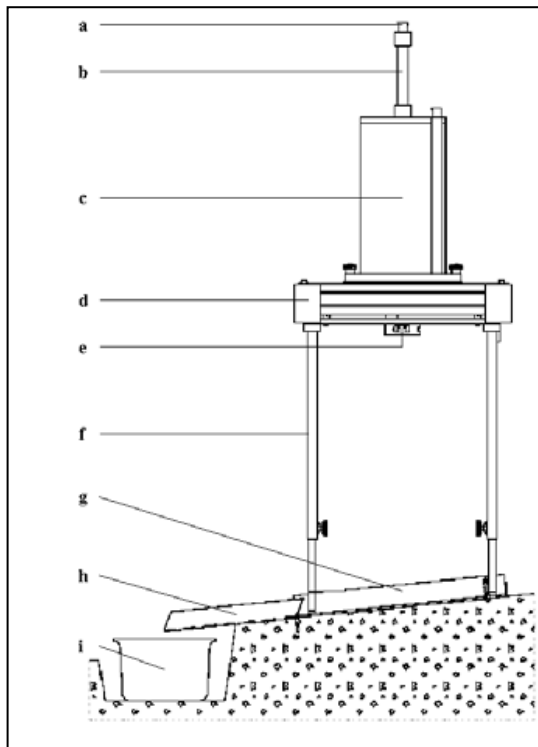


Figure 22 Rainfall simulator (Source: Eijkelkamp).



Figure 21 Rainfall simulator installed at the study site Spinas (Source: P. Polich).

- | | |
|-------------------------------|--------------------------|
| a: plug | f: adjustable support |
| b: aeration pipe | g: ground frame |
| c: reservoir | h: gutter |
| d: sprinkler (49 capillaries) | i: sample collection box |
| e: bubble levels | |

In order to measure the surface runoff and the sediment yield, an Eijkelkamp rainfall simulator was used (Figure 21). With the rainfall simulator one measures the runoff and soil loss generated by a standardized rain shower on a plot with a standard surface area. The duration, intensity and kinetic energy of the shower results in a high sensitivity for differences in soil properties in the test results (Eijkelkamp, 2005).

In a first step the aluminum ground frame (g) was installed solidly on the ground with 4 nails. This frame set the boundaries of the investigated plot and also prevented the lateral movement of water from the test plot to the surrounding soil. The triangular gutter (h) was placed on the downhill side of the frame to collect the surface runoff and sediment yield and to transfer it into the sample collection box (i), which was placed in a small excavated hole. In order to prevent the loss of runoff and sediment into the resulting gap between soil patch and gutter, this gap was sealed with synthetic modeling clay (see Figure 22).

In a next step a picture of the plot was taken and the soil parameters, indicated in chapter 2.5, was recorded. After these preparations, the support (f) for the rainfall simulator was installed on the ground frame. The two bubble levels (e) on this support ensured a perfectly horizontal setup. The height of the aeration pipe (b) on top of the water tank can be varied. In this way the amount of water coming out of

the tank during a rainfall simulation can be controlled. The pressure head on the capillaries can be increased or decreased by moving the aeration tube (b) upward or downward. The magnitude of this pressure head regulation is sufficient to correct the influence of the viscosity of the water used on the discharge rate of the capillaries. It is meant to control the intensity of the required standard shower (Eijkelkamp, 2005). The appropriate height h of the aeration pipe has to be calculated according to a formula that includes the current air temperature:

$$h = 100\text{mm} - 0.65 * \text{air temperature } (^{\circ}\text{C}) \text{ (Eijkelkamp, 2005).}$$

After this the sprinkler head (a-d) was filled with water and placed on top of the support. The sprinkler head consists of a calibrated cylindrical reservoir (c) which has a capacity of approximately 2300ml and is directly connected to the sprinkler (d) (Eijkelkamp, 2005). The water level in the reservoir (c) was noted before and after every simulation, in order to make sure that the amount of the sprinkled water was the same in each case (approx. 1125ml). The rainfall simulation was started by removing the plug (a) from the aeration pipe (b). The duration of the simulation was measured with a stop watch. During the three minutes of the rainfall simulation the sprinkler head (a-d) was moved slowly in the horizontal level in order to ensure an equal distribution of sprinkling across the investigated plot. After three minutes the simulation was stopped and the collection box (i) with the surface runoff and sediment yield was sealed, labeled and indexed.

After each replicated event duplicate samples of undisturbed soil was collected from the topsoil of the investigated patch in order to examine soil properties (see chapter 2.6.2).

2.5 Plot survey

As stated in the last chapter, several soil parameters were investigated on every plot before the rainfall simulations were conducted. The different soil parameters are listed below.



Figure 23 Plot survey (GPS measurement) of plot 22 at Bever (Source: P. Polich).

pH value

The pH of the topsoil was determined twice, at first in the field and then in the laboratory (see chapter 2.6) for a more precise result. A simple pH meter (Hellige) was used in the field. It consists of a plate with a dent and a color scale, as well as the Hellige pH indicator solution. By mixing a small soil sample with the indicator solution, the pH value can be estimated by comparing the color of the indicator with the color scale.

Vegetation cover and soil texture

The vegetation cover (%) and the soil texture (gravel content %) were roughly estimated, by sight. To do this a hole was dug and the exposed soil compared to a graphic illustration of different degrees of surface coverage.

Slope and exposition

The slope (inclination in °) of each plot was measured with a clinometer. For this purpose, the measuring instrument was positioned next to the ground frame of the rainfall simulator. The exposition (° N) was also determined with the clinometer.

Position

The exact position of each plot was measured with a global positioning system (GPS). The coordinates and the altitude above sea level were recorded in this way (Figure 23).

Permafrost

Another important characteristic was whether the measurement points were on permafrost-influenced soil or not. The two study sites were also used in two other research studies. The first one was carried out by the University of Würzburg, and in that study the permafrost was detected with geo-electric measurements. The other research study is a PhD project at the University of Zürich, where soil temperatures were measured with a temperature logger at several points at the study sites and over a period of more than a year. Building on the results of these studies one could estimate the distribution of permafrost at the two study sites.

Physical properties of the soil

In order to measure (1) the temperature of the soil, (2) its water conductivity and (3) the moisture in the soil before the rainfall simulation, a measurement with a Time-Domain Reflectometer (TDR) was conducted in the immediate radius of the investigated plot. In this way potential falsifications due to infiltration of the simulated rain into the insertion holes of the measurement probe inside the soil patches could be prevented. The same measurement was also taken after the rainfall simulation within the plot, which made monitoring the change inside the soil possible (its ability to absorb water).

Soil samples

In addition to the parameter recording described above, two soil samples of the topsoil (Ah-horizon) were taken at every measurement point. In the end 120 soil samples were analyzed in the laboratory (see chapter 2.6). Since there were two soil samples per investigated soil patch, one could always calculate the mean between the values of the two soil samples. This makes the results more representative.

The results of these plot surveys, shown as diagrams, can be seen In “Appendix A: Illustrations of the plot survey”.

2.6 Laboratory work and data preparation

The collected erosion, runoff and soil samples were evaluated at the University of Zürich, and a clearer picture and more information about the different soil types at the two study sites Spinas and Bever was obtained.

2.6.1 Sediment yield and runoff measurement

In this study the “change in weight” method was applied to analyze the point scale measurements of interrill water erosion. This method enables the collection of detachment through rain splash erosion, so that it can be weighed at a later stage (Stroosnijder, 2005). Runoff and sediment yield of each rainfall simulation was collected in a sample collection box on the downhill side of the investigated soil plot. The collection boxes were weighed (1) before the simulations (deadweight) and (2) after the runoff and the sediment yield had been collected. Then the collection boxes were put in a drying cabinet for 24 to 48 hours at a temperature of 70 °C so that the fluid runoff could evaporate. They were then weighed for a (3) third time.

Surface runoff was then calculated by subtracting the deadweight and the dry sediment (3) from the weight of the collection box containing runoff and sediment (2). Sediment yield was calculated by subtracting the deadweight (1) from the weight after evaporation (2).

2.6.2 Soil Samples

The 120 topsoil samples collected at the 60 soil patches rested for 24 hours in a drying oven at a temperature of 100°C, so that the water content was reduced to a minimum.

Ratio: coarse grained and fine grained

A subject of interest was also the size distribution of the topsoil in the two study sites. Two size fractions were obtained in order to determine the ratio between the coarse grained and the fine grained fraction. The soil samples were weighed after the drying process. Subsequently the dry samples were sieved with a 2mm filter and the exact weight of the fine grained portion (<2mm) was noted. The weight of the coarse grained fraction was calculated by subtracting the weight of the <2mm fraction from the dry weight of the soil samples.

PH value measurements

The pH value of the soil samples were measured in the field and at a later stage also in the laboratory. Therefore the fine grained particles (<2mm) were mixed with a 0.1 mole CaCl₂-Solution in a proportion of 1 to 2.5. Some samples with a large amount of organic matter had to be mixed in a proportion of 1 to 5, otherwise the solution would have been completely absorbed by the soil particles. These mixtures were stirred with a magnetic mixer for 20 minutes and then left to rest for another 20 minutes. After these preparations, each solution was measured with a calibrated pH-measuring instrument.

Ratio: carbon and nitrogen

For the determination of the ratio between carbon (org. C) and nitrogen (N_{tot}) the fine grained fraction (<2mm) of the dried soil samples were analyzed at ZHAW (Zürcher Hochschule der angewandten Wissenschaft) in Rapperswil. The amount of hydrogen (H), carbon (C) and nitrogen (N) in a 0.1g soil

sample was detected by means of a combustion process. The percentages of the components could easily be transferred to the required C-N-ratio.

The collected data regarding the size distribution, the pH measurement and the CHN-measurements were stored in *Microsoft Office Excel*. The average between the values of the two soil samples was then calculated. By collecting duplicate soil samples for the determination of an average value, the reliability of the particular values was enhanced.

2.7 Statistical analyses

For the validation of the study hypothesis, the collected data were analyzed statistically with the statistics program *Statistical Package for the Social Science (SPSS)*. In hypothesis 1 the difference between two variables (permafrost and non-permafrost) had to be tested. For this the T-test for Independent Samples (normal distribution required) or the Man-Whitney U-test (no normal distribution required) could be applied. In hypothesis 2 the relation between two variables (surface runoff / sediment yield and slope / vegetation cover) had to be verified. For that reason a correlation analysis was conducted.

For this master thesis the following levels of significance were used (Table 1):

Table 1 Explanations of the levels of significance.

marginally significant	low presumption against null hypothesis	$0.1 > P \geq 0.05$
significant	presumption against null hypothesis	$P = 0.05$
highly significant	strong presumption against null hypothesis	$P < 0.01$
very highly significant	very strong presumption against null hypothesis	$P < 0.001$

The p-value or calculated probability of the statistical tests is the estimated probability for rejecting the null hypothesis (H_0). In scientific studies the null hypothesis will often be rejected when the p-value turns out to be less than a certain significance level (0.05). In the following results of the statistical tests the calculated p-value is indicated as “Sig. (2-tailed)”.

Hypothesis 1

In hypothesis 1, a significant difference in sediment yield and surface runoff was predicted between permafrost soil and non-permafrost soil. In order to test this statement, a Kolmogorov-Smirnov Test (K-S Test) had first of all to be done to see whether the data were normally distributed.

In the case of a normal distribution (Spinas: sediment yield, surface runoff; Bever: surface runoff), the T-test for Independent Samples was applied. When the K-S Test showed non-normal distribution, a Mann-Whitney U-test was applied instead.

Hypothesis 2

Hypothesis 2 claims a correlation between the amount of sediment yield and surface runoff, and the slope inclination (°) and vegetation cover (%). This proposition was tested with a bivariate correlation analysis. Because other factors besides the two factors of slope and vegetation were of interest, other variables were tested as well. These variables were: (1) the gravel content (%) of the soil, (2) the moisture difference of the soil (difference between TDR measurement before and after the rainfall simulation), (3) the soil moisture before the rainfall simulation, (4) the ratio between fine grained and coarse grained soil particles, (5) the average amount of carbon in the soil and (6) the ratio between carbon and nitrogen. In this way a broad overview of the different soil variables and their influence on soil erosion could be established.

Data preparation

The first attempt at correlation analysis did not show convincing results. In order to generate a more significant and meaningful result as well as to see whether the outliers distorted the outcome, the outliers were eliminated. These outliers were located by means of a box plot which showed the distribution of the data as well as the outliers. At Spinas (see Figure 26 in chapter 3.1.1) the data of sediment yield were more or less uniform. Only in the box plot of the surface runoff one can see two striking outliers (see Figure 28 in chapter 3.1.2).

The following outliers were removed from the data set of Spinus (Table 2):

Table 2 Outliers removed from the dataset of Spinus.

Surface runoff (ml)	Sediment yield (g)
21.84	0.06
65.92	0.02

At the study site Bever the distribution of neither of the data variables (sediment yield and surface runoff) was uniform (see Figure 28 in chapter 3.1.1 and Figure 30 in chapter 3.1.2).

In the case of Bever the following four extreme outliers were removed (Table 3):

Table 3 Outliers removed from the dataset of Bever.

Surface runoff (ml)	Sediment yield (g)
430.56	3.44
809.18	11.63
585.54	0.56
129.06	3.01

2.8 Soil cartography

Aerial photographs and a map of the two study sites Spinas and Bever served as a starting point for the soil maps. By means of the spatial variations on the photograph of the study sites possible soil orders were classified according to the FAL (Eidgenössische Forschungsanstalt für Agronomie und Landbau) system (Brunner et al., 1997) and noted in the form of separated polygons on the map (Figure 24). These assumptions were then reviewed and corrected by means of a field investigation (by Markus Egli). Approximately 100 small soil core drillings were made and used as reference profiles for mapping. The resulting soil maps already contained a certain generalization. Small scale variations could not be considered.

The verified soil maps were then digitalized with ArcGIS, software by Esri for mapping and analyzing (Figure 25). The joined table of content included (1) soil order, (2) soil depth, (3) parent material, (4) vegetation, (5) topography, (6) soil hydrology, (7) terrain form, (8) pH value, (9) organic carbon content, (10) soil skeleton, (11) granulometry, (12) aggregates and (13) humus form.

For better visualization, the different soil orders were then colored and exported into a soil map (Figure 26).

In the following figures one can see the three steps in the production of the soil maps of Spinas, as described above. Figure 24 shows an extract of the first draft that was afterwards verified in the field. Figure 25 shows the outlines of the polygons digitalized with ArgGIS and in Figure 26 the polygons were joined with the attribute table and the polygons were colored in specific colors for each soil order.

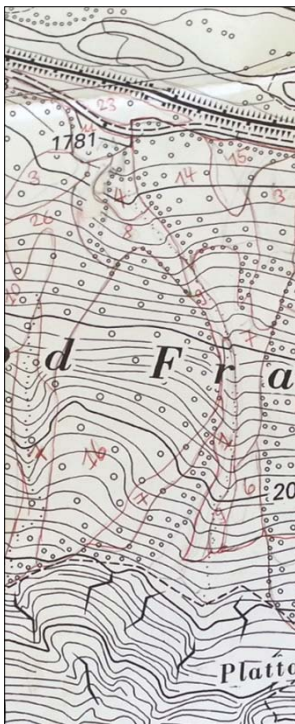


Figure 24 Step 1
(Source: P. Polich).

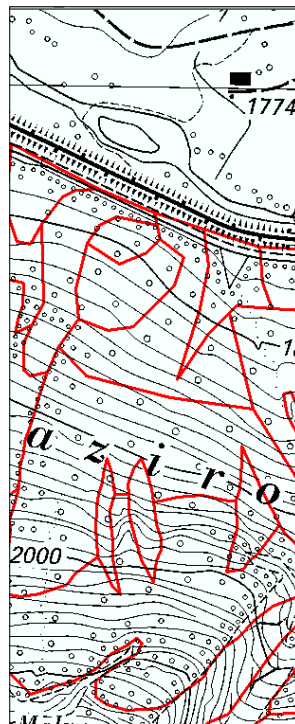


Figure 25 Step 2
(Source: P. Polich).

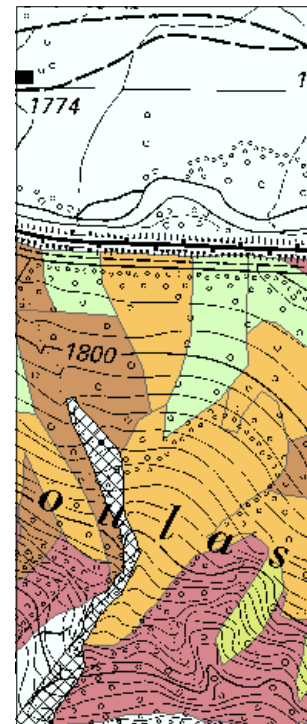


Figure 26 Step 3
(Source: P. Polich).

3 Results

3.1 General results

In this chapter some general results of the dataset are summarized without undertaking a close examination of the two hypotheses.

3.1.1 Sediment yield

In the figures below one can see the general data distribution of the sediment yield at Spinas (Figure 27) and Bever (Figure 28) in terms of box plots generated with SPSS.

Box plots serve as a quick way of graphically examining a set of data by showing their distribution. Box plots are non-parametric. The spacings between the different parts of the box help to indicate the degree of dispersion (spread) and skewness in the data and to identify outliers.

The brown boxes of the box plots comprise the 25% and the 75% quartiles and therefore contain 50% of all the data. The black horizontal bar in the middle of the box represents the median. Error bars show the smallest as well as the biggest value that were not defined as outliers. Outliers and extreme values are represented as points and asterisks. A data point is defined as an outlier (°) as soon as it is situated more than 1.5 block lengths away from the 75% resp. 25% quartile. An extreme value (*) is therefore a data point situated more than 3 block lengths away from the quartiles.

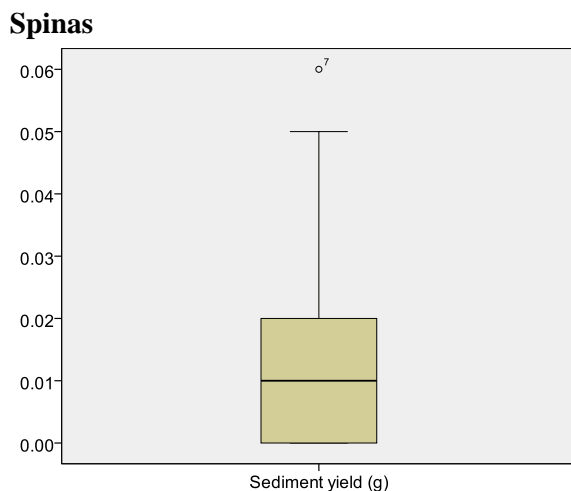


Figure 27 Box plot of the sediment yield at Spinas (SPSS).

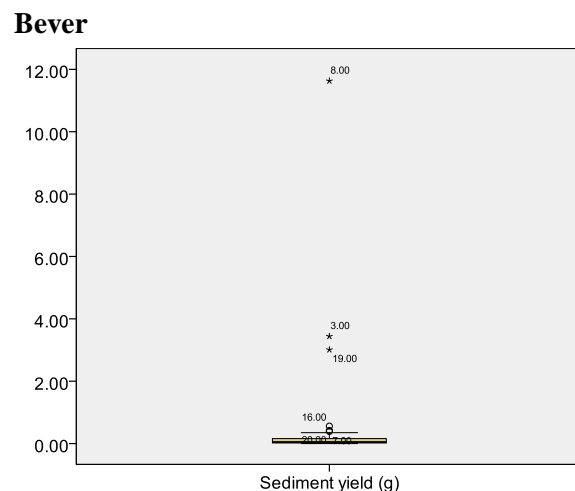


Figure 28 Box plot of the sediment yield at Bever (SPSS).

At Spinas the mean of the measured values of sediment yield were 0.015 ± 0.004 g (on a $25\text{cm} \times 25\text{cm}$ patch). This would be 0.24 g m^{-2} . After the removal of the outliers, the mean of sediment yield at Spinas was 0.012 ± 0.004 g. This corresponds with 0.1952 g m^{-2} .

At Bever the raw data show a mean of 0.54 ± 0.30 g (8.72 g m⁻²) and the dataset without outliers a mean of 0.09 ± 0.02 g (1.4 g m⁻²).

Generally one could see a larger amount of sediment yield descending at the study site of Bever (Table 4).

Table 4 Amount of sediment yield (raw data and without outliers) at Spinas and Bever.

	Spinas	Bever
Mean: sediment yield (raw data)	0.24 g m ⁻²	8.72 g m ⁻²
Mean: sediment yield (without outliers)	0.19 g m ⁻²	1.4 g m ⁻²

The SPSS outputs of the descriptive statistics of the datasets described above can be seen in chapter 8.2.

3.1.2 Surface runoff

In the figures below one can see the general data distribution of the sediment yield in Spinas (Figure 29) and Bever (Figure 30) in terms of box plots generated by SPSS.

Spinas

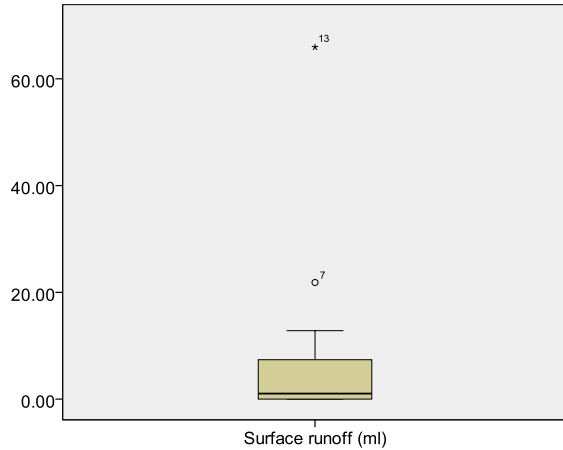


Figure 29 Box plot of the surface runoff at Spinas (SPSS).

Bever

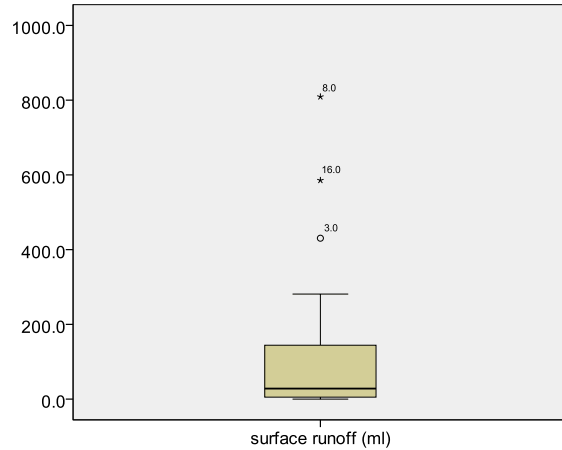


Figure 30 Box plot of the surface runoff at Bever (SPSS).

At Spinas the mean of the measured values for the surface runoff was 7.00 ± 3.36 ml (on a $25\text{cm} \times 25\text{cm}$ patch). This would be 16.01 ml m^{-2} . After the removal of the outliers, the mean of surface runoff at Spinas was 2.90 ± 0.97 ml, which corresponds with 46.44 ml m^{-2} .

At Bever the raw data showed a mean of 110.84 ± 26.98 ml g ($1773.47 \text{ ml m}^{-2}$) and the dataset without outliers a mean of 68.87 ± 14.27 ml ($1101.92 \text{ ml m}^{-2}$).

To sum up, the surface runoff at the study site Bever was generally higher than at Spinas (Table 5) (analogous to the sediment yield).

Table 5 Amount of surface runoff (raw data and without outliers) at Spinas and Bever.

	Spinas	Bever
Mean: surface runoff (raw data)	16.01 ml m^{-2}	$1773.47 \text{ ml m}^{-2}$
Mean: surface runoff (without outliers)	46.44 ml m^{-2} .	$1101.92 \text{ ml m}^{-2}$

The SPSS outputs of the descriptive statistics of the above described datasets can be seen in chapter 8.2.

3.1.3 Correlation: surface runoff and sediment yield

An interesting question is whether the amount of surface runoff and sediment yield in the measurements correlate with each other. Therefore the following graphs are shown.

3.1.3.1 Spinus

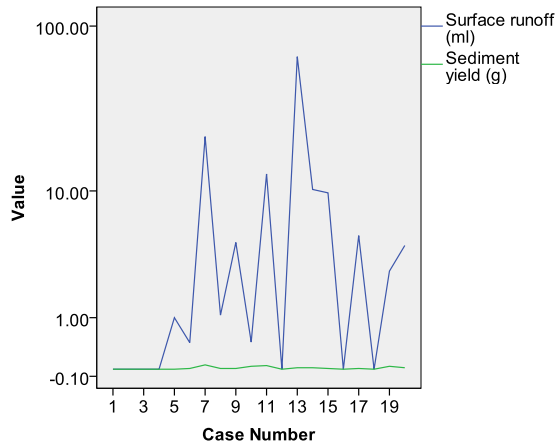


Figure 31 Amount of surface runoff (ml) and sediment yield (g) at Spinus (SPSS).

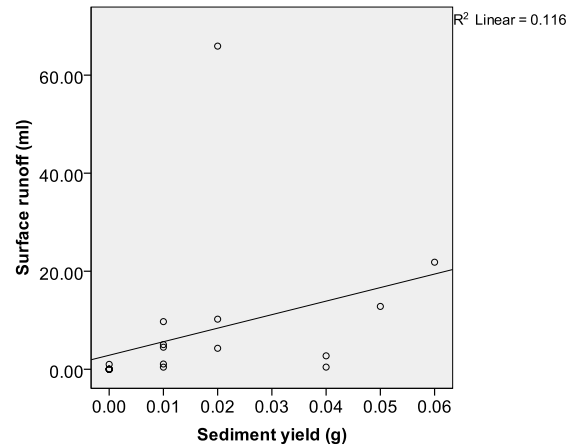


Figure 32 Scatter plot of surface runoff (ml) and sediment yield (g) at Spinus (SPSS).

In Figure 31 the amounts of surface runoff (ml) (blue) and sediment yield (g) (green) are illustrated by means of two curves. Due to the small amounts of sediment yield (many measurements were 0g), one cannot clearly see a proper relation in the peaks of the two curves even when the y-axis is transformed to a logarithmic scale, so that the differentiation in the curve of sediment yield is more distinct. This also applies to the scatter plot of sediment yield (g) and surface runoff (ml) in Figure 32 and the correlation analysis in Table 6. There is no significant correlation between the two variables, surface runoff and sediment yield. The reason for that is most certainly the small number of measurements ($n = 20$) as well as the few measurements showing no erosion.

Table 6 Correlation analysis between surface runoff (ml) and sediment yield (g) at Spinus (SPSS).

		Surface runoff (ml)
Sediment yield (g)	Pearson Correlation	0.30
	Sig. (2-tailed)	0.142
	N	20

The same correlation analysis with the dataset without the outliers illustrated a correlation significance of 0.015, what is highly significant. Consequently one can say that the results above are highly influenced by outliers.

3.1.3.2 Bever

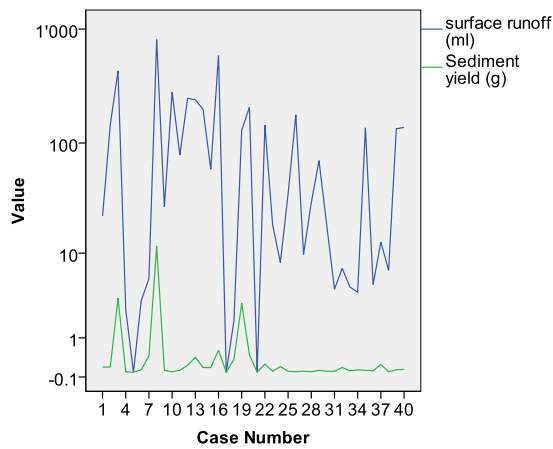


Figure 33 Amount of surface runoff (ml) and sediment yield (g) at Bever (SPSS).

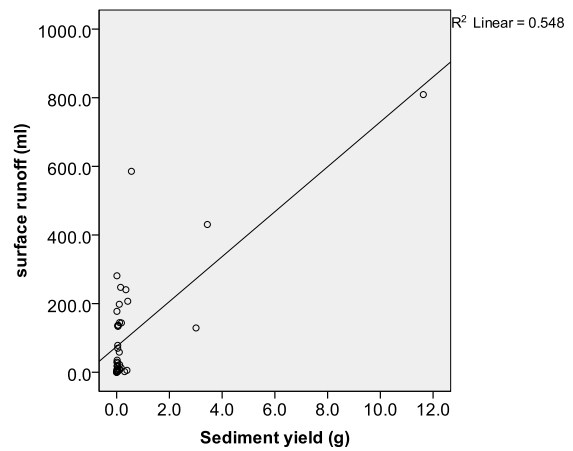


Figure 34 Scatter plot of surface runoff (ml) and sediment yield (g) at Bever (SPSS).

In Figure 33 the value curves of sediment yield (g) (green) and surface runoff (ml) (blue) are illustrated. One can see the congruence of the peaks in two of the curves. On the right (Figure 34) the correlation between sediment yield (g) and surface runoff (ml) is shown with a scatter plot. The assumed correlation is demonstrated with a correlation analysis. In Table 7 one sees that the two-tailed p-value is 0.000, which is very highly significant.

Table 7 Correlation analysis between surface runoff (ml) and sediment yield (g) at Bever (SPSS).

		Sediment yield (g)
Surface runoff (ml)	Pearson Correlation	0.70**
	Sig. (2-tailed)	0.00
	N	40

3.1.4 C/N-Ratio

The ratio between carbon and nitrogen in the soil samples collected at every investigated soil plot was calculated out of the average C (%) and N (%) percentage which had been measured at ZHAW in Rapperswil with a CHN analyzer. The values displayed in the histograms below (Figure 35 and Figure 36) were the result of the calculation of the mean value between the C/N ratios of the two individual soil samples, taken at every measurement point at Spinas and Bever.

In statistics, a histogram is a graphical representation of the distribution of a dataset. A histogram allows a visual interpretation of numerical data by indicating the number of data points that lie within a range of values, called a class. The frequency of the data that falls in each class is depicted by the use of a bar. The height of each bar is equal to the frequency density of the interval. The total area of the histogram is equal to the total number of data. The horizontal line represents the mean of the values in the two datasets.

Spinas

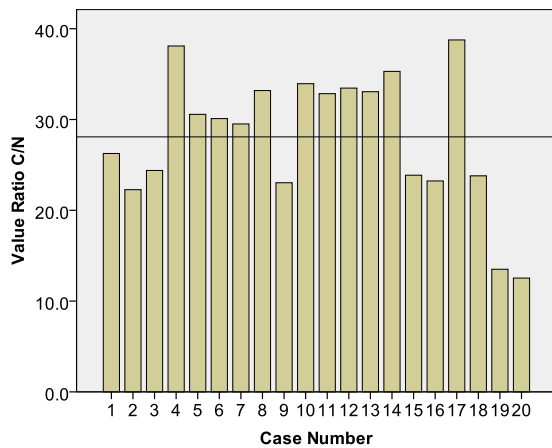


Figure 35 C/N ratio of the investigated soil plots at Spinas (with mean) (SPSS).

Bever

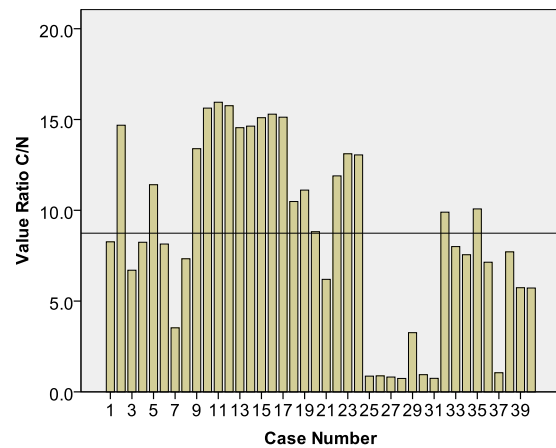


Figure 36 C/N ratio of the investigated soil plots at Bever (with mean) (SPSS).

In general one can see a higher C/N ratio at Spinas than at Bever. For the study site Spinas the mean C/N ratio is 28.08 ± 7.27 , for Bever 8.74 ± 5.05 .

In absolute values, the mean of the carbon in the soil at Spinas is 26.48 ± 13.58 volume percent, and the mean of nitrogen 0.95 ± 0.42 . At Bever the mean of carbon is 5.30 ± 5.76 volume percent, and the mean of nitrogen 0.44 ± 0.33 .

Prominent are the very low C/N ratio values at Bever, as seen in Figure 36 (case numbers 25-31). The soil samples of these measurement points also show a very low amount of carbon (0.1-0.38 vol. %) and nitrogen (0.1-0.7 vol. %). By defining these seven measurement points as outliers and removing them from the dataset, one can see whether they have a significant influence on the mean values. This is not the case. The total amount of carbon at Bever after the removal of the outliers is 6.39 ± 5.77 , and the amount of nitrogen 0.51 ± 0.33 . This is still far less than at Spinas. The C/N ratio (10.34 ± 3.96) is also still smaller than at Spinas.

The difference in C/N ratios in permafrost-influenced soil and non-permafrost soils was also tested in SPSS, but there was no significant difference between the C/N ratios of soil patches on permafrost and patches without permafrost conditions.

In the tables below (Table 8, Table 9 and Table 10), the information of all measured 120 soil samples are listed. The amount of carbon and nitrogen is translated into g/kg.

Table 8 C/N ratio and the amount of carbon and nitrogen in the 40 soil samples of Spinus.

Sample Nr.	C g/kg	N g/kg	C/N ratio	Sample Nr.	C g/kg	N g/kg	C/N ratio
1a	129	5.4	23.9	11a	49.5	1.1	43.2
1b	63	1.9	33.3	11b	101	3.4	29.4
2a	196	9.7	20.1	12a	117	3.8	31
2b	189	7.5	25	12b	131	3.6	36
3a	193	8.6	22.4	13a	443	13.1	33.7
3b	138	4.9	27.7	13b	443	13.6	32.4
4a	361	8.8	41.1	14a	461	13.9	33.2
4b	365	10.3	35.5	14b	454	12	37.8
5a	434	12.4	35	15a	374	15.7	23.8
5b	425	15.7	27	15b	289	12.1	23.9
6a	413	13.4	30.9	16a	370	16.2	22.8
6b	338	11.6	29.2	16b	380	16	23.7
7b	293	10.5	27.9	17a	409	10.3	39.7
7a	425	13.8	30.7	17b	419	11.1	37.8
8a	168	5.3	31.9	18a	374	14.9	25.1
8b	129	3.7	34.9	18b	341	15.2	22.5
9a	225	9.8	23	19a	35.5	3.8	9.2
9b	204	8.8	23	19b	171	11.4	14.9
10b	114	3.4	33.8	20a	73.2	6.6	11.1
10a	209	6.1	34	20b	146	10.9	13.4

Table 9 C/N ratio and the amount of carbon and nitrogen in the 60 soil samples of Bever (Part 1).

Sample Nr.	C g/kg	N g/kg	C/N ratio	Sample Nr.	C g/kg	N g/kg	C/N ratio
21a	26.3	3.5	9	41a	13.3	1.9	6.8
21b	31.3	3.5	7.5	41b	11.8	2.1	5.7
22b	225	14.7	15.3	42a	86.7	7.5	11.5
22a	133	9.7	13.8	42b	75.2	6.1	12.3
23a	20.7	3.2	6.4	43a	136	9.3	14.7
23b	22.1	3.1	7	43b	60.4	5.7	10.6
24a	32.7	4	8.2	44a	65.7	6	10.9
24b	31.7	3.8	8.3	44b	119	8.1	14.6
25a	48.5	4.4	11.1	45a	1	1.3	0.7
25b	46.3	3.9	11.8	45b	1	0.9	1
26a	40.5	4.6	8.7	46a	1	1.4	0.7
26b	17.7	2.5	7	46b	1	0.9	1.1
27a	5.1	1.9	2.7	47a	1	1.6	0.6
27b	8.4	1.9	4.3	47b	1	0.9	1.1
28a	17.3	2.3	7.3	48a	1	1.3	0.7
28b	16.5	2.3	7.3	48b	1	1.4	0.7
29a	84.8	6	14	49a	1	1	0.9
29b	78.1	6.1	12.7	49b	6.7	1.3	5.1
30a	137	8.6	15.9	50a	1	1.1	0.9
30b	271	17.5	15.4	50b	1	1	0.9

Table 10 C/N ratio and the amount of carbon and nitrogen in the 60 soil samples of Bever (Part 2).

Sample Nr.	C g/kg	N g/kg	C/N ratio	Sample Nr.	C g/kg	N g/kg	C/N ratio
31a	168	10.3	16.2	51a	1.2	1.4	0.9
31b	156	9.9	15.6	51b	1	1.7	0.6
32a	149	9.4	15.8	52a	34.9	3.2	10.8
32b	194	12.3	15.7	52b	19	2.2	8.5
33a	98.2	6.9	14.2	53a	21.9	2.9	7.4
33b	98.4	6.6	14.9	53b	25.5	2.9	8.6
34a	81.6	5.5	14.8	54a	17.3	2.5	6.9
34b	130	8.9	14.5	54b	16.8	2	8.3
35a	153	9.4	16.3	55b	36.7	3.5	10.5
35b	91.6	6.8	13.4	55a	27.6	2.9	9.6
36a	82.3	5.7	14.3	56a	16.6	2.4	6.9
36b	85.2	5.2	16.3	56b	16.6	2.2	7.4
37a	106	7.5	14.1	57a	1.5	1.5	1
37b	203	12.9	15.7	57b	0.9	0.8	1.1
38a	44.2	4.2	10.4	58a	25.1	3.4	7.3
38b	44.9	4.3	10.5	58b	21.6	2.6	8.2
39a	51.3	4.5	11.3	59a	13.5	2.1	6.5
39b	38.5	3.5	10.9	59b	6.2	1.4	4.6
40a	45.7	3.9	11.8	60a	14.5	3.2	4.6
40b	7.3	2.1	3.4	60b	11.9	1.4	8.2

3.1.5 pH value

The soil pH (in 0.01 M CaCl₂) was determined on air-dried samples using a soil / CaCl₂ solution ratio of 1 to 2.5. The soil pH is a measure for the concentration of protons in the CaCl₂-extract of the fine soil. In the following histograms (Figure 37 and Figure 38), the data distribution of the variable pH value is shown.

Spinas

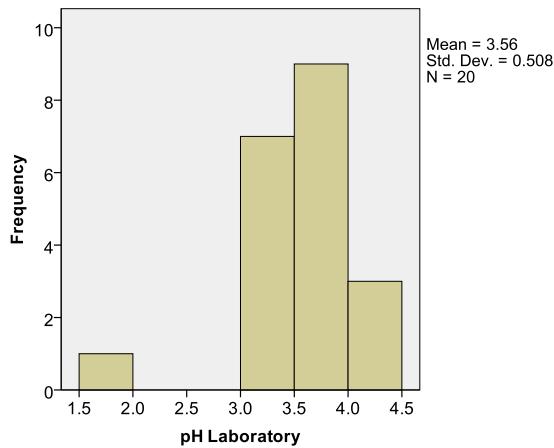


Figure 37 Histogram of the pH value (Laboratory) at the investigated soil plots at Spinas (SPSS).

Bever

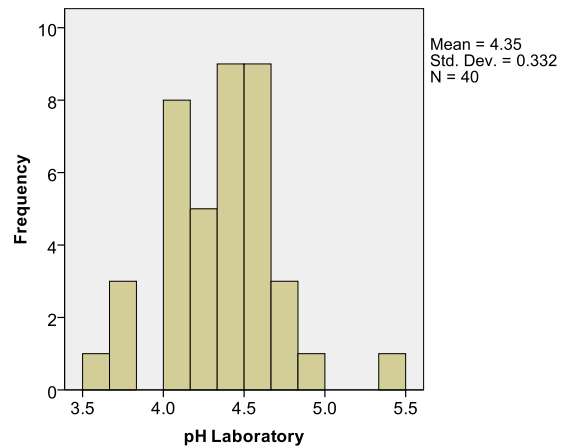


Figure 38 Histogram of the pH value (Laboratory) at the investigated soil plots at Bever (SPSS).

The pH values of the soil plots at Spinas were between 1.9 and 4.5, at Bever between 3.5 and 5.5. Consequently the investigated soil plots at the study sites Spinas and Bever are acid. The descriptive statistics show a mean pH value of 3.56 ± 0.11 for Spinas and 4.35 ± 0.05 for Bever. Therefore the two study sites have the same degree of acidity (extreme acidity).

The box plots show one outlier each for the two study sites. At Spinas (Figure 39) one can see an excessively low value of 1.9. At Bever (Figure 40) the outlier shows a pH value of 5.3.

Spinas

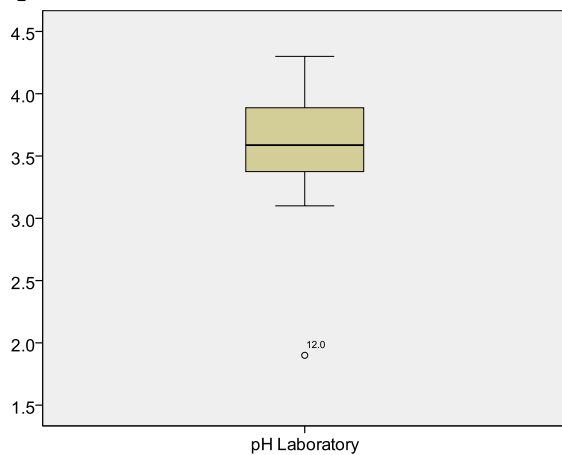


Figure 39 Box plot of the pH value (Laboratory) at the investigated soil plots at Spinas (SPSS).

Bever

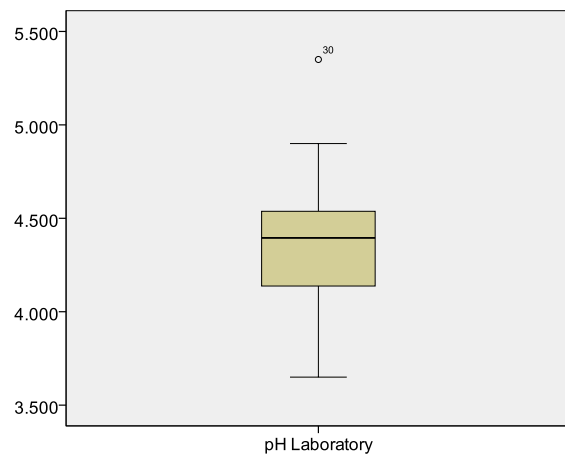


Figure 40 Box plot of the pH value (Laboratory) at the investigated soil plots at Bever (SPSS).

In the two tables below (Table 11 and Table 12), one can see a list of the pH-values of all 120 measured soil samples.

Table 11 List of the pH-values measured in the laboratory (Spinas).

Sample Nr.	pH-value						
1a	4.05	6a	3.35	11a	3.7	16a	3.25
1b	3.9	6b	3.3	11b	3.8	16b	3.6
2a	4	7a	4.15	12a	1.9	17a	3.2
2b	3.5	7b	4.05	12b	3.8	17b	3
3a	4.4	8a	3.5	13a	3.4	18a	3.5
3b	4.2	8b	3.4	13b	3.15	18b	3.4
4a	4	9a	3.65	14a	3.95	19a	3.6
4b	3.65	9b	3.5	14b	3.75	19b	4.25
5a	3.2	10a	3.55	15a	3.7	20a	4.05
5b	3.1	10b	3.5	15b	3.5	20b	2.05

Table 12 List of the pH-values measured in the laboratory (Bever).

Sample Nr.	pH-value						
21a	4.1	31a	4	41a	4.3	51a	4.55
21b	4.05	31b	4	41b	4.6	51b	4.55
22a	3.75	32a	3.8	42a	4.3	52a	4.55
22b	3.7	32b	3.85	42b	4.3	52b	4.6
23a	4.3	33a	4.35	43a	4.2	53a	4.45
23b	4.4	33b	3.95	43b	4.6	53b	4.55
24a	4.35	34a	4.4	44a	4.5	54a	4.5
24b	4.35	34b	4.5	44b	4.4	54b	4.5
25a	4.1	35a	4	45a	4.33	55a	4.5
25b	4.05	35b	4.05	45b	4.45	55b	4.55
26a	4.35	36a	4.25	46a	4.5	56a	4.3
26b	4.15	36b	4.05	46b	4.45	56b	4.5
27a	4.1	37a	3.95	47a	4.6	57a	4.75
27b	4.25	37b	3.7	47b	4.6	57b	4.5
28a	4.5	38a	4.3	48a	5	58a	4.6
28b	4.55	38b	4.2	48b	4.8	58b	4.85
29a	4.05	39a	4.25	49a	4.7	59a	4.75
29b	4	39b	4	49b	4.7	59b	4.8
30a	3.6	40a	4.2	50a	5.6	60a	4.7
30b	3.7	40b	4.4	50b	5.1	60b	4.5

3.2 Hypothesis 1

3.2.1 Spinas

An independent T-Test was done to ascertain whether the amounts of surface runoff and sediment yield on permafrost-influenced plots and plots not influenced by permafrost were significantly different or not.

Surface runoff and permafrost

The test output (Table 13) shows no significant difference in surface runoff on plots with permafrost compared to non-permafrost plots (Sig. 0.526). This implies the rejection of hypothesis 1: *“There is a significant difference in susceptibility to soil erosion (sediment yield and surface runoff) between measurements on permafrost and those without permafrost”*.

In Figure 41 and Figure 42 one can see the distribution of the data (surface runoff) on permafrost soil and on non-permafrost soil in terms of a box plot. In Figure 42 the y-axis has been changed to a logarithmic scale in order to eliminate the statistical compression caused by the outliers.

Table 13 Independent T-Test for surface runoff at Spinas (SPSS)

		Levene's Test for Equality of Variances		t-test for Equality of Means						
		F	Sig.	t	df	Sig. (2-tailed)	Mean Difference	Std. Error Difference	95% Confidence Interval of the Difference	
Surface Runoff (ml)	Equal variances assumed	1.527	0.232	0.65	18	0.521	4.46	6.81	-9.85	18.78
	Equal variances not assumed			0.65	11.199	0.526	4.46	6.81	-10.50	19.43

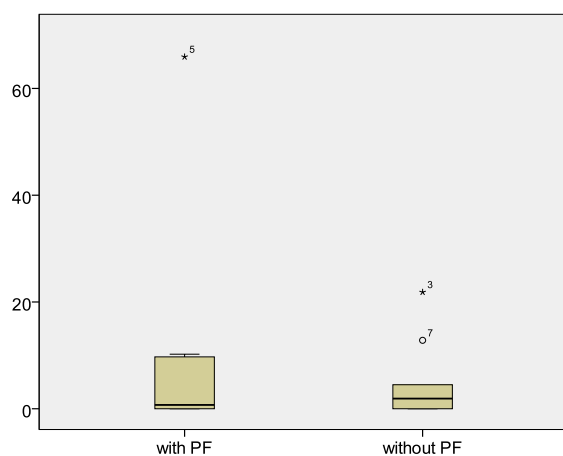


Figure 41 Box plots of the surface runoff on PF and on soil without PF at Spinas (SPSS).

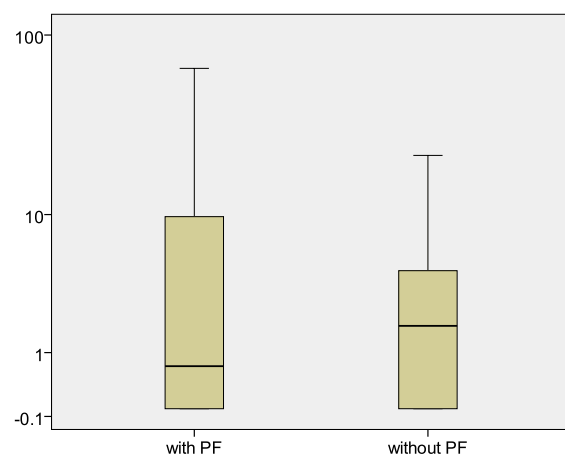


Figure 42 Box plots of the surface runoff on PF and on soil without PF at Spinas, logarithmic scale (SPSS).

Sediment yield and permafrost

A similar result shows the test (Table 14) between the variable sediment yield on permafrost and non-permafrost. The difference indicates an extremely low significance (Sig. 0.059, marginally significant). One can see a tendency to a greater sediment yield on plots without permafrost influence. The average sediment yield on plots with permafrost influence is 0.007 g, and on non-permafrost plots it is 0.023 g. As a consequence one can say that hypothesis 1 (*There is a significant difference in susceptibility to soil erosion (sediment yield and surface runoff) between measurements on permafrost and such without permafrost*) is only partly true for Spinass. Measurements show that there is no difference in susceptibility to surface runoff between permafrost soil and soil without permafrost, but that there is a tendency to a higher sediment yield.

Table 14 Independent T-Test for the sediment yield at Spinass (SPSS)

		Levene's Test for Equality of Variances		t-test for Equality of Means						
		F	Sig.	t	df	Sig. (2-tailed)	Mean Difference	Std. Error Difference	95% Confidence Interval of the Difference	
									Lower	Upper
Sediment Yield (g)	Equal variances assumed	16.083	0.001	-2.101	18	0.050	-0.016	0.008	-0.032	0.000
	Equal variances not assumed			-2.101	11.341	0.059	-0.016	0.008	-0.033	0.001

In Figure 43 one can see an illustration of the data for sediment yield on soil patches with and without permafrost influence.

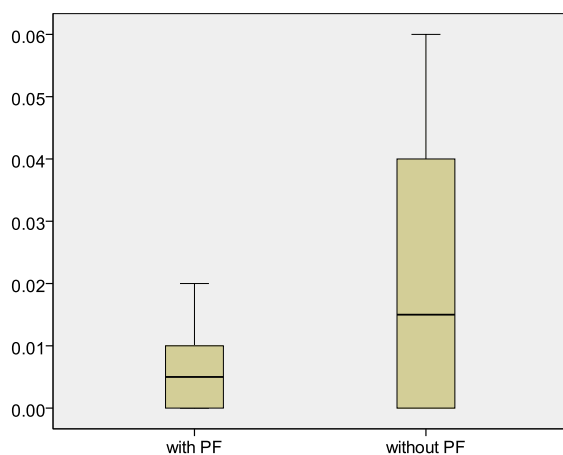


Figure 43 Box plots of the sediment yield on soil with PF and on soil without PF at Spinass (SPSS).

3.2.2 Bever

In hypothesis 1 of this study a significant difference in susceptibility to soil erosion (sediment yield and surface runoff) between soil with permafrost and soil without permafrost was predicted. The difference in surface runoff and sediment yield on plots with permafrost influence and those without were tested with SPSS at Bever, as had been done at Spinus.

Surface runoff and permafrost

Table 15 Independent T-Test for surface runoff at Bever (SPSS)

		Levene's Test for Equality of Variances		t-test for Equality of Means						
		F	Sig.	t	df	Sig. (2-tailed)	Mean Difference	Std. Error Difference	95% Confidence Interval of the Difference	
Surface Runoff (ml)	Equal variances assumed	4.04	0.052	-1.85	38	0.072	-97.03	52.35	-203.01	8.94
	Equal variances not assumed			-1.85	27.67	0.074	-97.03	52.35	-204.32	10.26

c. PF = 2.00

An Independent T-Test was done to ascertain whether the surface runoff on permafrost-influenced soil plots and plots without permafrost is significantly different. The results of this test (Table 15) shows that there is no significant difference in the amount of surface runoff between plots with permafrost-influenced soil and those without. The significance of 0.072 (marginally significant) is higher than the significance level of 0.05. The points made above support the null hypothesis, namely that “the population means from the two unrelated groups are equal”.

This implies that hypothesis 1 (*There is a significant difference in susceptibility to soil erosion (sediment yield and surface runoff) between measurements on permafrost and such without permafrost*) has to be rejected when one refers to surface runoff.

In the following box plots (Figure 44 and Figure 45) one can see the distribution of the surface runoff on permafrost-influenced soil and non-permafrost soil. The figure on the right has a logarithmic scale.

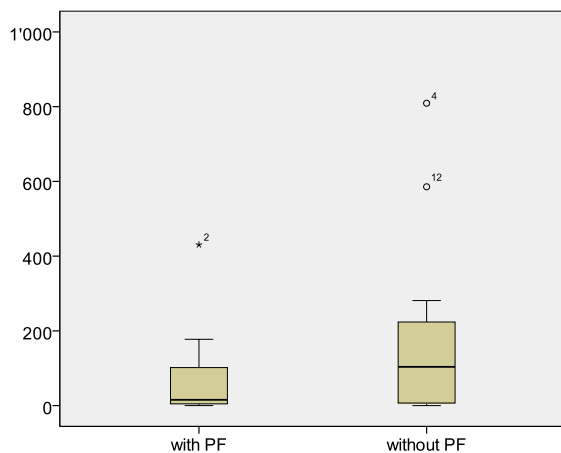


Figure 44 Box plots of the surface runoff on PF and on soil without PF at Bever (SPSS).

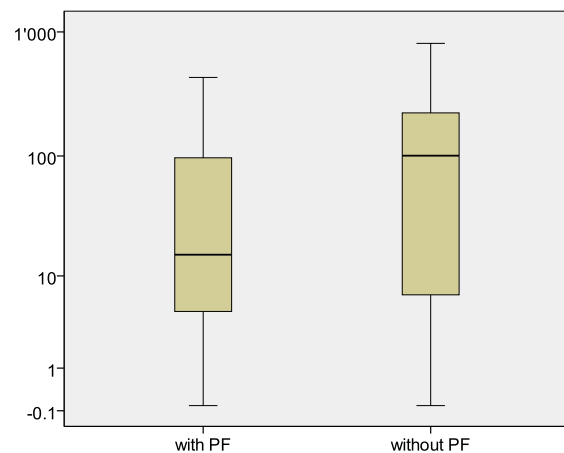


Figure 45 Box plots of the surface runoff on PF and on soil without PF at Bever, logarithmic scale (SPSS)

Sediment yield and permafrost

In order to test whether there is a significant difference between the amount of sediment yield on permafrost-influenced plots and non-permafrost plots, the Wilcoxon Signed-Rank Test was applied (for paired samples). This was done because of the non-normal distribution of the data.

Table 16 Signed-Rank Test for sediment yield at Bever (SPSS)

	Sediment yield
Mann-Whitney U	111.00
Wilcoxon W	321.00
Z	-2.41
Asymp. Sig. (2-tailed)	0.016
Exact Sig. [2*(1-tailed Sig.)]	0.015^a

The test shows a significant difference between sediment yield on permafrost and sediment yield on non-permafrost plots (Sig. 0.015) (see Table 16). The average amount of sediment yield on permafrost-influenced soil is 0.21g; on non-permafrost soil it is 0.88g. This supports hypothesis 1 (*There is a significant difference in susceptibility to soil erosion (sediment yield and surface runoff) between measurements on permafrost and such without permafrost*) regarding sediment yield.

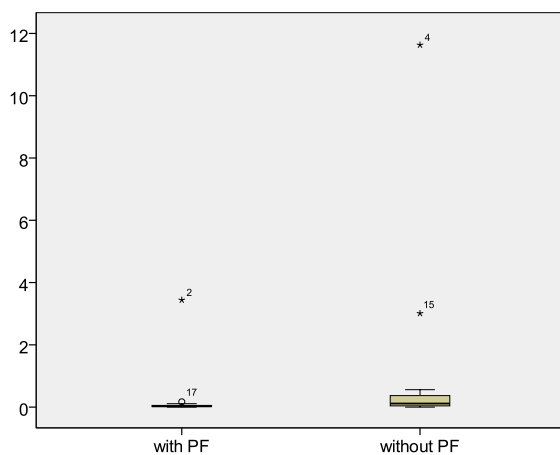


Figure 46 Box plot of the sediment yield on PF and on soil without PF at Bever (SPSS).

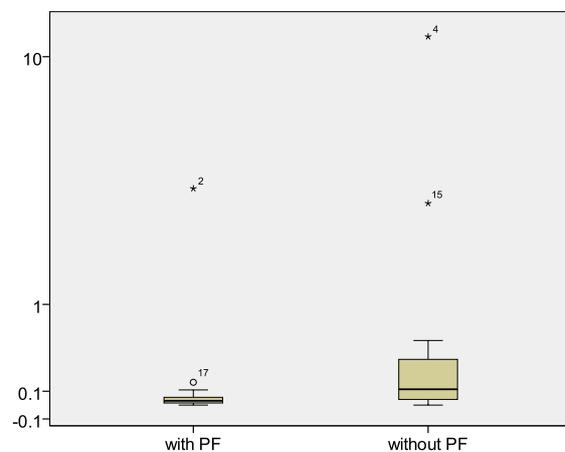


Figure 47 Box plot of the sediment yield on PF and on soil without PF at Bever, logarithmic scale (SPSS).

The measurement data of sediment yield is illustrated in the box plots above (Figure 46 and Figure 47). The figure on the left has a linear scale and the figure on the right a logarithmic scale.

3.3 Hypothesis 2

3.3.1 Spinas

In hypothesis 2 a positive correlation between soil erosion and vegetation cover and a negative correlation between soil erosion (sediment yield and surface runoff) and slope was predicted. The influence of the different soil parameters on surface runoff and sediment yield was tested with the Pearson correlation analysis (see Table 17).

Correlation analysis

Table 17 Correlation analysis of soil parameters and soil erosion at Spinas (SPSS)

		Surface runoff (ml)	Sediment yield (g)
Slope (°)	Pearson Correlation	-.105	-0.030
	Sig. (2-tailed)	0.659	0.901
	N	20	20
Vegetation cover (%)	Pearson Correlation	0.052	-0.379
	Sig. (2-tailed)	0.827	0.100
	N	20	20
Gravel content (%)	Pearson Correlation	-0.437	-0.500*
	Sig. (2-tailed)	0.054	0.025
	N	20	20
Moisture (before)	Pearson Correlation	-0.208	-0.139
	Sig. (2-tailed)	0.378	0.560
	N	20	20
Ratio fine/coarse	Pearson Correlation	0.011	-0.274
	Sig. (2-tailed)	0.963	0.242
	N	20	20
C (%)	Pearson Correlation	0.347	-0.178
	Sig. (2-tailed)	0.134	0.452
	N	20	20
C/N Ratio	Pearson Correlation	0.187	-0.003
	Sig. (2-tailed)	0.429	0.990
	N	20	20

*. Correlation is significant at the 0.05 level (2-tailed).

Table 17 shows that the correlation of surface runoff and sediment yield of the gravel content in the soil is significant (sig. 0.025).

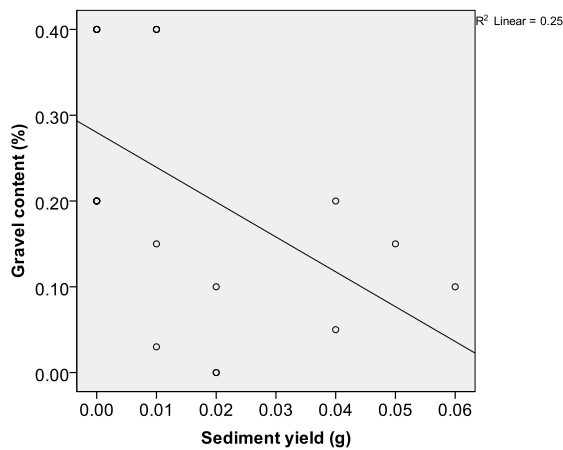


Figure 48 Gravel content (%) and sediment yield (g) at Spinas (SPSS).

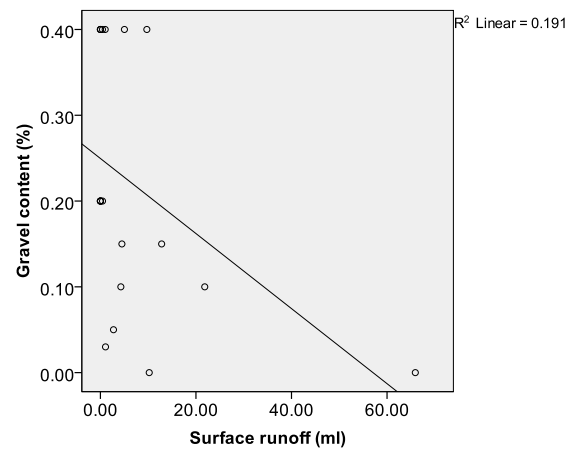


Figure 49 Gravel content (%) and surface runoff (ml) at Spinas (SPSS).

Figure 48 shows the correlation between sediment yield and gravel content in the soil. The more gravel in the soil, the less sediment yield was collected during the rainfall simulations. Therefore a negative correlation between the variables sediment yield and gravel content can be observed at the study site Spinas. In Figure 49 the correlation between gravel content (%) and surface runoff (ml) is illustrated. These two variables show a sig. of 0.054, which is barely significant (marginally significant). To see whether these outcomes were distorted by outliers, the same correlation analyses were conducted, but with the outliers removed.

Table 18 Correlation analysis of soil parameters and soil erosion at Spinas (without outliers) (SPSS)

		Surface runoff (ml)	Sediment yield (g)
Slope (°)	Pearson Correlation	0.531*	-0.041
	Sig. (2-tailed)	0.023	0.873
	N	18	18
Vegetation cover (%)	Pearson Correlation	-0.444	-0.284
	Sig. (2-tailed)	0.065	0.254
	N	18	18
Gravel content (%)	Pearson Correlation	-0.263	-0.482*
	Sig. (2-tailed)	0.292	0.043
	N	18	18
Moisture (before)	Pearson Correlation	-0.211	0.115
	Sig. (2-tailed)	0.401	0.650
	N	18	18
Ratio fine/coarse	Pearson Correlation	-0.295	-0.325
	Sig. (2-tailed)	0.234	0.188
	N	18	18
C (%)	Pearson Correlation	0.042	-0.467
	Sig. (2-tailed)	0.869	0.051
	N	18	18
C/N Ratio	Pearson Correlation	0.091	-0.056
	Sig. (2-tailed)	0.719	0.826
	N	18	18

*. Correlation is significant at the 0.05 level (2-tailed).

The results of the correlation analysis of the dataset without the outliers show a significant influence of slope on surface runoff and also a significant influence of the gravel content in the soil on the sediment yield (Table 18). In the case of Spinax Hypothesis 2 (*Independent of the influence of permafrost, a decrease in soil erosion (sediment yield and surface runoff) is expected with increasing vegetation cover and decreasing slope*) cannot be rejected completely. The results of the test with the raw data (Table 17) show that neither the vegetation cover nor the slope inclination had a significant influence on the measured soil erosion (sediment yield and surface runoff). When one removes the outliers, one can see a significant influence of the slope inclination on the surface runoff and a slight and insignificant influence of vegetation cover on the surface runoff. This, however, does not apply to the sediment yield.

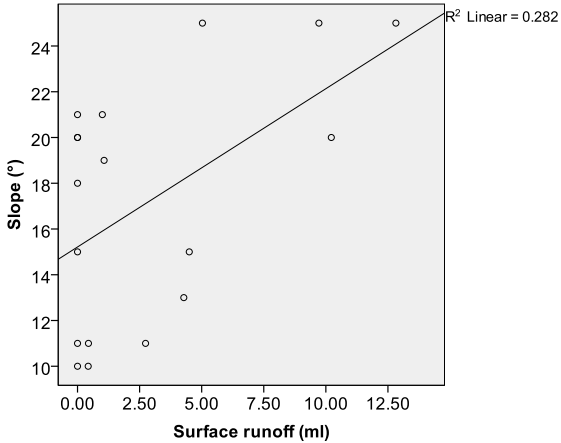


Figure 50 Slope (°) and surface runoff (ml) at Spinax (without outliers) (SPSS).

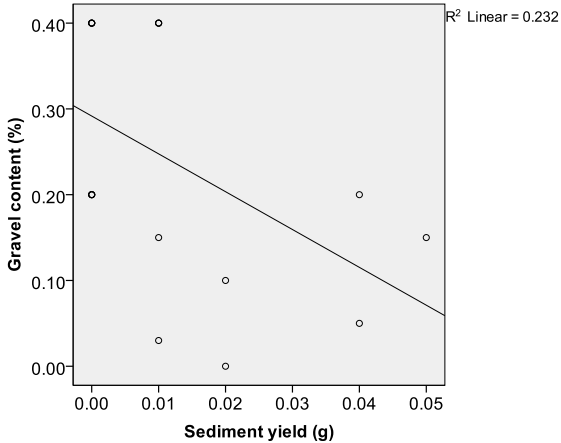


Figure 51 Gravel content (%) and sediment yield (g) at Spinax (without outliers) (SPSS).

In Figure 50 and Figure 51, the two significant correlations are illustrated with scatter plots. After the elimination of the outliers the correlation between gravel content (%) and sediment yield (g) remains insignificant. Nevertheless, there is a difference in the correlation of surface runoff (ml). In the raw data above a significant correlation with gravel content (%) can be seen, but when outliers are removed, there is a significant correlation with slope.

3.3.2 Bever

In hypothesis 2 a positive correlation between soil erosion (sediment yield and surface runoff) and vegetation cover as well as a negative correlation between soil erosion (sediment yield and surface runoff) and slope was predicted. The influence of the different soil parameters on surface runoff and sediment yield was tested with a Pearson correlation analysis.

Correlation analysis

Table 19 Correlation analysis of soil parameters and soil erosion in Bever (SPSS)

		surface runoff (ml)	Sediment yield (g)
Slope (°)	Pearson Correlation	0.176	0.077
	Sig. (2-tailed)	0.277	0.637
	N	40	40
Vegetation cover (%)	Pearson Correlation	-0.060	-0.203
	Sig. (2-tailed)	0.715	0.209
	N	40	40
Gravel content (%)	Pearson Correlation	-0.079	0.105
	Sig. (2-tailed)	0.628	0.519
	N	40	40
Moisture diff.	Pearson Correlation	0.011	0.062
	Sig. (2-tailed)	0.946	0.703
	N	40	40
Moisture before	Pearson Correlation	0.051	-0.151
	Sig. (2-tailed)	0.753	0.351
	N	40	40
Ratio fine/coarse	Pearson Correlation	-0.117	0.168
	Sig. (2-tailed)	0.474	0.301
	N	40	40
C/N Ratio	Pearson Correlation	0.225	-0.027
	Sig. (2-tailed)	0.163	0.871
	N	40	40
C (%)	Pearson Correlation	0.168	-0.120
	Sig. (2-tailed)	0.300	0.460
	N	40	40

** . Correlation is significant at the 0.01 level (2-tailed).

* . Correlation is significant at the 0.05 level (2-tailed).

In Table 19 one cannot observe any significant correlation between surface runoff, sediment yield and any of the soil parameters. In this case hypothesis 2 would be rejected. To see whether these outcomes are influenced in any way by outliers, the same correlation analyses were conducted without the four measurements which showed the biggest outliers in sediment yield and surface runoff.

Table 20 Correlation analysis of soil parameters and soil erosion at Bever (without outliers)

		Surface runoff (ml)	Sediment yield (g)
Ratio C/N	Pearson Correlation	0.374*	0.148
	Sig. (2-tailed)	0.025	0.388
	N	36	36
Ratio fine/coarse grained	Pearson Correlation	-0.374*	0.064
	Sig. (2-tailed)	0.025	0.710
	N	36	36
C (%)	Pearson Correlation	0.484**	0.042
	Sig. (2-tailed)	0.003	0.810
	N	36	36
Slope (°)	Pearson Correlation	0.213	-0.027
	Sig. (2-tailed)	0.212	0.876
	N	36	36
Vegetation cover	Pearson Correlation	0.326	-0.052
	Sig. (2-tailed)	0.053	0.764
	N	36	36
Gravel content	Pearson Correlation	-0.139	-0.232
	Sig. (2-tailed)	0.420	0.173
	N	36	36
Moisture before	Pearson Correlation	0.142	0.065
	Sig. (2-tailed)	0.408	0.706
	N	36	36

*. Correlation is significant at the 0.05 level (2-tailed).

**. Correlation is significant at the 0.01 level (2-tailed).

The results of the correlation analysis with the dataset without the outliers show a significant correlation between the variables “surface runoff” and the “C/N ratio”, “ratio between fine and coarse soil particles”, as well as between “surface runoff” and the “amount of carbon in the soil” (Table 20). The sediment yield does not show a correlation to any of the measured soil parameters. In this case, hypothesis 2 (*Independent of the influence of permafrost, a decrease in soil erosion (sediment yield and surface runoff) is expected with increasing vegetation cover and decreasing slope*) is rejected for the sediment yield at the study site Bever. Additionally, no significant correlation can be observed between surface runoff and slope, but one can see a slight influence of the vegetation cover on the surface runoff (sig. 0.053, marginally significant).

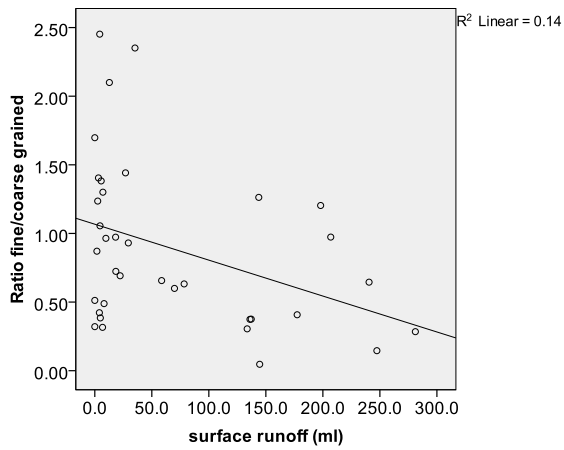


Figure 53 Scatter plot of the ratio fine/coarse grained and surface runoff (ml) at Bever (without outliers) (SPSS).

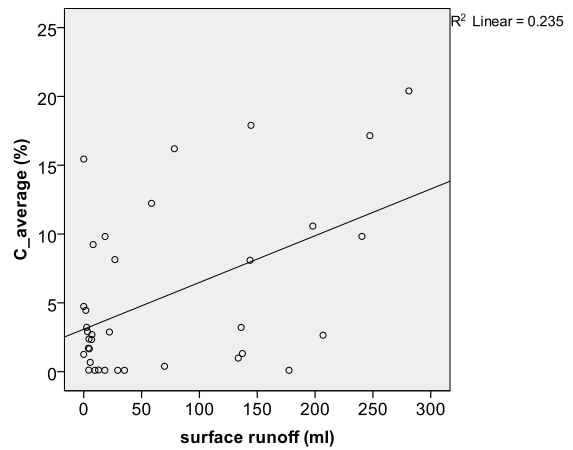


Figure 52 Scatter plot of the average amount of carbon in the soil and surface runoff (ml) at Bever (without outliers) (SPSS).

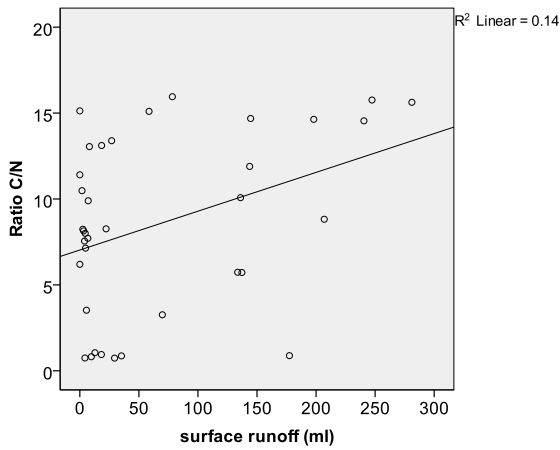


Figure 54 Scatter plot of the C/N ratio and surface runoff (ml) at Bever (without outliers) (SPSS).

In the three figures above (Figure 52, Figure 53 and Figure 54) the correlation between the variables “surface runoff” and the “ratio between fine and coarse grained soil particles”, as well as between “surface runoff” and “the average of carbon in the soil” are plotted.

3.4 Soil cartography

3.4.1 Spinass

In Figure 55 the different soil types of Spinass are illustrated in a soil map. Shallow and rather weakly developed Letosols dominated on the scree slope, while well developed Albic Podzols, as well as Haplic Podzols and Haplic Cambisol Dystric, were found in the lower area. Fluvisols have developed in the lowest part of the valley because of the activity of the river Beverin.

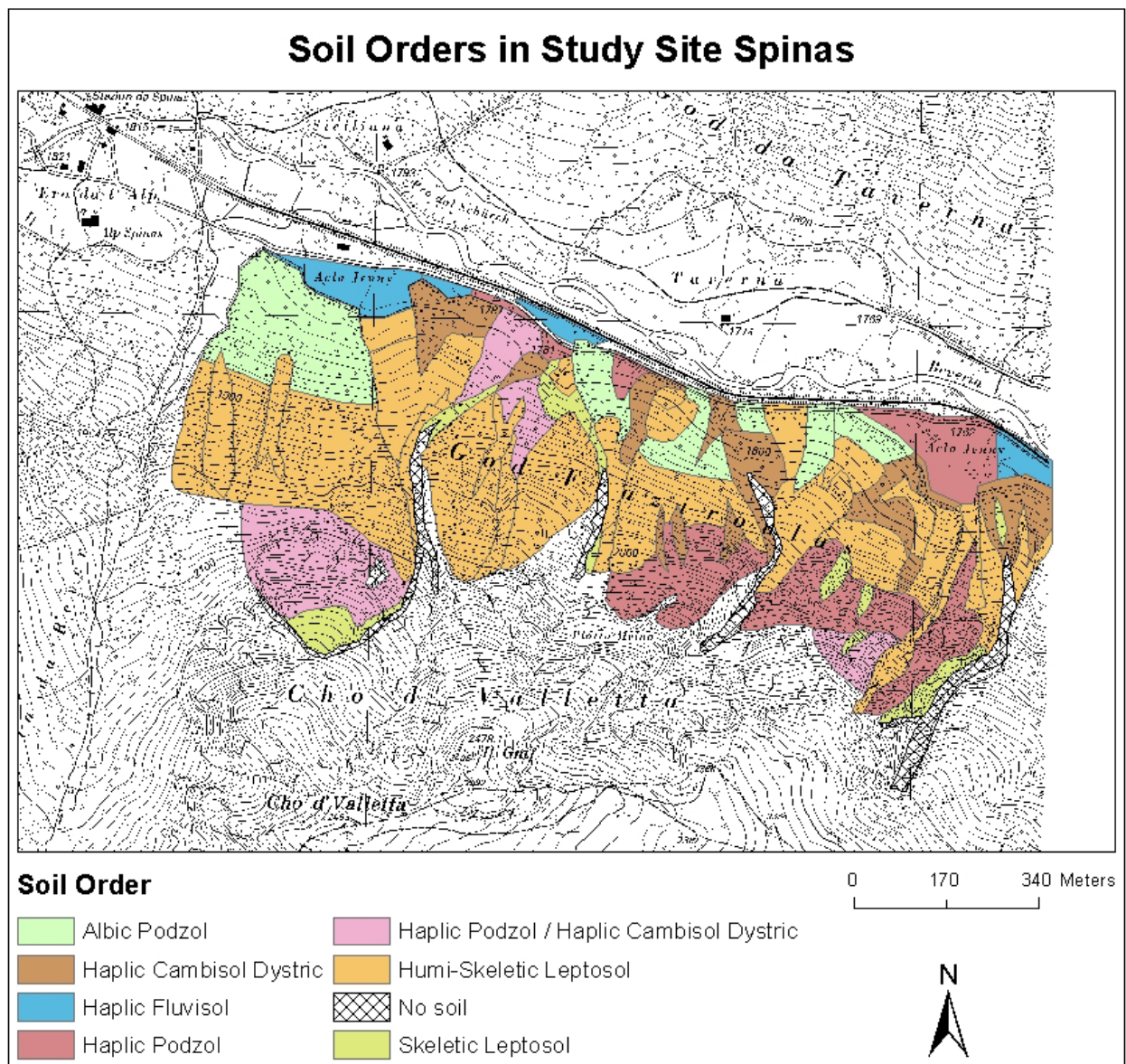


Figure 55 Representation of the different soil types at Spinass (ArcGIS).

3.4.2 Bever

At the study site Bever Skeletic Leptosols dominated. Haplic Podzols and Haplic Cambisol Dystric were also found in the lower parts of the area (Figure 56).

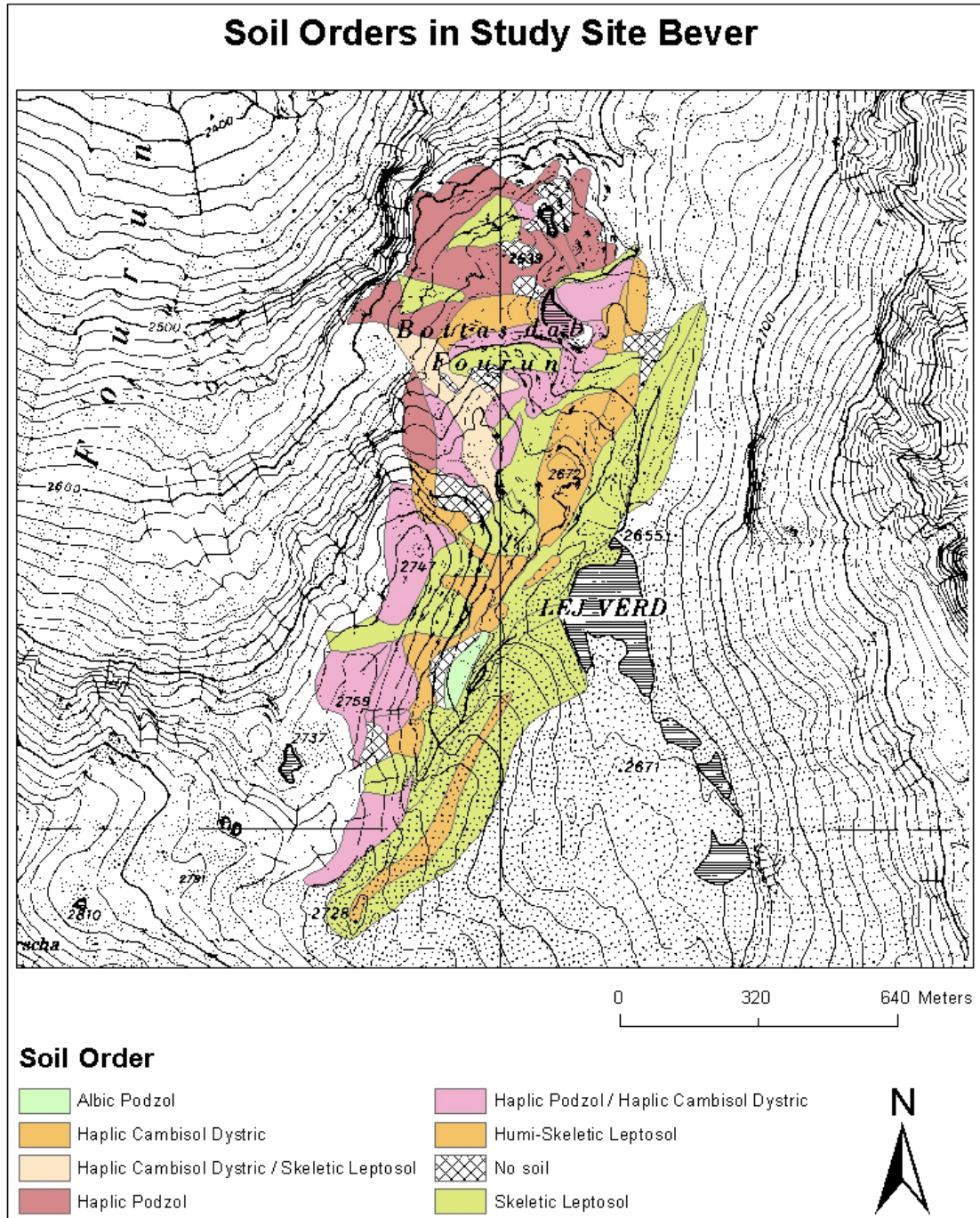


Figure 56 Representation of the different soil types at Bever (ArcGIS).

4 Discussion

4.1 Surface runoff and sediment yield

In general, higher amounts of surface runoff and sediment yield were measured at Bever - the upper study site - than at Spinas. A possible explanation for this could be the vegetation cover at Spinas. The majority of the investigated soil plots were covered with moss (Figure 57). Most species of moss tend to have a large water holding capacity, which prevents surface runoff of the soil. The physiology of moss is very different from that of other plants. Mosses lack roots and a vascular system, so they have to take up water directly through leaf surfaces. The hydrologic consequence of this physiological necessity is that moss colonies have a large capacity for retaining the water which has moved from the canopy above (Skre et al., 1983; Busby et al., 1978). Additionally, moss stabilizes the soil surface. As it increases the surface roughness, it acts as a trap for massing sediment (Witter et al., 1991).



Figure 57 Photo of soil patch nr. 5 at Spinas (Source: P. Polich).

The results indicated a positive correlation between surface runoff and sediment yield (at Spinas only for the dataset without outliers). This was probably mainly due to the fact that with an increasing runoff volume, more soil particles detached by raindrop impact were transported downhill and not because of the effect of increased shear stress between runoff and soil surface.

4.2 PH Value and Vegetation

The descriptive statistics revealed a mean pH value of 3.56 ± 0.11 for Spinas and 4.35 ± 0.05 for Bever. Therefore both study sites show an acid soil pH value for the topsoil. The low pH values are the consequence of the fact that both study sites are situated in siliceous bedrock. Soil types formed out of siliceous rock are naturally more acid than for instance soil formed out of carbonate rock. In addition, soil in a conifer forest is known to be acidic, as is the case at Spinas. At Spinas the dominant soil orders are different forms of Podzols - grey colored, acidic and nutrient-poor types of soil. The magnitude of the current pH values seem to be realistic since Zollinger et al. (2013) measured similar values for the upper horizons at Bever and Spinas (see also chapter 8.4). They also measured lower pH at Spinas (\varnothing 3.8) than at Bever (\varnothing 4.2).

The optimum pH range for most plants is between 5.5 and 7.0. However, many plants have adapted to thrive at pH values outside this range. At Spinas, where the vegetation cover was more developed than at Bever, plants adapted to acidic soil were found, such as alpine rose (Figure 58), cranberry and blueberry in the herbaceous layer. At Bever the vegetation is also influenced by the acidic soil, and *Caricetum curvulae* (Figure 59), an acidification indicator, is widespread.



Figure 59 Alpine rose at Spinas (Source: P. Polich).



Figure 58 *Caricetum curvulae* at soil patch nr. 30 at Bever (Source: P. Polich).

4.3 C/N ratio

The results showed a higher C/N ratio in the topsoil of Spinas (\bar{x} 28.08) than of Bever (\bar{x} 8.67). The absolute values were also higher at Spinas (\bar{x} C 26.48, \bar{x} N 0.95) than at Bever (\bar{x} C 5.29, \bar{x} N 0.44).

Several explanations are possible for these differences between the two study sites. Firstly, the amount of carbon and nitrogen depends on the input as well as on the rate of degradation in the soil. Most of the measurement points at Spinas were within a conifer forest, where the soil is covered by moss and grass. The input of carbon and nitrogen there is naturally higher than at Bever, where the vegetation cover was only marginally developed. Secondly, coniferous litter is difficult to break down. At Spinas the input as well as the degradation is therefore higher than at Bever. This explains the higher mean in the amounts of carbon and nitrogen in the soil samples of Spinas.

In the chapter on the results (see 3.1.4) one can see very small C/N ratios at seven different measurement points at Bever. These measurement points were all situated on permafrost and were constantly influenced by fresh gravel rolling down the hill. Because of that, the vegetation cover in these soil patches is not highly developed. The small amounts of carbon and nitrogen in these soil patches, as well as the small C/N ratios, might have occurred because of thinning through a continuous input of fresh gravel as well as a small input of carbon and nitrogen because of the marginally developed vegetation cover.

It can be said that, when compared to the values recorded in articles on the C/N ratio of alpine soils (see Egli et al., 2001; Zollinger et al., 2013), the results of this study are reasonable. In the two alpine sites of Egli et al. (2001), the C/N ratios of the topsoil horizons were between 13 and 23. In the three study sites of Zollinger et al. (2013), the values of the C/N ratios were between 5 and 21. The amounts of carbon and nitrogen as well as the C/N ratios listed in these two reference articles can be seen in Appendix C (8.3).

The statistical test on whether the C/N ratio showed significantly different values on permafrost soil patches and soil patches without permafrost conditions showed no significant differences.

4.4 Rainfall simulator

Soil erosion research data obtained with rainfall simulators are influenced by the kind of rainfall simulator used and its characteristics. In the case of the current study, a small portable rainfall simulator was used. Besides the advantages of simple transportation and installation, these simulators have several disadvantages, as have all rainfall simulators.

In the implemented statistical tests, one cannot always see a significant reason for the soil erosion and surface runoff at the two study sites, Spinas and Bever. In this chapter several possible causes for these results are listed.

The fundamental problem with simulated rainfall is the limited accuracy with which simulators replicate the characteristics of a natural rainstorm (Agassi & Bradford, 1999; Bryan, 1974; Bryan, 1981; Lal, 1988). Furthermore, several additional complications arise in simulator use, such as limited plot size, edge effects and the plot boundaries, differences in the drop size distribution and energy characteristics of natural and simulated rainfall, and the intricate variability of natural rainfall compared to the controlled nature of simulated rainfall (Bowyer-Bower & Burt, 1989).

Several other authors mentioned the problem of limited time. Measurements should be taken frequently for a sufficiently long duration (Lal, 1994). Frequency is the number of times measurements are taken during the measuring campaign and duration is the length of time that measurements are taken. But time and special coverage are often limited (Stroosnijder, 2005).

Regarding the result of hypothesis 2, where the soil erosion did not show the expected correlation with the variable slope, the argument of Vahabi and Nikkami (2008) can be used. They stated that a possible explanation for the slight effect of land slope in their study could be related to the short lengths of slopes when one works with small plots (Vahabi & Nikkami, 2008). The soil plots used with the Eijkelkamp rainfall simulator in this study were only 25cm×25cm. The size of the plot means that one has neither a large investigation area, nor a long slope.

The choice of the individual soil plots might also have had an influence on the result. After this study and the discovery that the presence of permafrost in the soil has a limited effect on soil erosion, one can say that the first priority in the selection of the measurement points should not have been an equal distribution between permafrost-influenced soil and non-permafrost soil. A greater range in the other patch properties (e.g. vegetation cover, slope and gravel content) would have made more sense for testing the impact of these variables.

In general one can also say that there might perhaps have been more significant results if more measurements could have been taken. Here the factors of time and accessibility are the main reasons for not doing so. The time between snow melt and first snowfall was limited; furthermore, reaching the upper study site (Bever) required about 3 hours of travelling.

In addition, the topography and also locational factors at both study sites were changing within a small scale. The effect of this could have been reduced by a higher number of rainfall simulations.

5 Conclusion

When the two study sites Spinas and Bever are compared, both measured variables (sediment yield and surface runoff) show higher amounts at Bever than at Spinas (the raw data as well as the dataset without outliers). Possible reasons are the marginal vegetation cover at Bever and the high moss density as well as the forest cover at Spinas. The datasets of sediment yield and surface runoff correlate with each other (at Spinas only in the dataset without outliers); in other words, a larger amount of water falling on the surface resulted in a higher sediment yield.

The calculated C/N ratios at Spinas and Bever differed. In absolute values, the amount of carbon and nitrogen in the topsoil of the measurement points was higher at Spinas than at Bever. This can be explained by the higher input at Spinas due to the forest and the dense vegetation cover on the ground, as well as the slow breakdown of coniferous litter. In addition, there is a constant thinning of the topsoil at Bever, caused by gravel sliding downhill. The C/N ratios of the permafrost and non-permafrost sites did not differ significantly.

Both study sites show acidic pH values in the topsoil layers of the investigated soil patches. These results are corroborated by the presence of acidophilic plants such as alpine roses, blueberry and cranberry at Spinas and widespread *Caricetum curvulae*, an acidification indicator, at Bever. Crucial for the acidity of the soil is the siliceous bedrock out of which the current Podzols and Leptosols were formed.

Neither hypothesis 1 (*There is a significant difference in susceptibility to soil erosion (sediment yield and surface runoff) between measurements on permafrost and such without permafrost*) nor hypothesis 2 (*Independent of the influence of permafrost, a decrease in soil erosion (sediment yield and surface runoff) is expected with increasing vegetation cover and decreasing slope*) can be accepted without reservation.

Hypothesis 1 does not apply to surface runoff, either at Spinas or at Bever. In both cases there is no significant difference between measurements of surface runoff on permafrost-influenced soil and on soil without permafrost. In contrast, however, the sediment yield during rainfall simulations show a nearly significant difference at Spinas (sig. 0.059, marginally significant) and a significant difference at Bever (sig. 0.015) between measurements conducted on permafrost-influenced soil and on non-permafrost soil.

The second hypothesis cannot be accepted regarding the amount of sediment yield at both study sites. No significant correlation between sediment yield and slope inclination (°) or vegetation cover (%) was found. By contrast, the relation between surface runoff and the two soil parameters (slope and vegetation cover) is only partially unclear. There is a significant correlation (sig. 0.023) between surface runoff and slope inclination (°) at the study site Spinas when outliers are removed. In addition, there is an insignificant correlation (sig. 0.053, marginally significant) between surface runoff and vegetation cover (%) at the study site Bever after the elimination of the outliers in the dataset.

The results of this study can be improved in several ways. First of all the selection of the measurement points should be modified. A more equal distribution of the soil properties tested (e.g. vegetation cover, slope and gravel content) may show the correlation between soil erosion and these factors more clearly. Secondly, the number of measurements should be extended. With a larger number of investigated soil patches, the influence of the outliers and possible errors is smaller. And, finally, the time

factor is of great influence. The measurements for the current study were made during the summer months (June, July and August) of one year. Measurements over a longer period of time would have been better.

Generally speaking, permafrost has an influence on the amount of soil erosion (surface runoff and sediment yield). Even though this influence is not always statistically significant and other influences may have a stronger effect on soil erosion, the melting of permafrost could in fact exacerbate the problem of soil erosion in alpine regions.

In order to improve the results of this study on the effect of melting alpine permafrost on the susceptibility of soil to erosion, further research has to be done. Apparently the direct and indirect influences of the current climate change enhance the melting of permanently frozen soil globally. But investigations made in this master thesis were not able to illustrate the influence of this trend on soil erosion definitively. Various measurements at different study sites have to be done before a better assessment of future trends will be possible.

6 Bibliography

- Agassi, M., Bradford, J. M.**, 1999. Methodologies for interrill soil erosion studies. IN: Soil and Tillage Research. Vol. 49.
- Aksoy, A., Unal, E. N., Cokgor, S., Gedikli, A., Yoon, J., Koca, K., Inci, B. S., Eris, E.**, 2012. A rainfall simulator for laboratory-scale assessment of rainfall-runoff-sediment transport processes over a two-dimensional flume. IN: Catena, Vol. 98.
- Angima, S. D., Stott, D. E., O'Neill, M. K., Ong, C. K., Weesies, G. A.**, 2003. Soil erosion prediction using RUSLE for central Kenyan highland conditions. IN: Agriculture, Ecosystems and Environment, Vol. 97.
- Assouline, S., Ben-Hur. M.**, 2006. Effects of rainfall intensity and slope gradient on the dynamics of interrill erosion during soil surface sealing. IN: Catena, Vol. 66.
- Auerswald, K.**, 1998. Bodenerosion, Analyse und Bilanz eines Umweltproblems. Kapitel in „Bodenerosion, Analyse und Bilanz eines Umweltproblems“, Richter (Hrsg) 1998. Wissenschaftliche Buchgesellschaft, Darmstadt.
- Auerswald, K., Kainz, M., Schöder, D., Martin, W.**, 1991. Comparison of german and swiss rainfall simulators - experimental setup. IN: Zeitschrift für Pflanzenernährung und Bodenkunde, Vol.155.
- Bagnold, R. A.**, 1941. The physics of blown sand and desert dunes. Methuen, London.
- Beuselinck, L., Govers, G., Hairsine, P. B., Sander, G. C., Breynaert, M.**, 2002. The influence of rainfall on sediment transport by overland flow over areas of net deposition. IN: Journal of Hydrology, Vol. 257.
- Bhardwaj, A., Singh, R.**, 1992. Development of a portable rainfall simulator infiltrometer for infiltration, runoff and erosion studies. IN: Agricultural Water Management, Vol. 22.
- Birot, P.**, 1981. Les processus d'érosion à la surface des continents. Masson, Paris.
- Boardman, J.**, 2010. A short history of muddy floods. IN: Land Degradation and Development, Vol. 21.
- Boardman, J., Shepherd, M. I., Walker, E., Foster, I. D. L.**, 2009. Soil erosion and risk-assessment for on- and off-farm impacts: a test case using the Midhurst area, West Sussex, UK. IN: Journal of Environmental Management, Vol. 90.
- Bochet, E., Poesen, J., Rubio, J. L.**, 2000, Mound development as an interaction of individual plants with soil, water erosion and sedimentation processes on slopes. IN: Earth Surface Processes and Landforms, Vol. 25.
- Bowyer-Bower, T. A. S., Burt, T. P.**, 1989. Rainfall simulators for investigating soil response to rainfall. IN: Soil Technology. Vol. 2.
- Bryan, R. B.**, 1974. A simulated rainfall test for the prediction of soil erodibility. IN: Zeitschrift für Geomorphologie, Supp. Bard., 21d.

- Bryan, R. B.**, 1981. Soil erosion under simulated rainfall in the field and laboratory: variability of erosion under controlled conditions. *Erosion and Sediment Transport Measurements*, IAHS publ. no. 133.
- Bryan, R. B.**, 2000. Soil erodibility and processes of water erosion on hillslope. IN: *Geomorphology*, Vol. 32.
- Brunner, J., Jäggli, F., Nievergelt, J., Peyer, K.**, 1997. Kartieren und Beurteilen von Landwirtschaftsböden. Schriftenreihe der FAL (Eidgenössische Forschungsanstalt für Agrarökologie und Landbau) 24, Zürich-Reckenholz.
- Bull, L. J., Kirkby, M. J.**, 1997. Gully processes and modelling. IN: *Progress in Physical Geography*, Vol. 21.
- Busby, J. R., Bliss, L. C., Hamilton, C. D.**, 1978. Microclimate control of growth rates and habitat of boreal forest mosses, *Thomopterygium nitens* and *Hylocomium splendens*. IN: *Ecological Monographs*, Vol. 48.
- Canali, G. E.**, 1992. The Impact of Watershed Dynamics and Homogeneity on Sedimentation. PhD. Dissertation, Colorado State University.
- Cantón, Y., Solé-Benet, A., Asensio, C., Chamizo, S., Puigdefàbregas, J.**, 2008. Aggregate stability in range sandy loam soils Relationships with runoff and erosion. IN: *Catena*, Vol. 77.
- Cerdà, A.**, 1998. Soil aggregate stability under different Mediterranean vegetation types. IN: *Catena*, Vol. 32.
- Chepil, W. S.** 1945. Dynamics of wind erosion: Nature of movement of soil by wind. IN: *Soil Science*, Vol. 60.
- Clarke, M.A., Walsh, R.P.D.**, 2007. A portable rainfall simulator for field assessment of splash and slope wash in remote locations. IN: *Earth Surface Processes and Landforms*, Vol. 32.
- Corona, R., Wilson, T., D'Adderio, L. P., Porcù, F., Montaldo, N., Albertson, J.**, 2013. On the estimation of surface runoff through a new plot scale rainfall simulator in Sardinia, Italy. IN: *Procedia Environmental Sciences*, Vol. 19.
- De Baets, S., Poesen, J., Gysels, G., Knapen, A.**, 2006. Effects of grass roots on the erodibility of topsoils during concentrated flow. IN: *Geomorphology*, Vol. 76.
- De Ploey, J., Poesen, J.**, 1985. Aggregate stability, runoff generation and interrill erosion. IN: *Geomorphology and Soils*, Richards, K. S., Arnett, R. R., Ellis, S..George Allen & Unwin, London.
- Descroix, L., González Barrios, J. L., Viramontes, D., Poulenard, J., Anaya, E., Esteves, M., Estrada, J.**, 2008. Gully and sheet erosion on subtropical mountain slopes: Their respective roles and the scale effect. IN: *Catena*, Vol. 72.
- Dhakal, A. und Sidle, R.**, 2003. Longterm modelling of landslides for different forest management practices. IN: *Earth Surface Processes Landforms*, Vol. 28.
- Dlamina, P., Orcharda, C., Jewitta, G., Lorentza, S., Titshall, L., Chaplota, V.**, 2011. Controlling factors of sheet erosion under degraded grasslands in the sloping lands of KwaZulu-Natal, South Africa. IN: *Agricultural Water Management*, Vol. 98.
- Egl, M., Fitze, P., Mirabella, A.**, 2001. Weathering and evolution of soils formed on granitic, glacial deposits: results from chronosequences of Swiss alpine environments. IN: *Catena*, Vol. 45.

- Eijkelkamp**, 2005. Operating Instructions, 09-06 Rainfall Simulator. Eijkelkamp, Agrisearch Equipment.
- Faust D., Schmidt, M.**, 2009. Soil erosion processes and Sediment fluxes in a Mediterranean Marl landscape, campiña de cádiz, SW Spain. IN: Zeitschrift Für Geomorphologie, Vol. 53.
- Forster, G. R., Young, R. A., Ronkens, M. J. M., Onstand, C. A.**, 1985. Processes of soil erosion by water. IN: Soil erosion and crop productivity, Follet F. R, Steward, B. A., American Society of Agronomy and Crop Science Society of America.
- Fox, D. M., Bryan, R. B.**, 1999. The relationship of soil loss by interrill erosion to slope gradient. IN: Catena, Vol. 38.
- Gobin, A., Jones, R., Kirkby, M., Campling, P., Goversa, G., Kosmas C., Gentile, A. R.**, 2004. Indicators for pan-European assessment and monitoring of soil erosion by water. IN: Environmental Science & Policy, Vol. 7.
- Govers, G., Giménez, R., Van Oost, K.**, 2007. Rill erosion: exploring the relationship between experiments, modeling and field observations. IN: Earth-Science Reviews, Vol. 84.
- Govers, G., Poesen, J.**, 1988. Assessment of the interrill and rill contributions to total soil loss from an upland field plot. IN: Geomorphology, Vol. 1.
- Gray, D. H., Sotir, R. B.**, 1996. Biotechnical and soil bioengineering slope stabilization: a practical guide for erosion control. Wiley, New York.
- Gross, C. M., Angle, J. S., Hill, R. L., Welterlen, M.**, 1991. Runoff and sediment losses from tall fescue under simulated rainfall. IN: Journal of Environmental Quality, Vol. 20.
- Gyssels, G., Poesen, J.**, 2003. The importance of plant root characteristics in controlling concentrated flow erosion rates. IN: Earth Surf Process and Landforms, Vol. 28, Issue 4.
- Gyssels, G., Poesen, J., Bochet, E., Li, Y.**, 2005. Impact of plant roots on the resistance of soils to erosion by water: a review. IN: Progress in Physical Geography, Vol. 29.
- Haerberli, W.**, 1975. Untersuchungen zur Verbreitung von Permafrost zwischen Flüelapass und Piz Grialetsch (Graubünden). IN: Mitteilungen der Versuchsanstalt für Wasserbau, Hydrologie und Glaziologie, ETH Zurich Vol. 17.
- Haerberli, W.**, 2013. Mountain permafrost — research frontiers and a special long-term challenge. IN: Cold Regions Science and Technology, Vol. 96.
- Hagen L. J., van Pelt, S., Sharratt B.**, 2010. Estimating the saltation and suspension components from field wind erosion. IN: Aeolian Research, Vol. 1.
- Halsey, L.A., Vitt, D.H., Zoltai, S.C.**, 1995: Disequilibrium response of permafrost in boreal continental western Canada to climate change. IN: Climate Change, Vol. 30.
- Hancock, G. R., Cawter, D., Fityus, S. G., Chandler, J., Wells, T.**, 2008. The measurement and modelling of rill erosion at angle of repose slopes in mine spoil. IN: Earth Surface Processes and Landforms, Vol. 33.
- Harris, S. A., Pedersen, D. E.**, 1998. Thermal regimes beneath coarse blocky materials. IN: Permafrost and Periglacial Processes, Vol. 9.

- Hinzman, L.D., Bettez, N. D., Bolton, R., Chapin, F. S., Dyurgerov, M. B., Fastie, C. L., Griffith, B., Hollister, R. D., Hope, A., Huntington, H., P., Jensen, A., M., Jia, G. J., Jorgenson, T., Kane, D. L., Klein, D. R., Kofinas, G., Lynch, A. H., Lloyd, A. H., McGuire, A. D., Nelson, F. E., Oechel, W. C., Osterkamp, T. E., Racine, C. H., Romanovsky, V. E., Stone, R. S., Stow, D. A., Sturm, M., Tweedie C. E., Vourlitis, G. V., Walker, M. D., Walker, D. A., Webber, P. J., Welker, J. M., Winker, K. S., Yoshikawa, K., 2005:** Evidence and implications of recent climate change in northern Alaska and other arctic regions. IN: *Climate Change*, Vol. 72.
- Horikawa, K., Shen H. W., 1960.** Sand movement by wind action. IN: Beach Erosion Board., Corps of Engineers, Technical Memo. No. 119. Washington, DC.
- Huang, C., Bradford, J., 1993.** Analyses of slope and runoff factors based on the WEPP erosion model. *Soil Science Society of America Journal*, Vol. 57.
- Iserloh T., Ries J. B., Arnáez, J., Boix-Fayos, C., Butzen, V., Cerdà, A., Echeverría, M. T., Fernández-Gálvez, J., Fister, W., Geißler, C., Gómez, J. A., Gómez-Macpherson, H., Kuhn, N. J. Lázaro, R., León, F. J., Martínez-Mena, M., Martínez-Murillo, J. F., Marzen, M., Mingorance, M. D., Ortigosa, L., Peters, P., Regüés, D., Ruiz-Sinoga, J. D., Scholten, T., Seeger, M., Solé-Benet, A., Wengel, R., Wirtz, S., 2013.** European small portable rainfall simulators: A comparison of rainfall characteristics. IN: *Catena*, Vol. 110.
- Jasrotia, A. S., Singh, R., 2006.** Modeling runoff and soil erosion in a catchment area, using the GIS, in the Himalayan region, India. IN: *Environmental Geology*, Vol. 51.
- Jorgenson, T. M., Racine, C. H., Walters, J. C., Osterkamp, T. E., 2001.** Permafrost Degradation and Ecological Changes associated with awarming Climate in Central Alaska. IN: *Climate Change*, Vol. 48.
- Kääb, A., Chiarle, M., Raup, B., Schneider, C., 2007.** Climate change impacts on mountain glaciers and permafrost. IN: *Global and Planetary Change*, Vol. 56.
- Kinnell, P., 1990,** Modelling erosion by rain-impacted flow. In: Bryan, R.B. _Ed., *Soil Erosion, Experiments and Models*. IN: *Catena*, Vol. 17.
- Kinnell, P., McLachlan, C., 1989.** Shallow soil monoliths for laboratory studies on soil erosion from undisturbed soil surfaces. IN: *Australian Journal of Soil Research*, Vol. 27.
- Kirkby, M. J., Bracken, L. J., 2009.** Gully processes and gully dynamics. IN: *Earth Surface Processes and Landforms*, Vol. 1851.
- Knapen, A., Poesen, J., Govers, G., Gyssels, G., Nachtergaele, J., 2007.** Resistance of soils to concentrated flow erosion: a review. IN: *Earth-Science Reviews*, Vol. 80.
- Kneisel, C., Hauck, C., 2003.** Multi-method geophysical investigation of a sporadic permafrost occurrence. IN: Schrott, L., Hoerdt, A., Dikau, R. (Eds.), *Geophysical methods in geomorphology. Zeitschrift für Geomorphologie*, Suppl. 132.
- Kneisel, C., Hauck, C., Vonder Mühl, D., 2000.** Permafrost below the Timberline Confirmed and Characterized by Geoelectrical Resistivity Measurements, Bever Valley, Eastern Swiss Alps. IN: *Permafrost and Periglacial Processes*, Vol. 11.
- Kohl, B., Klosterhuber, R., Hotter, M., Markart, G., 2008.** Steuerung des Oberflächenabflusses durch standortoptimierte Waldbewirtschaftung. IN: *Interpraevent, Conference Proceedings*, Vol. 2.

- Kottek, M., Grieser, J., Beck, C., Rudolf, B., Rubel, F.,** 2006. World Map of Köppen–Geiger Climate Classification Updated. IN: Meteorologische Zeitschrift, Vol. 15.
- Lal, R.,** 1994. Soil Erosion Research Methods, 2nd edition. SWSC.
- Lal, R., Steward, B. A.,** 1990. Soil degradation. New York: Springer Verlag.
- Lattanzi, A., Meyer, L., Baumgardner, M.,** 1974. Influences of mulch rate and slope steepness on interrill erosion. Soil Science Society of America Proceedings, Vol. 38.
- Lemke, P., J. Ren, R.B. Alley, I. Allison, J. Carrasco, G. Flato, Y. Fujii, G. Kaser, P. Mote, R.H. Thomas and T. Zhang,** 2007: Observations: Changes in Snow, Ice and Frozen Ground. In: Climate Change 2007: The Physical Science Basis. Contribution of Working Group I to the Fourth Assessment Report of the Intergovernmental Panel on Climate Change [Solomon, S., D. Qin, M. Manning, Z. Chen, M. Marquis, K.B. Averyt, M. Tignor and H.L. Miller (eds.)]. Cambridge University Press, Cambridge, United Kingdom and New York, NY, USA.
- Lewkowicz, A. G.,** 1992: Factors influencing the distribution and initiation of active-layer detachment slides on Ellesmere Island, arctic Canada. IN: Periglacial Geomorphology [Dixon, J.C. and A.D. Abrahams (eds.)]. Wiley, New York.
- Lyles, L., Cole, G. W., Hagen, L. J.,** 1985. Wind Erosion: Processes and Prediction. IN: Soil Erosion and Crop Productivity, Follett, R. F., Stewart, B. A., Agricultural Research Service.
- Martin, C., Pohl, M., Alewell, C., Körner, C., Rixen, C.,** 2010. Interrill erosion at disturbed alpine sites: Effects of plant functional diversity and vegetation cover. IN: Basic and Applied Ecology, Vol. 11.
- Mattia, C., Bischetti, G., Gentile, F.,** 2005. Biotechnical characteristics of root systems of typical Mediterranean species. IN: Plant Soil Vol. 278
- McCool, D., Brown, L., Foster, G., Mutchler, C., Meyer, L.,** 1987. Revised slope steepness factor for the Universal Soil Loss Equation. IN: Transactions of the American Society of Agricultural Engineers, Vol. 30.
- McCool, D. K., Foster, G. R., Renard, K. G., Yoder, D. C., Weesies, G. A.,** 1995. The Revised Universal Soil Loss Equation.
- Meyer, L. D.,** 1965. Simulations of rainfall for soil erosion research. IN: Transactions of the American Society of Agricultural Engineers, Vol. 8.
- Meyer, L.D.,** 1988. Rainfall simulators for soil conservation research. IN: Lal, R. (Ed.), Soil Erosion Research Methods. Soil and Water Conservation Society. Ankeny, IO, U.S.A..
- Meyer, L. D., Foster, G. R., Römkens, M. J. M.,** 1975. Source of soil eroded by water from upland areas. IN: Present and Prospective Technology for Predicting Sediment Yields and Sources. U.S. Agriculture Research Service.
- Miller, R. M., Jastrow, J. D.,** 1990. Hierarchy of root and mycorrhizal fungal interactions with soil aggregation. IN: Soil Biology and Biochemistry, Vol. 22.
- Millward, A. A., Mersey, J. E.,** 1999. Adapting the RUSLE to model soil erosion potential in a mountainous tropical watershed. IN: CATENA, Vol. 38.
- Moore, I.D., Hirschi, M.C., Barfield, B.J.,** 1983. Kentucky rainfall simulator. Transactions of American Society of Agricultural Engineers, Vol. 26.

- Morgan, R. P. C.**, 1999. Bodenerosion und Bodenerhaltung, Enke im Georg-Thieme Verlag, Stuttgart.
- Morgan, R. P. C.**, 2005. Soil Erosion and Conservation, 2nd edition Blackwell Publishing Limited, USA.
- Moss, A.J.**, 1988. The effects of flow–velocity variations on rain-driven transportation and the role of rain impact in the movement of solids. IN: Australian Journal of Soil Research, Vol. 26.
- Mullan, D.**, 2013. Soil erosion under the impacts of future climate change: Assessing the statistical significance of future changes and the potential on-site and off-site problems. IN: Catena, Vol. 109.
- Muller, S. W.**, 1947. Permafrost or permanently frozen ground and related engineering problems. J.W. Edwards, Ann Arbor,
- Munn, J. R., Huntington, G. L.**, 1976. A portable rainfall simulator for erodibility and infiltration measurements in rugged terrain. IN: Soil Science Society of America, Journal, Vol. 40.
- Nelson, F. E., Anisimov, O. A., Shiklomanov, N. I.**, 2001: Subsidence risk from thawing permafrost. IN: Nature, Vol. 410.
- Nilaweera, N. S., Nutalaya, P.**, 1999. Role of tree roots in slope stabilization. IN: Bulletin of Engineering Geology and the Environment, Vol. 57.
- Nötzli, J., Gruber, S.**, 2005. Alpiner Permafrost – Ein Überblick. IN: Jahrbuch des Vereins zum Schutz der Bergwelt, 70.
- Osterkamp, T. E.**, 1983. Response of Alaskan Permafrost to Climate. IN: Proceedings of the Fourth International Conference on Permafrost, Vol. 2, National Academy Press, Washington, D.C.
- Osterkamp, T. E., Esch, D. C., and Romanovshy, V. E.**, 1998. Permafrost. IN: Weller, G. and Anderson, P. A. (eds.), Implications of Global Change in Alaska and the Bering Sea Region, Center for Global Change and Arctic System Research, University of Alaska.
- Péwé T.L.**, 1975. Quaternary Geology of Alaska. U.S. Geological Survey Professional Paper 835.
- Pimentel, D., Harvey, C., Resosudarmo, P., Sinclair, K., Kurz, D., MnCair, M., Crist, S., Shpritz, L., Fitton, L., Saffouri, R., Blair, R.**, 1995. Environmental and economic costs of soil erosion and conservation benefits. IN: Science Vol. 267.
- Pimentel, D., Kounang, N.**, 1998. Ecology of Soil Erosion in Ecosystems. IN: Ecosystems.
- Poesen, J., Nachtergaele, J., Verstraeten, G., Valentin, C.**, 2003. Gully erosion and environmental change: importance and research needs. IN: Catena, Vol. 50.
- Pohl, M., Alig, D., Körner, C., Rixen, C.**, 2009. Higher plant diversity enhances soil stability in disturbed alpine ecosystems. IN: Plant Soil, Vol. 324.
- Prasannakumar, V., Vijith, H., Abinod, S., Geetha N.**, 2012. Estimation of soil erosion risk within a small mountainous sub-watershed in Kerala, India, using Revised Universal Soil Loss Equation (RUSLE) and geo-information technology. IN: Geoscience Frontiers, Vol. 3.
- Pruski, F. F., Nearing, M. A.**, 2002. Climate-induced changes in erosion during the 21st century for eight U.S. locations. IN: Water Resources Research, Vol. 38.
- Punz, W., Sieghardt, H., Maier, R., Engenhardt, M., Christian, E.**, 2005. Kaltlöcher im Ostalpenraum. IN: Verh. Zoologische-Botanische Gesellschaft Österreich, Vol. 142.

- Renard, K. G., Foster, G. R., Weesies, G. A., McCool, D. K., Yoder, D. C.,** 1997. Predicting Soil Erosion by Water: A Guide to Conservation Planning with the Revised Universal Soil Loss Equation (RUSLE). IN: Agriculture Handbook, Vol. 703. US Department of Agriculture, Washington, DC.
- Renard, K. G., Foster, G. R., Weesies, G. A., Porter, J. P.,** 1991. RUSLE – Revised Universal Soil Loss Equation. IN: Journal of Soil and Water Conservation, Vol. 46.
- Reubens, B., Poesen, J., Danjon, F., Geudens, G., Muys, B.,** 2007. The role of fine and coarse roots in shallow slope stability and soil erosion control with a focus on root system architecture: a review. IN: Trees-Structure and Function, Vol. 21.
- Rey, F., Isselin-Nondedeu, F., Bédécarrats, A.,** 2007. Vegetation Dynamics on Sediment Deposits Upstream of Bioengineering Works in Mountainous Marly Gullies in a Mediterranean Climate (Southern Alps, France). IN: Plant and Soil, Vol. 278.
- Ramos, M. C., Nacci, S., Pla, I.,** 2003. Effect of raindrop impact and its relationship with aggregate stability to different disaggregation forces. IN: Catena, Vol. 55.
- Scheffer, F., Schachtschabel, P.,** 2002. Lehrbuch der Bodenkunde, 15th edition. Spektrum Akademischer Verlag GmbH, Heidelberg, Berlin.
- Schwarb, M., Daly, C., Frei, C, Schär, C.,** 2000. Mittlere jährliche Niederschlagshöhe im europäischen Alpenraum 1971-1990. IN: Hydrologischer Atlas der Schweiz.
- Shit, P. K., Bhunia, G. S., Maiti, R.,** 2012: Effect of Vegetation Cover on Sediment Yield: An Empirical Study through Plots Experiment. IN: Journal of Environment and Earth Science, Vol. 2, No. 5.
- Shur, Y. L., Jorgenson M. T.,** 2007. Patterns of Permafrost Formation and Degradation in Relation to Climate and Ecosystems. IN: Permafrost and Periglacial Process. Vol. 18:
- Singh, T. V., Kaur, J.,** 1989. Studies in Himalayan ecology and development strategies. New Dehli,: Hymalayan.
- Skidmore, E. L.,** 2000. Air, soil, and water quality as influenced by wind erosion and strategies for mitigation. IN: Agronenviron 2000, Second International
- Skre, O., Oechel, W. C., Miller, P. M.,** 1983. Moss water leaf content and solar radiation at the moss surface in mature black spruce forest in central Alaska. IN: Canadian Journal of Forest Research, Vol. 13.
- Stroosnijder, L.,** 2005. Measurement of erosion: Is it possible? IN: Catena. Vol. 64.
- Styczen, M. E., Morgan, R. P. C.,** 1995. Engineering properties of vegetation. IN: Slope Stabilization and Erosion Control: A Bioengineering Approach, Morgan, R. P. C., Rickson, R. J..
- UNEP (United Nations, Environment Programme),** 1994. IN: Environmental Data Report 1993–94, United Nations Environmental Programme, Oxford.
- USDA (U. S. Department of Agriculture), NRCS (Natural Resources Conservation Service),** 2000. Index – Revised Universal Soil Loss Equation (RUSLE).
- Vahabi, J., Nikkami, D.,** 2008. Assessing dominant factors affecting soil erosion using a portable rainfall simulator. IN: International Journal of Sediment Research, Vol. 23.

- Vonder Mühl, D., Delaloye, R., Haerberli, W., Hölzle, M., Krummenacher B.,** 2001. Permafrost Monitoring Switzerland PERMOS 1. Jahresbericht 1999/2000, Schweizerische Akademie der Naturwissenschaften (SANW)
- Walsh, J., Anisimov, O., Hagen, J. O. M., Jakobsson, T., Oerlemans, J., Prowse, T. D., Romanovsky, V., Savelieva, N., Serreze, M., Shiklomanov, A., Shiklomanov, I., Solomon, S.,** 2005: Cryosphere and hydrology. IN: Arctic Climate Impact Assessment. Cambridge University Press, Cambridge and New York, pp. 183–242.
- Ward T. J., Bolton, S. M.,** 1991. Hydrology parameters for selected in Arizona and New Mexico as determined by rainfall simulation.
- Wardle, D. A., Bardgett, R. D., Klironomos, J. N., Setälä, H., van der Putten, W. H., Wall, D. H.,** 2004. Ecological linkages between aboveground and below ground biota. IN: Science. Vol. 304
- Warrington, I., Shainberg, I., Agassi, M., Morin, J.,** 1989. Slope and phosphogypsum effect on runoff and erosion. IN: Soil Science Society of America Journal, Vol. 53.
- Watson, D., Laflen, J.,** 1986. Soil strength, slope, and rainfall intensity effects on interrill erosion. IN: Transactions of the American Society of Agricultural Engineers, Vol. 29.
- White, B. R., and J. C. Schulz,** 1977. Magnus effect in saltation. IN: Journal of Fluid Mechanics, Vol. 81, Issue 3.
- Wirtz, S., Iserloh, T., Rock, G., Hansen, R., Marzen, M., Seeger, M., Betz, S., Remke, A., Wengel, R., Butzen, V., Ries, J. B.,** 2012. Soil Erosion on Abandoned Land in Andalusia: A Comparison of Interrill- and Rill Erosion Rates. IN: ISRN Soil Science.
- Witter, J. V., Jungerius, P. D., ten Harkel, M. J.,** 1991. Modelling Water Erosion and the Impact of Water Repellency. IN: Catena, Vol. 18.
- Woodward, D. E.,** 1999. Method to predict cropland ephemeral gully erosion. IN: Catena, Vol. 37.
- Wu, T. H., Wang, Q. X., Watanabe, M., Chen, J., Battogtokh, D.,** 2009. Mapping vertical profile of discontinuous permafrost with ground penetrating radar at Nalaikh depression, Mongolia. IN: Environmental Geology Vol. 56.
- Yang, Z., Ou, Y. H., Xu, X., Zhao, L., Song, M., Zhou, C.,** 2010. Effects of permafrost degradation on ecosystems. IN: Acta Ecologica Sinica. Vol. 30.
- Zhang, T., Barry, R. G., Knowles, K., Heginbottom, J. A., Brown, J.,** 1999. Statistics and characteristics of permafrost and ground-ice distribution in the northern hemisphere. IN: Polar Geography, Vol. 23.
- Zhang, T., Nelson, F. E., Gruber, S.,** 2007. Introduction to special section: permafrost and seasonally frozen ground under a changing climate. IN: Journal of Geophysical Research Vol. 1

7 Source of Figures

Table 21 Sources of the used figures (Part 1).

Figure Number:	Source:	Date of access:	Link:
Figure 1	WWF (World Wide Fund for Nature)	24.03.2014	https://worldwildlife.org/photos/soil-erosion-and-degradation
Figure 2	Pascale Polich (own photograph)	2013	–
Figure 3	Wind erosion research, Kansas State University	19.02.2014	http://www.weru.ksu.edu/weps/wepshome.htm
Figure 4	Landloch	24.03.2014	http://www.landloch.com.au/facilities/rainfall-simulator/
Figure 5	Clark, T., Dahlhauser, Q., Holtz, B., 2002. Small-Scale Rainfall Simulator, Iowa State University	31.03.2014	http://www3.abe.iastate.edu/ae445/SmallScaleRainfallSimulator.pdf
Figure 6	Permos (Swiss Permafrost Monitoring Network)	24.03.2014	http://www.permos.ch/info.html
Figure 7	Larry Hinzmann, Next Generation, Ecosystem Experiment	12.02.2014	http://ngee-arctic.blogspot.ch/2011/08/this-was-wonderful-trip-from-all.html
Figure 8	Schweizerische Eidgenossenschaft, map.geo.admin	01.04.2013	https://map.geo.admin.ch/?X=190000.00&Y=660000.00&zoom=1&lang=en&topic=ech&bgLayer=ch.swisstopo.pixelkarte-farbe

Table 22 Sources of the used figures (Part 2).

Figure Number:	Source:	Date of access:	Link:
Figure 9	Schweizerische Eidgenossenschaft, map.geo.admin	01.04.2013	https://map.geo.admin.ch/?X=190000.00&Y=660000.00&zoom=1&lang=en&topic=ech&bgLayer=ch.swisstopo.pixelkarte-farbe
Figure 10	Barbara Zollinger (University of Zurich)	2013	–
Figure 11	Barbara Zollinger (University of Zurich)	2013	–
Figure 12	Pascale Polich (own photograph)	2013	–
Figure 13	Schweizerische Eidgenossenschaft, map.geo.admin	01.04.2013	https://map.geo.admin.ch/?X=190000.00&Y=660000.00&zoom=1&lang=en&topic=ech&bgLayer=ch.swisstopo.pixelkarte-farbe
Figure 14	Barbara Zollinger (University of Zurich)	2013	–
Figure 15	Barbara Zollinger (University of Zurich)	2013	–
Figure 16	Pascale Polich (own photograph)	2013	–
Figure 20	Pascale Polich (own photograph)	2013	–
Figure 21	Eijkkelkamp, Agrisearch Equipment	06.02.2014	http://pkd.eijkkelkamp.com/Portals/2/Eijkkelkamp/Files/Manuals/M1-0906e%20Rainfall%20simulator.pdf
Figure 55	Pascale Polich (own photograph)	2013	–
Figure 58	Pascale Polich (own photograph)	2013	–

8 Appendix

8.1 Appendix A: Illustrations of the plot survey

In the following appendix, the mean results of the plot survey are illustrated in histograms, divided in the two study sites Spinass and Bever. In the histograms, the measured values as well as the frequencies of the specific values are shown. In an ideal case these variables would have been uniformly frequent over the ranges. Unfortunately that was not possible, even though it was planned in the first place. But the high gravel content in the soil in the two study sites restricted the range of soil plots, due to an impossible fixation of the ground frame. As well the fact that the rain simulator does not work properly on large slope inclinations ($>30^\circ$) reduced the selection of measurement points. The equal number of plots on permafrost influenced soil and non permafrost soil was a more important selection criterion.

Slope

Spinas

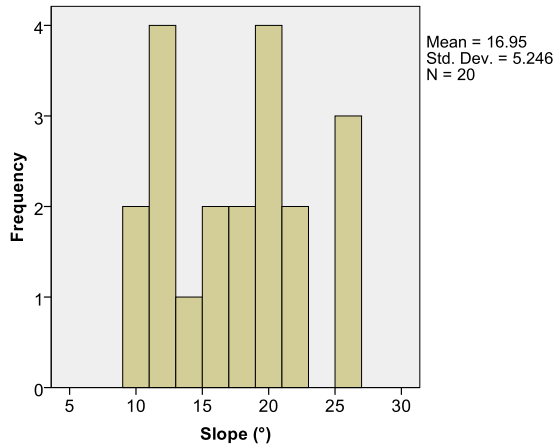


Figure 60 Histogram of the slope inclination at the investigated soil plots at Spinas (SPSS).

Bever

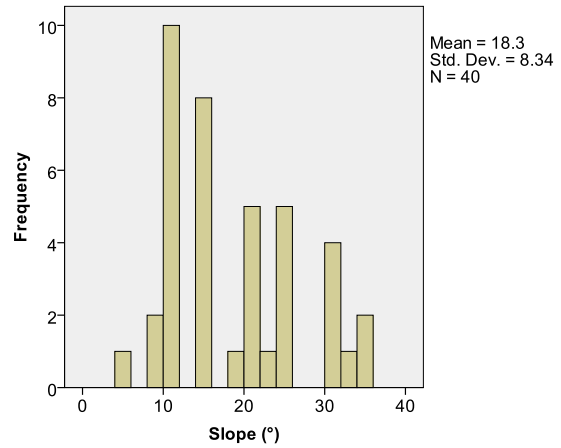


Figure 61 Histogram of the slope inclination at the investigated soil plots at Bever (SPSS).

In the diagrams above (Figure 60 and Figure 61), one can see the slope inclination of the investigated soil plots. At Spinas (left) the slope inclinations were located between 10 and 20°, at Bever (right) between 5 and 35°. The mean slope inclination over the plots at Bever (18.3°) was a bit steeper than at Spinas (16.95°) and also the steepest investigated plot was measured at Bever (35°).

Neither in the box plot of Spinas nor in the one of Bever one can perceive noticeable outliers or extreme values (Figure 62 and Figure 63).

Spinas

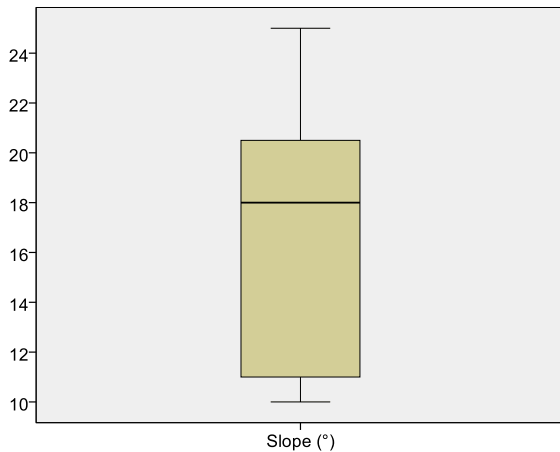


Figure 62 Box plot of the slope inclination at the investigated soil plots at Spinas (SPSS).

Bever

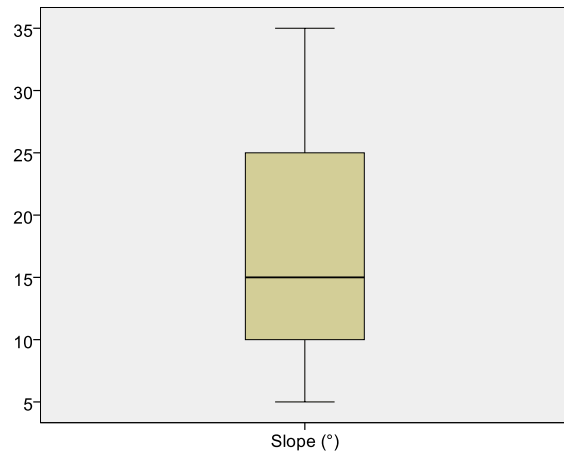


Figure 63 Box plot of the slope inclination at the investigated soil plots at Bever (SPSS).

Vegetation cover

Spinas

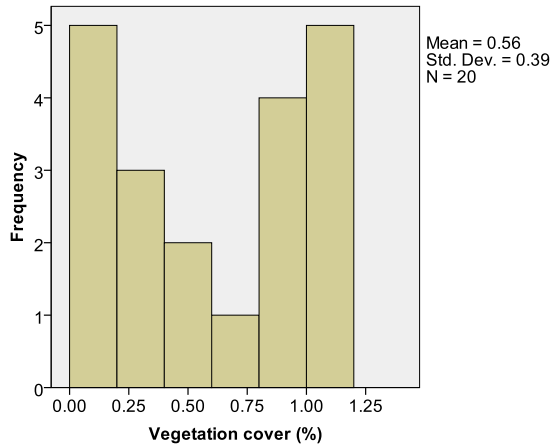


Figure 65 Histogram of the vegetation cover at the investigated soil plots at Spinas (SPSS).

Bever

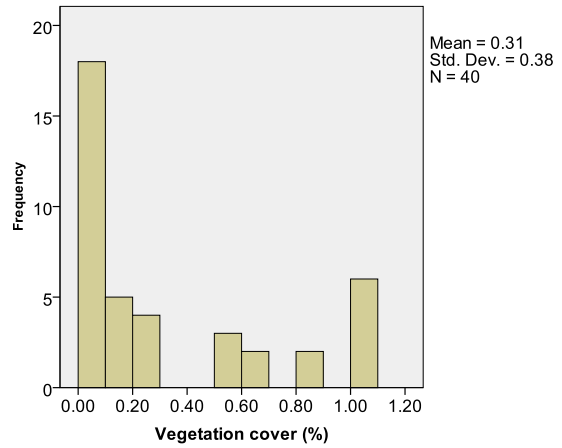


Figure 64 Histogram of the vegetation cover at the investigated soil plots at Bever (SPSS).

In Figure 64 and Figure 65 the vegetation cover of the investigated plots are illustrated. The values are situated between 0 and 1 (0 and 100%). In the comparison of the two diagrams, one can see that the analyzed plots at Spinas (Mean: 0.56) have a greater vegetation cover as such at Bever (Mean: 0.31). This fact might explain the low values in surface runoff and sediment yield at Spinas.

The box plots below (Figure 66 and Figure 67) show the same conditions as the ones of the slope dataset. One cannot see any outliers.

Spinas

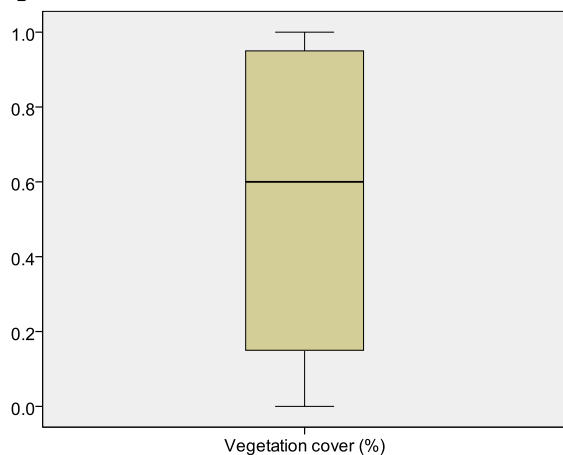


Figure 67 Box plot of the vegetation cover at the investigated soil plots at Spinas (SPSS).

Bever

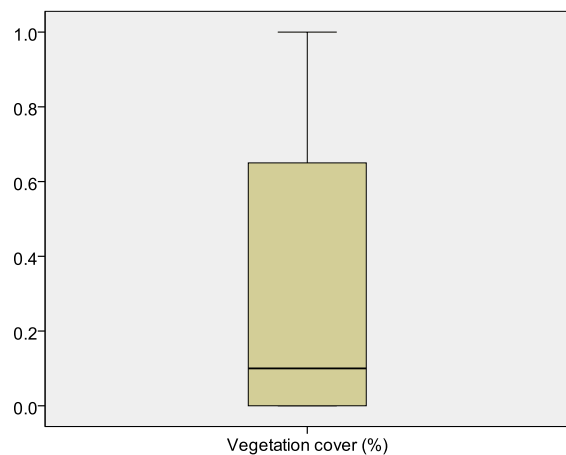


Figure 66 Box plot of the vegetation cover at the investigated soil plots at Bever (SPSS).

Gravel content

Spinas

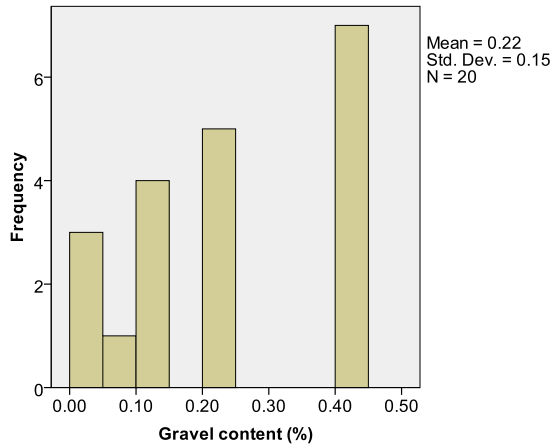


Figure 68 Histogram of the gravel content at the investigated soil plots at Spinas (SPSS).

Bever

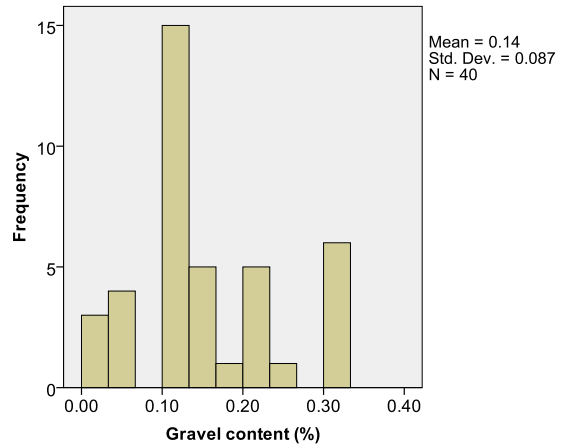


Figure 69 Histogram of the gravel content at the investigated soil plots at Bever (SPSS).

In the graphs above (Figure 68 and Figure 69), the gravel content of the soil plots are posed. At Spinas the gravel content is situated between 0 and 0.4 (0 and 40%), at Bever between 0 and 0.3 (0 and 30%). One can see that the mean gravel content at Spinas is higher (22%) than at Bever (14%).

Also for the gravel content, the box plots (Figure 70 and Figure 71) show no remarkable outliers or extreme values.

Spinas

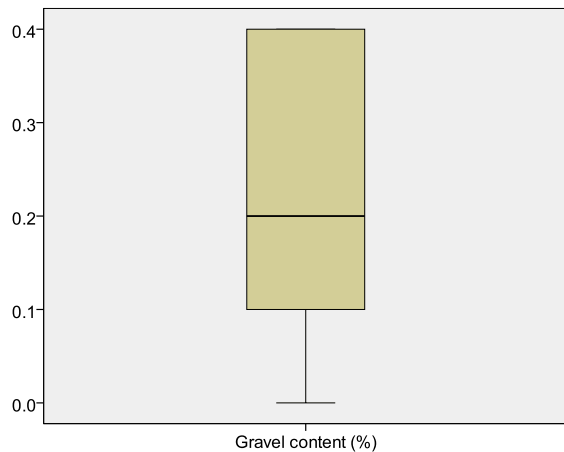


Figure 71 Box plot of the gravel content at the investigated soil plots at Spinas (SPSS).

Bever

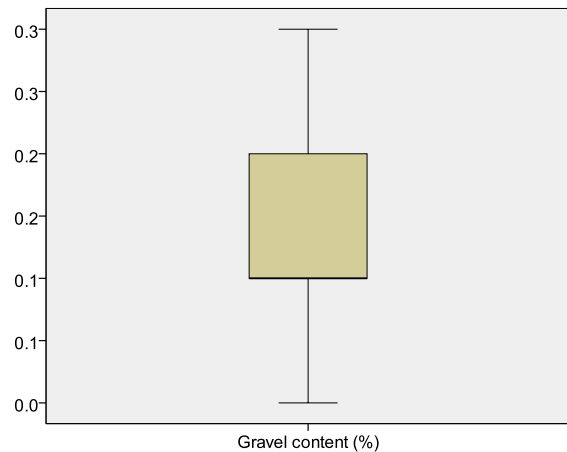


Figure 70 Box plot of the gravel content at the investigated soil plots at Bever (SPSS).

Soil moisture

The following graphs show the results of the TDR-measurements of soil moisture. The blue columns represent the soil moisture before the rainfall simulation, the green ones the soil moisture afterwards. In orange, the difference between the two soil moisture values is illustrated.

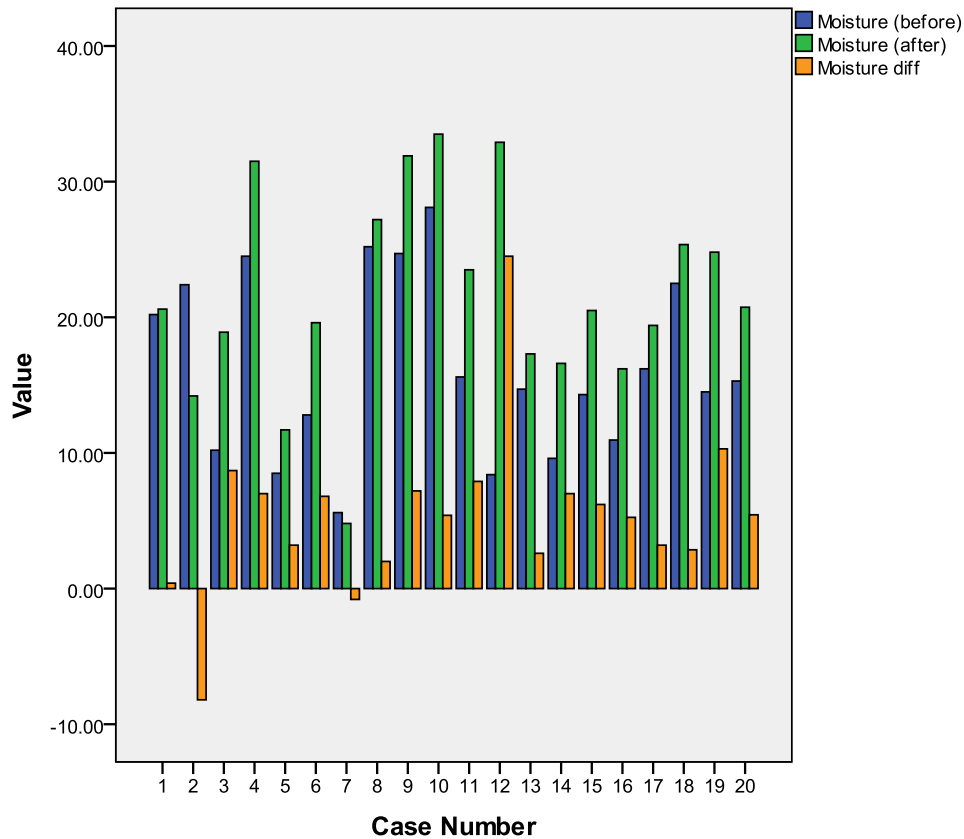


Figure 72 Soil moisture before and after the rain simulations and the soil moisture difference at Spinus (SPSS).

In the both cases, Spinus (Figure 72) and Bever (Figure 73), some columns of the soil moisture difference show a negative value. A possible explanation for this case could be the difference in measurement position between the two measurements. As mentioned in the chapter about soil plot survey, the soil moisture measurement before the rainfall simulation was conducted next to the investigated soil plot, the one after the simulation within the patch. Due to large difference in soil moisture on a small-scale as a result of as example small depressions, this case can happen.

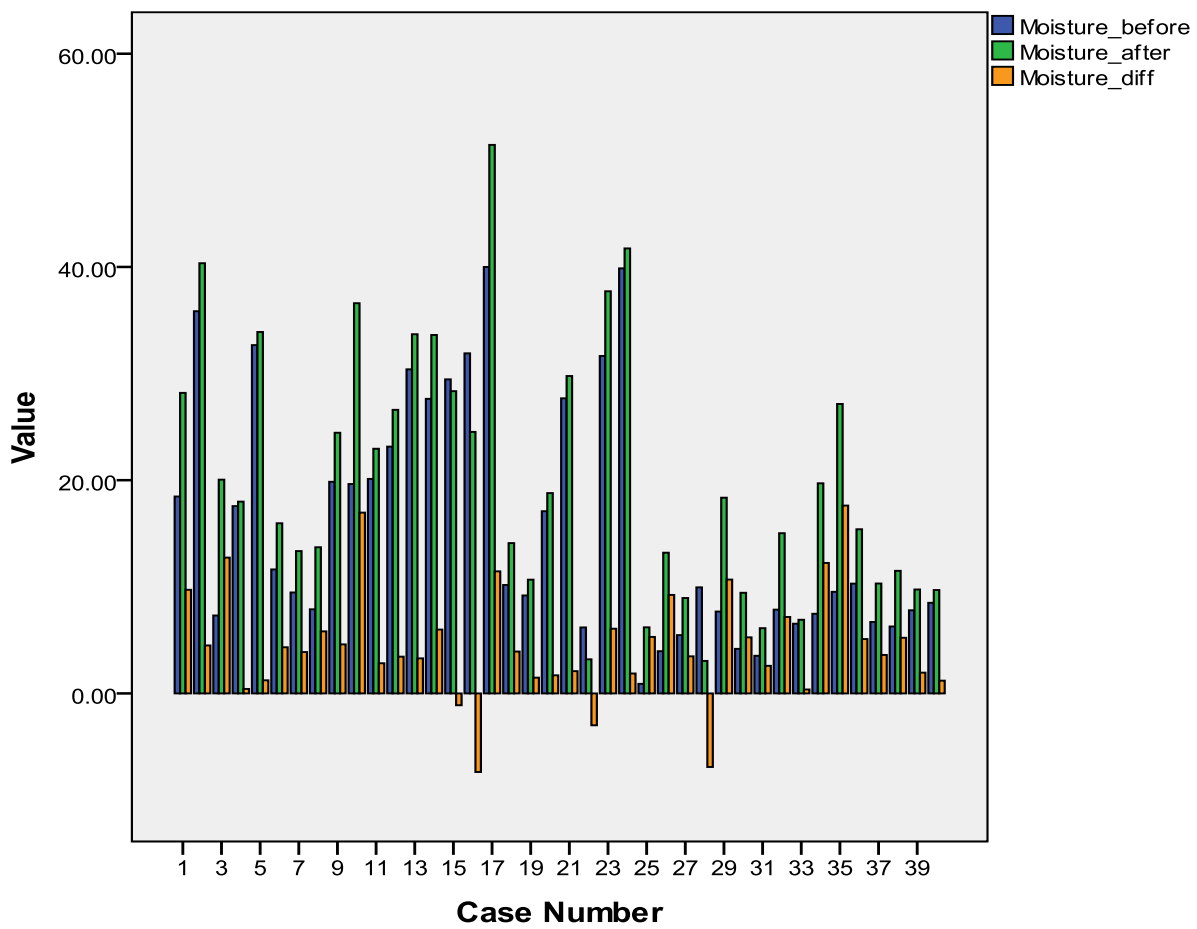


Figure 73 Soil moisture before and after the rain simulations and the soil moisture difference at Bever (SPSS).

8.2 Appendix B: Descriptive statistics

In this appendix one can see the descriptive statistics of several variables described in the results of this study. In this tables (1) the number of samples (N Statistic), (2) the range of values (Range Statistic), (3) the minimum, or the smallest value of the variable (Minimum Statistic), (4) the maximum, or the largest value of the variable (Maximum Statistic) (5) the mean / average, this is the arithmetic mean across the observations. It is the most widely used measure of central tendency. The mean is sensitive to extremely large or small values (Mean Statistic), (6) the standard error of the Mean (Mean Std. Error), (7) the standard deviation is the square root of the variance. It measures the spread of a set of observations. The larger the standard deviation is, the more spread out the observations are (Std. Deviation Statistics) and (8) the variance, a measure of variability. It is the sum of the squared distances of data value from the mean divided by the variance divisor (Variance Statistic).

Sediment yield

In Table 23 the descriptive statistics of the variable sediment yield at Spinas is showed for the raw dataset. In Table 24 the same descriptive statistics are showed for the adapted dataset without outliers. One can see a reduction of the standard error after the elimination of the outliers.

Table 23 Spinas: descriptive statistics of the sediment yield (raw data).

	N	Range	Minimum	Maximum	Mean		Std. Deviation	Variance
	Statistic	Statistic	Statistic	Statistic	Statistic	Std. Error	Statistic	Statistic
Sediment yield (g)	20	0.06	0.00	0.06	0.01	0.004	0.02	0.00
Valid N (listwise)	20							

Table 24 Spinas: descriptive statistics of the sediment yield (without outliers).

	N	Range	Minimum	Maximum	Mean		Std. Deviation	Variance
	Statistic	Statistic	Statistic	Statistic	Statistic	Std. Error	Statistic	Statistic
Sediment yield (g)	18	0.05	0.00	0.05	0.012	0.003	0.01	0.00
Valid N (listwise)	18							

In Table 25 the descriptive statistics of the variable sediment yield at Bever is showed for the raw dataset. In Table 26 the same descriptive statistics are showed for the adapted dataset without outliers.

Table 25 Bever descriptive statistics of the sediment yield (raw data).

	N	Range	Minimum	Maximum	Mean		Std. Deviation	Variance
	Statistic	Statistic	Statistic	Statistic	Statistic	Std. Error	Statistic	Statistic
Sediment yield (g)	40	11.63	0.00	11.63	0.54	0.30	1.93	3.72
Valid N (listwise)	40							

Table 26 Bever descriptive statistics of the sediment yield (without outliers).

	N	Range	Minimum	Maximum	Mean		Std. Deviation	Variance
	Statistic	Statistic	Statistic	Statistic	Statistic	Std. Error	Statistic	Statistic
Sediment yield (g)	36	0.42	0.00	0.42	0.09	0.02	0.11	0.01
Valid N (listwise)	36							

Surface runoff

In Table 27 the descriptive statistics of the variable surface runoff at Spinas is showed for the raw dataset. In Table 28, the same descriptive statistics are showed for the adapted dataset without outliers.

Table 27 Spinas: descriptive statistics of the surface runoff (raw data).

	N	Range	Minimum	Maximum	Mean		Std. Deviation	Variance
	Statistic	Statistic	Statistic	Statistic	Statistic	Std. Error	Statistic	Statistic
Surface runoff (ml)	20	65.92	0.00	65.92	7.00	3.35	15.01	225.23
Valid N (listwise)	20							

Table 28 Spinas: descriptive statistics of the surface runoff (without outliers).

	N	Range	Minimum	Maximum	Mean		Std. Deviation	Variance
	Statistic	Statistic	Statistic	Statistic	Statistic	Std. Error	Statistic	Statistic
Surface runoff (ml)	18	12.82	0.00	12.82	2.90	0.96	4.10	16.79
Valid N (listwise)	18							

In Table 29 the descriptive statistics of the variable surface runoff at Spinas is showed for the raw dataset. In Table 30, the same descriptive statistics are showed for the adapted dataset without outliers.

Table 29 Bever descriptive statistics of the surface runoff (raw data).

	N	Range	Minimum	Maximum	Mean		Std. Deviation	Variance
	Statistic	Statistic	Statistic	Statistic	Statistic	Std. Error	Statistic	Statistic
surface runoff (ml)	40	809.18	0.00	809.18	110.84	26.98	170.64	29117.37
Valid N (listwise)	40							

Table 30 Bever descriptive statistics of the surface runoff (without outliers).

	N	Range	Minimum	Maximum	Mean		Std. Deviation	Variance
	Statistic	Statistic	Statistic	Statistic	Statistic	Std. Error	Statistic	Statistic
surface runoff (ml)	36	281.11	0.00	281.11	68.87	14.27	85.62	7331.24
Valid N (listwise)	36							

C/N ratio

In the following tables the descriptive statistics of the C/N ration at Spinus (Table 31) and Bever (Table 32) are showed.

Table 31 Descriptive statistics of the C/N ration at Spinus (SPSS).

	N	Range	Mini- mum	Maxi- mum	Mean		Std. Devia- tion	Variance
	Statistic	Statistic	Statistic	Statistic	Statistic	Std. Error	Statistic	Statistic
Ratio C/N	20	26.23	12.54	38.76	28.09	1.63	7.27	52.93
Valid N (listwise)	20							

Table 32 Descriptive statistics of the C/N ration at Bever (SPSS).

	N	Range	Mini- mum	Maxi- mum	Mean		Std. Devia- tion	Variance
	Statistic	Statistic	Statistic	Statistic	Statistic	Std. Error	Statistic	Statistic
Ratio C/N	40	15.21	0.74	15.95	8.74	0.80	5.05	25.47
Valid N (listwise)	40							

Below, also the absolute values of carbon and nitrogen in the topsoil are showed (volume percent) (Table 33 and Table 34).

Table 33 Descriptive statistics of the carbon and nitrogen at Spinus.

	N	Range	Minimum	Maximum	Mean		Std. Devia- tion	Variance
	Statistic	Statistic	Statistic	Statistic	Statistic	Std. Error	Statistic	Statistic
C_mean (%)	20	38.22	7.52	45.75	26.48	3.03	13.58	184.45
N_mean (%)	20	1.38	0.23	1.61	0.95	0.09	0.42	0.18
Valid N (listwise)	20							

Table 34 Descriptive statistics of the carbon and nitrogen at Bever.

	N	Range	Minimum	Maximum	Mean		Std. Devia- tion	Variance
	Statistic	Statistic	Statistic	Statistic	Statistic	Std. Error	Statistic	Statistic
C_mean (%)	40	20.30	0.10	20.40	5.30	0.91	05.76	33.18
N_mean (%)	40	1.20	0.10	1.30	0.44	0.052	0.33	0.11
Valid N (listwise)	40							

pH value (laboratory)

In the following tables the descriptive statistics of the C/N ration at Spinus (Table 35) and Bever (Table 36) are showed.

Table 35 Descriptive statistics of the measured pH value (laobratory) at Spinus.

	N	Range	Minimum	Maximum	Mean		Std. Devia- tion	Variance
	Statistic	Statistic	Statistic	Statistic	Statistic	Std. Error	Statistic	Statistic
pH Laboratory	20	2.4	1.9	4.3	3.56	0.11	0.51	0.26
Valid N (listwise)	20							

Table 36 Descriptive statistics of the measured pH value (laobratory) at Bever.

	N	Range	Minimum	Maximum	Mean		Std. Devia- tion	Variance
	Statistic	Statistic	Statistic	Statistic	Statistic	Std. Error	Statistic	Statistic
pH Laboratory	40	1.7	3.6	5.3	4.35	0.05	0.33	0.11
Valid N (listwise)	40							

8.3 Appendix C: C/N ratios of alpine soils

Table 37 C/N ratio and the amount of carbon and nitrogen in alpine soils.

Horizon	C g/kg	N g/kg	C/N
Ah	25.7	1.1	23.4
Ah	38.6	2.4	16
Ah	98.2	6.1	16
Ah	114.6	7.9	14.5
Ah	120.5	9.0	13.4
O	217.6	13.4	16.2
O	142.8	8.7	16.4
O	383.3	18	21.3

In Table 37 one can see the amount of carbon and nitrogen, as well as the C/N ratio of topsoil samples at two alpine sites in Switzerland (measured by Egli et al., 2001).

Table 38 C/N ratio and the amount of carbon and nitrogen in the topsoil of “Albula”, “Bever”, and “Spinas”.

Horizon	C g/kg	N g/kg	C/N
O	197	15	13
A	99.3	7.7	13
O	110.0	7.8	14
AE	33.0	3.0	11
AE	73.9	5.5	13
A	79.6	7.4	11
E	58.4	3.2	18
E	63.5	5.8	11
A	65.7	3.2	21
A	71.7	6.6	11
A	81	5.9	14
A	31.6	4.1	8
A	146.5	9.0	16
A	128.0	8.5	15
A	15.8	3.1	5
Ah	19.6	3.1	6
Ah	29.6	3.8	8
A	27.4	2.3	12
AE	71.2	4.1	18
A	96.4	5.6	17

Table 38 shows a second reference from Zollinger et al., 2013. In their article they measured the carbon and the nitrogen in three different study sites. Two of them are alpine sites (Albula and Bever) and one is subalpine (Spinas). Thereby, Spinas and Bever are in the same area as the study sites of this current master thesis.

8.4 Appendix D: pH values Zollinger et al., 2013

In Table 39 and Table 40 one can see the measured pH values at Spinas and Bever published in Zollinger et al., 2013. They measured a mean pH of 3.8 at Spinas and 4.2 in Bever.

Table 39 Measured pH values at Spinas in Zollinger et al., 2013.

Site	Horizon	pH value
Spinas	E	4.0
Spinas	E	3.8
Spinas	A	3.8
Spinas	A	3.8
Spinas	A	3.9
Spinas	Ah	3.5
Spinas	AE	3.9

Table 40 Measured pH values at Bever in Zollinger et al., 2013.

Site	Horizon	pH value
Bever	O	4.0
Bever	A	4.1
Bever	O	3.9
Bever	A	4.5
Bever	Ah	4.6
Bever	Ah	4.4

8.5 Appendix E: Data sets

8.5.1 Spinas

In the following tables, the whole dataset of Spinas and Bever are illustrated. In Table 41 one can see the general information of the plots at Spinas, conducted with the plot survey in the field as well as the (in the laboratory) measured pH values.

Table 41 Dataset of Spinax (Part 1).

Plot Nr.	Coordinates	Elevation (asl)	Slope (°)	Exposition °N	PF / no PF	Vegetation cover (%)	Gravel content (%)	pH Hellige	pH Laboratory
1	N 46° 33.349 E 9° 51.460	1797 m	11 °	5°N	no	100%	20%	4.5	3.97
2	N 46° 33.345 E 9° 51.442	1801 m	15 °	80°N	no	30%	20%	4	3.75
3	N 46° 33.366 E 9° 51.439	1813 m	21 °	200°N	yes	70%	20%	4	4.3
4	N 46° 33.349 E 9° 51.450	1807 m	20 °	330°N	yes	50%	40%	4	3.82
5	N 46° 33.336 E 9° 51.467	1795 m	21 °	325°N	yes	100%	40%	4	3.15
6	N 46° 33.343 E 9° 51.463	1779 m	10 °	60°N	yes	100%	40%	4	3.32
7	N 46° 33.287 E 9° 51.684	1742 m	18 °	0°N	no	0%	10%	4	4.1
8	N 46° 33.302 E 9° 51.700	1754 m	19 °	335°N	no	80%	3%	4.5	3.45
9	N 46° 33.301 E 9° 51.719	1754 m	15 °	350°N	no	20%	15%	4.5	3.57
10	N 46° 33.304 E 9° 51.710	1785 m	11 °	15°N	no	10%	20%	4	3.52
11	N 46° 33.304 E 9° 51.700	1791 m	25 °	15°N	no	10%	15%	4.5	3.75
12	N 46° 33.309 E 9° 51.717	1800 m	10 °	25°N	no	3%	20%	4.5	1.9
13	N 46° 33.350 E 9° 51.471	1791 m	11 °	310°N	yes	100%	0%	4	3.27
14	N 46° 33.350 E 9° 51.471	1791 m	20 °	340°N	yes	10%	0%	4	3.85
15	N 46° 33.358 E 9° 51.323	1806 m	25 °	70°N	yes	20%	40%	4	3.6
16	N 46° 33.353 E 9° 51.491	1784 m	20 °	25°N	yes	100%	40%	4	3.42
17	N 46° 33.358 E 9° 51.333	1792 m	25 °	20°N	yes	80%	40%	4	3.1
18	N 46° 33.361 E 9° 51.331	1793 m	18 °	60°N	yes	50%	40%	4	3.45
19	N 46° 33.339 E 9° 51.334	1784 m	11 °	90°N	no	90%	5%	4.5	3.92
20	N 46° 33.367 E 9° 51.310	1785 m	13 °	100°N	no	90%	10%	4.5	4.02

In Table 42 the Soil physical properties (measured with the TDR) are listed for Spinas.

Table 42 Dataset of Spinas (Part 2).

Plot Nr.	Moisture before	Moisture after	Surface runoff (ml)	Sediment yield (g)	Temp °C before	Temp after °C	Conductivity before	Conductivity after
1	20.2	20.6	0	0	10.8	8.7	1.2	0.5
2	22.4	14.2	0	0	19	16.4	0.3	0.4
3	10.2	18.9	0	0	12	14.8	0.6	1.5
4	24.5	31.5	0	0	12.2	11.3	0.6	0
5	8.5	11.7	1	0	10.3	8.7	0.2	0.4
6	12.8	19.6	0.43	0.01	7.4	7.3	0.2	0
7	5.6	4.8	21.84	0.06	13.5	10.8	0	0
8	25.2	27.2	1.07	0.01	6.2	6.1	0.1	0
9	24.7	31.9	4.5	0.01	5.9	6.2	0.3	0.1
10	28.1	33.5	0.44	0.04	6.5	7	0.3	0.8
11	15.6	23.5	12.82	0.05	8.9	9.1	1.1	1.3
12	8.4	32.9	0	0	9.8	9.6	0.7	0.4
13	14.7	17.3	65.92	0.02	7.2	6.1	0	0
14	9.6	16.6	10.22	0.02	6.1	7	0.9	0.4
15	14.3	20.5	9.72	0.01	6.5	7.2	0.7	0
16	10.9	16.2	0	0	1.5	1.3	0	0
17	16.2	19.4	5.03	0.01	2.9	1.8	0.7	0.8
18	22.5	25.36	0	0	3.9	4	1.4	1.5
19	14.5	24.8	2.74	0.04	4.9	5.6	0.8	1
20	15.3	20.7	4.28	0.02	6.8	6.7	0.6	0.9

In Table 43 information about the grain size distribution, as well as the amount of carbon, hydrogen and nitrogen and the C/N ratio are listed.

Table 43 Dataset of Spinax (Part 3).

Plot Nr.	Ratio fine/coarse	C (%)	H (%)	N (%)	Ratio C/N
1	0.92	9.6	1.64	0.37	26.26
2	0.88	19.25	2.95	0.86	22.27
3	0.36	16.55	2.48	0.68	24.39
4	1.28	36.3	4.87	0.95	38.1
5	0.16	42.95	5.62	1.41	30.57
6	0.5	37.55	5.04	1.25	30.1
7	0.44	35.9	4.68	1.22	29.51
8	0.2	14.85	2.15	0.45	33.19
9	0.1	21.45	3.03	0.93	23.03
10	0.2	16.15	2.03	0.48	33.94
11	0.47	7.53	1.29	0.23	32.85
12	0.31	12.4	1.9	0.37	33.46
13	0.63	44.3	5.58	1.34	33.06
14	0.43	45.75	5.74	1.3	35.3
15	0.12	33.15	4.38	1.39	23.87
16	0.45	37.5	4.9	1.61	23.23
17	0.53	41.4	5.42	1.07	38.76
18	1.03	35.75	4.72	1.5	23.79
19	0.31	10.33	1.69	0.76	13.51
20	0.55	10.96	1.83	0.87	12.54

8.5.2 Bever

In the following tables, the whole dataset of Bever is illustrated. In Table 44 and Table 45 one can see the general information of the plots at Bever, conducted with the plot survey in the field as well as the (in the laboratory) measured pH values.

Table 44 Dataset of Bever (Part 1.1).

Plot Nr.	Coordinates	Elevation (asl)	Slope (°)	Exposition °N	PF / no PF	Vegetation cover (%)	Gravel content (%)	pH Hellige	pH Laboratory
21	N46.54339 E9.80053	2662 m	20 °	40 °N	yes	26%	15%	4.5	4.07
22	N46.54313 E9.80031	2664 m	25 °	220 °N	no	80%	5%	4	3.72
23	N46.54324 E9.79997	2666 m	10 °	92 °N	yes	0%	10%	5	4.35
24	N46.54322 E9.79962	2678 m	18 °	90 °N	yes	5%	15%	5	4.35
25	N46.54326 E9.79909	2683 m	15 °	45 °N	yes	5%	20%	4.5	4.07
26	N46.54302 E9.79886	2688 m	15 °	60 °N	no	10%	18%	5	4.25
27	N46.54277 E9.79881	2686 m	8 °	170 °N	no	0%	10%	4.5	4.17
28	N46.54252 E9.79863	2688 m	23 °	120 °N	no	0%	25%	5	4.52
29	N46.54248 E9.79853	2687 m	31 °	145 °N	no	70%	20%	4.5	4.02
30	N46.54105 E9.79768	2707 m	25 °	90 °N	no	100%	30%	4.5	3.65
31	N46.54118 E9.79720	2697 m	15 °	50 °N	no	70%	30%	4.5	4
32	N46.54133 E9.79770	2704 m	20 °	90 °N	no	100%	5%	4	3.82
33	N46.54160 E9.79769	2702 m	32 °	120 °N	no	50%	10%	5	4.15
34	N46.54169 E9.79782	2697 m	25 °	110 °N	no	50%	10%	4.5	4.45
35	N46.54182 E9.79844	2699 m	30 °	90 °N	no	85%	5%	5	4.02
36	N46.54220 E9.79844	2667 m	25 °	75 °N	no	0%	1%	4.5	4.15
37	N46.54216 E9.79855	2667 m	35 °	110 °N	no	100%	10%	4	3.82
8	N46.54219 E9.79860	2674 m	10 °	10 °N	no	0%	2%	4.5	4.25
39	N46.54219 E9.79859	2675 m	25 °	90 °N	no	0%	5%	4.5	4.12
40	N46.54218 E9.79863	2674 m	10 °	100 °N	no	0%	10%	4.5	4.3

Table 45 Dataset of Bever (Part 1.2).

Plot Nr.	Coordinates	Elevation (asl)	Slope (°)	Exposition °N	PF / no PF	Vegetation cover (%)	Gravel content (%)	pH Hellige	pH Labora- tory
41	N46.54198 E9.79851	2674 m	8	60 °N	no	0%	10%	4.5	4.45
42	N46.54205 E9.79829	2683 m	30	140 °N	no	100%	30%	4.5	4.3
43	N46.54210 E9.79825	2683 m	35	130 °N	no	100%	10%	4.5	4.4
44	N46.54208 E9.79823	2684 m	30	145 °N	no	100%	10%	4.5	4.45
45	N46.54207 E9.79901	2664 m	15	120 °N	yes	2%	30%	4.5	4.39
46	N46.54219 E9.79915	2661 m	5	60 °N	yes	5%	0%	4.5	4.475
47	N46.54244 E9.79948	2637 m	11	90 °N	yes	30%	10%	4.5	4.6
48	N46.54256 E9.79945	2636 m	15	150 °N	yes	10%	15%	5	4.9
49	N46.54258 E9.79942	2664 m	20	170 °N	yes	10%	15%	5	4.7
50	N46.54267 E9.79949	2663 m	15	50 °N	yes	15%	15%	5	5.35
51	N46.54266 E9.79867	2677 m	10	140 °N	yes	0%	30%	4.5	4.55
52	N46.54288 E9.79884	2682 m	10	90 °N	yes	0%	30%	4.5	4.575
53	N46.54300 E9.79887	2678 m	20	90 °N	yes	60%	20%	4.5	4.5
54	N46.54312 E9.79887	2675 m	10	110 °N	yes	5%	20%	4.5	4.5
55	N46.54332 E9.79892	2680 m	15	280 °N	yes	15%	10%	4.5	4.525
56	N46.54346 E9.79905	2681 m	15	30 °N	yes	30%	10%	4.5	4.4
57	N46.54361 E9.79901	2669 m	11	50 °N	yes	1%	20%	4.5	4.625
58	N46.54374 E9.79927	2667 m	10	0 °N	yes	1%	10%	4.5	4.725
59	N46.54380 E9.79935	2671 m	20	340 °N	yes	20%	10%	4.5	4.775
60	N46.54383 E9.79933	2669 m	10	310 °N	yes	0%	10%	4.5	4.6

In Table 46 and Table 47, the Soil physical properties (measured with the TDR) are listed for Bever.

Table 46 Dataset of Bever (Part 2.1)

Plot Nr.	Moisture before	Moisture after	Surface runoff (ml)	Sediment yield (g)	Temp before	Temp after	Conductivity before	Conductivity after
21	18.47	28.19	22.21	0.11	9	11.4	0.8	0.2
22	35.85	40.35	144.59	0.11	13.4	14.4	0.9	0.6
23	7.31	20.05	430.56	3.44	15.7	15.9	0	0.7
24	17.57	17.99	2.54	0.01	15.7	16.4	0.3	0.4
25	32.67	33.9	0	0	21.2	22.9	0	0
26	11.63	15.96	3.21	0.05	21	20.4	0.2	0.8
27	9.47	13.35	5.59	0.39	20.2	21	0.7	0.5
28	7.89	13.71	809.18	11.63	22.3	22.5	0.4	0
29	19.85	24.45	26.94	0.04	23.4	23.3	0.7	0.5
30	19.64	36.6	281.11	0.01	9.4	10.5	0.9	1.3
31	20.12	22.95	78.34	0.04	11.6	12.3	1.4	0.2
32	23.15	26.6	247.36	0.15	13.1	13.1	0.2	1.3
33	30.4	33.69	240.51	0.35	13.8	14.5	0.2	0.5
34	27.63	33.62	198.04	0.1	16.4	17.8	0.7	1.2
35	29.46	28.35	58.6	0.1	18	18.5	0.7	1.3
36	31.9	24.53	585.54	0.56	6.9	13.5	0	1.4
37	40	51.45	0	0	16.6	17.5	0.7	0.8
8	10.17	14.1	1.84	0.3	18	19.1	0.1	0.3
39	9.19	10.67	129.06	3.01	20.4	20.5	0.6	0
40	17.09	18.79	206.9	0.42	19.7	20.1	0	0.1

Table 47 Dataset of Bever (Part 2.2)

Plot Nr.	Moisture before	Moisture after	Surface runoff (ml)	Sediment yield (g)	Temp before	Temp after	Conductivity before	Conductivity after
41	27.68	29.77	0	0	2.9	5.6	0.8	0
42	6.19	3.2	143.79	0.18	12	13	1.1	0.8
43	31.65	37.72	18.44	0.02	16.7	19.4	10	0
44	39.87	41.74	8.12	0.12	20.1	24.7	0.9	0.6
45	0.9	6.2	35.24	0.019	20.5	25.4	0.1	0
46	3.96	13.2	177.46	0.01	20.2	19.9	0	0
47	5.47	8.95	9.72	0.02	18.3	18.4	0.8	0.8
48	9.95	3.05	29.4	0.01	16.5	15.9	0.6	0.4
49	7.68	18.36	69.87	0.04	14.9	15.3	0.2	0.8
50	4.18	9.44	18.24	0.02	16.2	17	0.9	1.1
51	3.53	6.12	4.32	0.02	17	16.2	0	0.6
52	7.86	15.03	7.09	0.1	15.1	15.3	1.2	0.6
53	6.54	6.91	4.56	0.03	16.2	17.1	0.6	0.9
54	7.47	19.71	4.01	0.05	12.4	11.8	0.6	0.1
55	9.53	27.15	136.07	0.04	11.1	10.9	0.5	0.3
56	10.3	15.4	4.85	0.03	10.81	9.6	0.6	0.4
57	6.7	10.31	12.78	0.17	10.5	10.9	0.8	0
58	6.28	11.5	6.79	0.01	11	10.31	1.5	0.8
59	7.8	9.75	133.62	0.05	10.8	12.5	0.5	0
60	8.5	9.7	137.18	0.06	11.4	10.67	1.2	0.9

In Table 48 and Table 49 information about the grain size distribution, as well as the amount of carbon, hydrogen and nitrogen and the C/N ratio are listed.

Table 48 Dataset of Bever (Part 3.1).

Plot Nr.	Ratio fine/coarse	C (%)	H (%)	N (%)	Ratio C/N
21	0.69	2.88	0.68	0.35	8.26
22	0.05	17.9	2.86	1.22	14.69
23	0.97	2.14	0.62	0.32	6.7
24	1.24	3.22	0.71	0.39	8.24
25	1.7	4.74	0.91	0.42	11.41
26	1.4	2.91	0.61	0.36	8.14
27	1.38	0.68	0.32	0.19	3.53
28	1.49	1.69	0.54	0.23	7.33
29	1.44	8.15	1.45	0.61	13.39
30	0.28	20.4	3.12	1.31	15.63
31	0.63	16.2	2.46	1.02	15.95
32	0.15	17.15	2.75	1.09	15.76
33	0.65	9.83	1.74	0.68	14.55
34	1.2	10.58	1.83	0.72	14.64
35	0.66	12.23	2.01	0.81	15.1
36	0.41	8.38	1.57	0.55	15.29
37	0.32	15.45	2.59	1.02	15.13
8	0.87	4.46	1.02	0.42	10.48
39	1.01	4.49	1.03	0.4	11.11
40	0.97	2.65	0.68	0.3	8.82

Table 49 Dataset of Bever (Part 3.2).

Plot Nr.	Ratio fine/course	C (%)	H (%)	N (%)	Ratio C/N
41	0.51	1.26	0.46	0.2	6.2
42	1.26	8.1	1.51	0.68	11.9
43	0.72	9.82	1.74	0.75	13.11
44	0.49	9.24	1.62	0.71	13.05
45	2.35	0.1	0.17	0.12	0.87
46	0.41	0.1	0.14	0.11	0.88
47	0.96	0.1	0.19	0.12	0.82
48	0.93	0.1	0.19	0.14	0.74
49	0.6	0.39	0.27	0.12	3.26
50	0.97	0.1	0.18	0.11	0.95
51	2.45	0.11	0.24	0.15	0.75
52	1.3	2.7	0.67	0.27	9.9
53	1.06	2.37	0.55	0.3	8
54	0.42	1.71	0.5	0.23	7.55
55	0.37	3.22	0.71	0.32	10.08
56	0.38	1.66	0.46	0.23	7.14
57	2.1	0.12	0.25	0.11	1.05
58	0.32	2.34	0.62	0.3	7.71
59	0.3	0.99	0.33	0.17	5.74
60	0.38	1.32	0.46	0.23	5.72

Personal declaration:

I hereby declare that the submitted thesis is the result of my own, independent, work. All external sources are explicitly acknowledged in the thesis.

Pascale Polich